

Summer 2019

A Nonlinear Parallel Model for Reversible Polymer Solutions in Steady and Oscillating Shear Flow

Erik Tracey Palmer

Follow this and additional works at: <https://scholarcommons.sc.edu/etd>



Part of the [Mathematics Commons](#)

Recommended Citation

Palmer, E. T.(2019). *A Nonlinear Parallel Model for Reversible Polymer Solutions in Steady and Oscillating Shear Flow*. (Doctoral dissertation). Retrieved from <https://scholarcommons.sc.edu/etd/5343>

This Open Access Dissertation is brought to you by Scholar Commons. It has been accepted for inclusion in Theses and Dissertations by an authorized administrator of Scholar Commons. For more information, please contact dillarda@mailbox.sc.edu.

A NONLINEAR PARALLEL MODEL FOR REVERSIBLE POLYMER SOLUTIONS IN
STEADY AND OSCILLATING SHEAR FLOW

by

Erik Tracey Palmer

Bachelor of Arts
University of California, Davis 2007

Master of Science
California State University, East Bay 2013

Submitted in Partial Fulfillment of the Requirements

for the Degree of Doctor of Philosophy in

Mathematics

College of Arts and Sciences

University of South Carolina

2019

Accepted by:

Paula A. Vasquez, Major Professor

Yi Sun, Committee Member

Hong Wang, Committee Member

Qi Wang, Committee Member

Guiren Wang, Committee Member

Cheryl L. Addy, Vice Provost and Dean of the Graduate School

© Copyright by Erik Tracey Palmer, 2019
All Rights Reserved.

ACKNOWLEDGMENTS

I would first like to thank my wife, Yulian Wu. Without her this would have never happened. To my children, thank you for sacrificing our time together. I am also thankful for the contributions from other family members. My mother and father unwaveringly supported my many educational pursuits over the years. My parents-in-law spared no effort in helping to get this project finished – particularly my mother-in-law. Her presence at crucial times allowed me space and energy to focus. My uncle, Owen Palmer, stepped up at several critical moments to offer timely support. I would like to thank him for responding with excessive patience and the willingness to invest time in my mathematical dilemmas.

I also want to thank a wonderful network of friends whose support was absolutely necessary. In particular, my friend Russell Mills Campisi, called me daily to keep me motivated and focused on my goals. My wife’s colleagues shared vast amounts of insider information and graduate school expertise as well as good food and drinks.

Because creeks flow into streams and streams into rivers, I would like to thank Moon Duchin. Her encouragement in a History of Mathematics class launched this journey. My experiences at Cal State East Bay were also crucial to the success of this project. Therefore, I would like to thank Stuart Smith who forged the mindset I needed to be successful, Julia Olkin for her support and Shirley Yap who told me ‘As long as you want to do math you will be able to’. My brief time as a summer intern at the Lawrence Berkeley Lab provided a lift that carried me through to the end of this project. For this reason, I want to thank Ann Almgren, Andy Nonaka and everyone else at the Center for Computational Sciences and Engineering.

I am also thankful for the many friendships I developed with my fellow graduate students. Classmates Xueping Zhao and Sameed Ahmed were supportive in every way and remain so to this day. With other classmates, I was inspired by their joy and motivated by their passion. My thanks to those who worked with me and listened to my ideas. These opportunities gave purpose to my studies. In particular, I want to express special thanks to the fellow students who stayed up late the night before my defense to give feedback and then woke up the next morning to show support by listening again. In all, our graduate student cohort looked out for one another and fostered an atmosphere I was happy to be a part of.

Finally, I would like to give thanks to my dissertation committee and the rest of the mathematics department for their support during this endeavor.

Erik Palmer

June 28, 2019

ABSTRACT

A mathematical model for reversible polymers in steady and oscillating shear flows is presented. Using a mean-field approach, the behavior of the polymer network is characterized by a finitely extensible nonlinear elastic bead-spring model that stochastically transitions between dumbbell states to represent attachments, detachments and loops. An efficient parallel scheme for computation on GPUs utilizes populations of over a million dumbbells to characterize steady, large and small amplitude oscillatory shear (SAOS) flows in Brownian dynamics simulations. In steady-shear a novel attachment species transition function enables shear thickening and shear thinning by the adjustment of either attachment or detachment parameters. Three species simulations show the inclusion of loops modifies the strength of these nonlinear flow responses. In SAOS simulations, three species simulations show an increase in dynamic moduli at higher frequencies not present in two species models. Two approaches for a looped segment transitioning to dangling are explored, and the choice found to have substantial impact on the effect of adding a third species. Pipkin diagrams are also generated using large amplitude oscillatory flows.

TABLE OF CONTENTS

ACKNOWLEDGMENTS	iii
ABSTRACT	v
LIST OF TABLES	viii
LIST OF FIGURES	ix
CHAPTER 1 INTRODUCTION	1
CHAPTER 2 MODEL DESCRIPTION	5
2.1 Block Copolymers	5
2.2 Dumbbell Evolution Equation	9
2.3 Attached, Dangling and Looped Transition Probability Functions	10
2.4 Additional Equations	17
2.5 Model Parameters	19
CHAPTER 3 SIMULATION METHOD	20
3.1 Brief Overview	20
3.2 Coding for the High Performance Computing Environment	21
3.3 Strain Simulations	24
3.4 Uncertainty Quantification	28

CHAPTER 4 RESULTS	33
4.1 Simple Shear	33
4.2 Small Amplitude Oscillatory Shear	43
4.3 Loop-to-Dangling Transition Methods	60
4.4 Large Amplitude Oscillatory Shear	63
CHAPTER 5 CONCLUSION	67
BIBLIOGRAPHY	69
APPENDIX A DERIVATION OF THE DUMBELL EQUATION	76
APPENDIX B NUMERICAL SCHEME	78
APPENDIX C CUDA C CODE	81

LIST OF TABLES

Table 2.1	Experimental measurements for triblock polymers containing PEO. All measurements were taken at 20°C. ^a Data from Kadam et al. [26]. ^b Data from Zhao et al. [67] with reported relative error: M_w , $\pm 5\%$; R_h , $\pm 2\%$; R_g , $\pm 8\%$	7
Table 2.2	Model Parameters: Description and Values.	19
Table 3.1	Table of computation environments and run combinations. The code has a small memory footprint on the GPU but fully utilizes the CPU core. Therefore, to saturate the hardware, multiple runs were executed simultaneously.	24
Table 3.2	Uncertainty in the steady state values from examples seen in figures 3.6 and 3.7.	31
Table 4.1	Dumbbell configuration term approximations.	58

LIST OF FIGURES

Figure 2.1	Cartoon of BAB-block copolymer. Hydrophobic and hydrophilic blocks in the polymer chain respond to the solvent by forming micelles.	6
Figure 2.2	Visual representation of the model conceptualization process; from experimental form (<i>left</i>), cartoon representation (<i>center</i>), to network diagram (<i>right</i>). <i>Left</i> . Image of a block copolymer hydrogel sample from Nykänen et al. [37]. <i>Center</i> . Cartoon representation of a polymer network showing fully formed micelles connected by polymer chains, as well as dangling and looped segments. <i>Right</i> . Network diagram containing the three species types used in the model: active (red), dangling (green), and looped (blue).	8
Figure 2.3	Elastic dumbbell. Dumbbells represent each, endpoint-edge-endpoint, segment of the polymer network. Notice that \mathbf{Q} tracks only the configuration (length and orientation) and not the location of the segment.	9
Figure 2.4	Diagram of a polymer chain with one attached end, and one free or dangling end. We model the area explored by the dangling end as the volume of a cone, thus leading to a αQ^2 dependence on the length in the probability of attachment.	13
Figure 2.5	Transition probability functions. <i>Top</i> . Probability of transitioning from an active to dangling species type. <i>Center</i> . Probability of transitioning from a dangling species to either an active or looped type. <i>Bottom</i> . Probability of transitioning from a looped to dangling species type. <i>All</i> . Parameters used for the plots are $\alpha = 1.7$, $\beta = 8.7$, $\chi = 1.0$, $Q_{\max} = 33.3334$ and $\Delta t = 5e - 3$	16

Figure 3.1	Code flow chart. The design of the code can be divided into CPU (left) and GPU (right) parts. Sending data between the CPU and GPU is a time intensive operation. The loop on the GPU represents a single thread and is run independently for each of the 1024000 dumbbells in the simulation. The term ‘RNG’ refers to random number generator.	23
Figure 3.2	Plot of a typical steady shear flow simulation. The left axis shows the stress response, σ_{xy} , versus time. The right axis indicates the fraction of each species type. The system is allowed to equilibrate with zero flow until $t = 100$ then the flow is imposed. The dashed line indicates the steady state stress value measured as an average over the last 10% of simulated flow time.	25
Figure 3.3	Figure illustrating the fitting of the coefficients of $G'\gamma_0 \sin(\omega t) + G''\gamma_0 \cos(\omega t)$ to the stress response of a SAOS simulation. The top plot shows the simulated stress response. The red curve is the fitted expression over the steady state period. The lower plot indicates the error between each data point and the computed curve.	26
Figure 3.4	Plot showing the Fourier transform of the stress response from a SAOS simulation. The single peak at 1 indicates there is only a clear first harmonic present and thus this response should be considered within the linear regime.	27
Figure 3.5	Plot showing the Fourier transform of the simulated stress response from a LAOS plot. The multiple peaks indicate additional harmonics present in the stress response. Harmonics automatically identified by the MATLAB routine are identified with a yellow circle.	28
Figure 3.6	Figure showing the stress response from 100 steady shear simulations. The largest plot shows the full runtime of a collection of 100 simulations. Insert A is an enlarged view of the transient period where variations are largest. Insert B is a plot of the 95% confidence interval. These areas were enlarged to highlight the variation between simulations.	29
Figure 3.7	Figure showing the stress response from 100 SAOS simulations. The largest plot shows the full runtime of a collection of 100 simulations. Insert A is an enlarged view of a selected time period. Insert B is a plot of the 95% confidence interval. These areas were enlarged to highlight the variation between simulations.	30

Figure 4.1	Viscosity η and First Normal Stress Coefficient Ψ_1 for steady shear flow simulations of a two species model. Each plot contains a single α/β ratio.	35
Figure 4.2	Species fractions in shear flow. Plots show the steady state species fraction of each type, active and dangling, for the simple shear simulations in 4.1.	35
Figure 4.3	Three species steady shear flow simulations. Plot shows steady state viscosity η and first normal coefficient Ψ_1 , organized by attachment, α/β , and looping, β/χ , ratios. The α/β ratio increases in the upward direction and the β/χ ratio increases left to right.	38
Figure 4.4	Two species, dangling and looped, steady shear flow simulations. Plots show the viscosity η and first normal stress coefficient Ψ_1 . Each plot shows the result of three data sets with the same χ/β ratio.	40
Figure 4.5	Dumbbell species transition diagram. Equations are simplified in that $F(Q)$ represents different functions of the length of a dumbbell, Q . Each ellipse represents a species type. Each arrow represents a species transition and is labeled with the parameter that affects the transition probability. In the two species model, only the area above the dashed line is considered. In the three-species model, the entire diagram is considered.	40
Figure 4.6	Transition function parameter dissymmetry in the three species model. Steady shear plots of viscous and first normal stress coefficient on the left axis. On the right axis, are species fractions. Plots on the first row include only active and dangling species. Plots on the second row also include loops.	42
Figure 4.7	Three measurements from a two species and three species SAOS simulation. (Left) Dynamic moduli plots indicate the strength of the network response, and describe elastic-like and viscous-like behavior of the fluid. (Center) Species fraction separated by state. (Right) Average normed length of dumbbell segments.	44

- Figure 4.8 Stress contributing species fractions. Plots show the ratio of active (top) and dangling (bottom) dumbbells to active and dangling combined. Three distinct regions in the three species model are apparent; A low frequency region where including loops decreases the ratio of active dumbbells and increase the ratio of dangling. A mid-frequency region, where both models show similar ratios. A high frequency region, where the three species models shows increasing numbers of active dumbbells and decreasing numbers of dangling dumbbells. 46
- Figure 4.9 Figure showing the dynamic moduli from the model and experimental data for hydrophobically modified ethoxylated urethane. Experimental data and model values have been shifted by constant multiples to align relaxation points. Model parameters were set to $\alpha = 1.7$ $\beta = 8.7$ $\chi = 0.002$ for this simulation. Filled symbols indicate the frequency range with the best match to the data. Unfilled symbols indicate values without experimental data for qualitative comparison. 48
- Figure 4.10 Intracycle analysis of a low frequency two species SAOS simulation. *Upper Left* Normalized σ_{xy} stress, strain, curve fit and species fractions over a single cycle. Error bars indicate the range of data over the steady state. Fit refers to the curve generated by fitting σ_{xy} to the function $A \cos \omega t + B \sin \omega t$. The right axis shows the species fractions over the cycle. Error bars indicate variation over the steady state. The numbered dots indicate the corresponding time in the cycle where the corresponding dumbbell configuration histogram is taken. *Right* Dumbbell configuration histograms. To generate the histograms, one end of the dumbbell is fixed at the origin. The placement of the other end is used to for the histogram. Colors represent the number of dumbbell ends in the bin. *Bottom Left* Dynamic moduli for the batch of runs from which the current data is taken. Dots indicate the frequency currently under examination. 49

Figure 4.11 Intracycle analysis of a low frequency three species SAOS simulation. *Upper Left* Normalized σ_{xy} stress, strain, curve fit and species fractions over a single cycle. Error bars indicate the range of data over the steady state. Fit refers to the curve generated by fitting σ_{xy} to the function $A \cos \omega t + B \sin \omega t$. The right axis shows the species fractions over the cycle. Error bars indicate variation over the steady state. The numbered dots indicate the corresponding time in the cycle where the corresponding dumbbell configuration histogram is taken. *Right* Dumbbell configuration histograms. To generate the histograms, one end of the dumbbell is fixed at the origin. The placement of the other end is used to for the histogram. Colors represent the number of dumbbell ends in the bin. *Bottom Left* Dynamic moduli for the batch of runs from which the current data is taken. Dots indicate the frequency currently under examination. 50

Figure 4.12 Intracycle analysis of a mid-frequency two species SAOS simulation. *Upper Left* Normalized σ_{xy} stress, strain, curve fit and species fractions over a single cycle. Error bars indicate the range of data over the steady state. Fit refers to the curve generated by fitting σ_{xy} to the function $A \cos \omega t + B \sin \omega t$. The right axis shows the species fractions over the cycle. Error bars indicate variation over the steady state. The numbered dots indicate the corresponding time in the cycle where the corresponding dumbbell configuration histogram is taken. *Right* Dumbbell configuration histograms. To generate the histograms, one end of the dumbbell is fixed at the origin. The placement of the other end is used to for the histogram. Colors represent the number of dumbbell ends in the bin. *Bottom Left* Dynamic moduli for the batch of runs from which the current data is taken. Dots indicate the frequency currently under examination. 51

Figure 4.13 Intracycle analysis of a mid-frequency three species SAOS simulation. *Upper Left* Normalized σ_{xy} stress, strain, curve fit and species fractions over a single cycle. Error bars indicate the range of data over the steady state. Fit refers to the curve generated by fitting σ_{xy} to the function $A \cos \omega t + B \sin \omega t$. The right axis shows the species fractions over the cycle. Error bars indicate variation over the steady state. The numbered dots indicate the corresponding time in the cycle where the corresponding dumbbell configuration histogram is taken. *Right* Dumbbell configuration histograms. To generate the histograms, one end of the dumbbell is fixed at the origin. The placement of the other end is used to for the histogram. Colors represent the number of dumbbell ends in the bin. *Bottom Left* Dynamic moduli for the batch of runs from which the current data is taken. Dots indicate the frequency currently under examination. 52

Figure 4.14 Intracycle analysis of a high frequency two species SAOS simulation. *Upper Left* Normalized σ_{xy} stress, strain, curve fit and species fractions over a single cycle. Error bars indicate the range of data over the steady state. Fit refers to the curve generated by fitting σ_{xy} to the function $A \cos \omega t + B \sin \omega t$. The right axis shows the species fractions over the cycle. Error bars indicate variation over the steady state. The numbered dots indicate the corresponding time in the cycle where the corresponding dumbbell configuration histogram is taken. *Right* Dumbbell configuration histograms. To generate the histograms, one end of the dumbbell is fixed at the origin. The placement of the other end is used to for the histogram. Colors represent the number of dumbbell ends in the bin. *Bottom Left* Dynamic moduli for the batch of runs from which the current data is taken. Dots indicate the frequency currently under examination. 53

- Figure 4.15 Intracycle analysis of a high frequency three species SAOS simulation. *Upper Left* Normalized σ_{xy} stress, strain, curve fit and species fractions over a single cycle. Error bars indicate the range of data over the steady state. Fit refers to the curve generated by fitting σ_{xy} to the function $A \cos \omega t + B \sin \omega t$. The right axis shows the species fractions over the cycle. Error bars indicate variation over the steady state. The numbered dots indicate the corresponding time in the cycle where the corresponding dumbbell configuration histogram is taken. *Right* Dumbbell configuration histograms. To generate the histograms, one end of the dumbbell is fixed at the origin. The placement of the other end is used to for the histogram. Colors represent the number of dumbbell ends in the bin. *Bottom Left* Dynamic moduli for the batch of runs from which the current data is taken. Dots indicate the frequency currently under examination. 54
- Figure 4.16 Progression of a single dumbbell. Plot shows the length and angle of a single dumbbell in the three species SAOS simulation. The background colors indicate the species state of the dumbbell. Oscillations occur in both directions when the dumbbell is not in the looped state. However, entering and exiting the looped state at opportune times allows the dumbbell to progressively extend in length. 56
- Figure 4.17 Orientation angle versus oscillation frequency and flow rate. There are three regions; a left region where the spring force is the largest factor influencing change in dumbbell configuration, a right region where frequency and flow rate are the larger factor, and a middle region where it depends on the dumbbell species type. Slope and position of dividing lines depend on the value of Z 59
- Figure 4.18 Intracycle behavior from a three species SAOS simulation where loops transition to dangling with length draw from a normal distribution. In these simulations, the looped-to-dangling dumbbells take configurations based on a truncated normal distribution. (Upper left) Plot showing intracycle stress, strain and species fractions. (Lower left) Dynamic moduli across a range of frequencies. The intra-cycle is taken from the run indicated by the black dot. (Right) Dumbbell configuration histograms separated by type and intracycle time. 62

Figure 4.19 Pipkin diagrams showing elastic Bowditch-Lissajou curves form a three species large amplitude oscillatory shear flow simulation. Each simulation was done with parameters $\alpha = 1$, $\beta = 10$ and $\chi = 0.01$. ω is the oscillation frequency, $\lambda_{eff} = 1/\tau = 14.1343$ 64

Figure 4.20 Pipkin diagrams showing viscous Bowditch-Lissajou curves form a three species large amplitude oscillatory shear flow simulation. Each simulation was done with parameters $\alpha = 1$, $\beta = 10$ and $\chi = 0.01$. ω is the oscillation frequency, $\lambda_{eff} = 1/\tau = 14.1343$ 65

CHAPTER 1

INTRODUCTION

Associative polymer models for viscoelastic fluids have held the attention of the scientific community for over 50 years. Interest remains high due to the numerous applications of transient polymers in industrial applications where control over their rheological behavior is crucial for achieving ideal performance. Transient polymers also serve important roles in the biomedical community as the material for soft sensors, drug carriers and in tissue engineering, just to name a few [2, 54, 24]. They are categorized as associative polymers due to the reversible cross-links of their molecular network that give rise to unique characteristics such as shear-thinning and shear-thickening.

The work of this dissertation focuses on the rheological behavior of tri-block polymers above the micelle concentration [42, 45, 34] . Tri-block polymers are defined as molecular chains that consist of a B-A-B configuration where the B-Blocks are hydrophobic and the A-blocks are hydrophilic. Above a certain concentration, interactions with the solvent cause the polymer chains to form micelles. At higher concentrations, thermodynamic vibration and flow forces then lead to bridging between micelles as the hydrophobic ends break out of their micelle cores and form bridges by embedding their hydrophobic ends in other micelle cores. Conversely, the same forces cause the destruction of bridges as polymer ends disassociate from either core. These mechanical behaviors are responsible for the dynamic characteristics of the polymer and is what leads scientists to classify them as telechelic or reversible associative polymers.

Since Green and Tobolsky [19] numerous models have been presented in an attempt to capture the characteristic behaviors of telechelic polymer networks [66, 65, 55, 62, 63, 64, 48, 49, 50] . An early history of constitutive models is well covered in the introduction of Tripathi et al. [51] and a thorough discussion in Wang and Larson [56] provides a recent update. Of present interest is the work done by Vaccaro and Marrucci in [53]. Based on theory and simulation results from van den Brule and Hoogerbrugge [8] , they model this system as finitely extensible dumbbells separated into two groups, active and dangling. Each segment has its own characteristics and thus effects the polymer network structure differently. In simulation, dumbbells stochastically switch between states. Representing each state as a single Fokker-Planck equation creates a system of equations which can be solved using closure approximations. A systematic evaluation of this approach is undertaken by [38]. On the other hand, Hernández Cifre [22] takes a Brownian Dynamics approach. Instead of Fokker-Plank equations, a Langevin equation describes the micro-scale dynamics of each dumbbell type. Macro-scale terms, such as the fluid stress, are then determined by averaging over many realizations -typically ensembles of 5000 dumbbells. In this way, Hernández Cifre shows the viscosity profile of associative polymers in simple shear flow can be captured without the closure approximations needed in other approaches.

In a more recent evolution of Vaccaro and Marrucci's approach, Sing et al [44]. adds a third looped dumbbell species. Through analysis of their three species Fokker-Plank system, they conclude that the inclusion of loops causes non-monotonic shear thickening and shear thinning at lower stresses. However, this type of simulation maybe more difficult to adapt to complex scenarios [32]. In this light, a Brownian Dynamics micro-macro scale approach provides a useful alternative.

A molecular dynamics model by Baljon et al. simulates telechelic polymers in small amplitude oscillatory shear flow and produces nonlinear stress responses [3,

60]. Their model is an extension of earlier work by Kremer and Grest [20, 29] where dynamics are driven by temperature and inter-chain interactions via energy potentials. The model by Baljon et al. adds the ability for endgroups on each chain to associate and detach from each other via Monte Carlo Dynamics. They simulate systems of 100 polymer chains with eight beads each. However, as they consider pairwise interactions between chains in the system, they are limited in the number of chains and beads they can model efficiently. To generate rheological data from SAOS flow, they attach polymer chains to an oscillating boundary and rely on strain rate-frequency superposition [61] to reconstruct a complete flow curve. While the complexities of this model make this admirable work, they also underscore the need for an efficient and straight forward method.

Although interest in elastic dumbbell models is high, the application of Brownian Dynamics models to associating polymers has not kept pace with advances in experimental techniques used to measure their rheology. In recent decades, small amplitude oscillatory shear (SAOS) has become the canonical method for rheological measurements [25]. Moreover, the developing field of non-linear rheology also relies on large amplitude oscillatory shear (LAOS) fluid flows that are more complex than steady shear and require additional sensitivity. However, few Brownian Dynamics models have yet to demonstrate capability in capturing rheological characteristics in this type of flow. The goal of this work is to present a micro-macro scale simulation capable of modelling associative polymers in steady, and small to large oscillatory shear flows. To this aim we present an extension of the mean-field method set forth in Hernández Cifre et al. and apply it to the more dynamic shear flows used in modern rheological measures. The parallel computation scheme allows for an efficient simulation of over a million dumbbells in the system and produces full flow curves with little stochastic noise or the need for additional frequency extension techniques. The inclusion of a third looping dumbbell species also creates a more dynamic non-linear

fluid response and results in a wider range of dynamic moduli. Finally, the additional fidelity makes it possible to simulate large amplitude oscillatory shear measurements for a wide range of frequencies and flow rates.

CHAPTER 2

MODEL DESCRIPTION

Our model builds off the approach taken by Hernández Cifre in [22] by adding a third species of dumbbells and adopting modifications for efficient parallel computation. The key differences are the use of nonlinear elastic finitely extendable (FENE) dumbbells, reworked species transition probability functions, including an adaptation of Sing's method for incorporating looped dumbbells, and the use of a constant instantaneous lifetime for dumbbell chains in the network. The most important feature of the model is the Mean-Field approach. In this approach, explicit positions for dumbbells and their connections are not tracked; forgoing direct tracking of the network topology. Instead, each dumbbell follows a stochastic differential equation according to its species type that also varies stochastically according to prescribed rules based on the length. These characteristics allow parallel computation of each dumbbell configuration and thus result in efficient modelling of large populations.

2.1 BLOCK COPOLYMERS

Our modelling approach is based on the structure of BAB block copolymers in solvent. BAB block copolymers are made of long molecule chains with a backbone of two segments, B and A, that show differing preference for the solvent.

For example, for a BAB copolymer in water, the A block is hydrophobic and the B block is hydrophilic.

At concentrations above the critical micelle concentration (CMC), the varying preference for water causes the formation of a core of A-type blocks as they attempt to

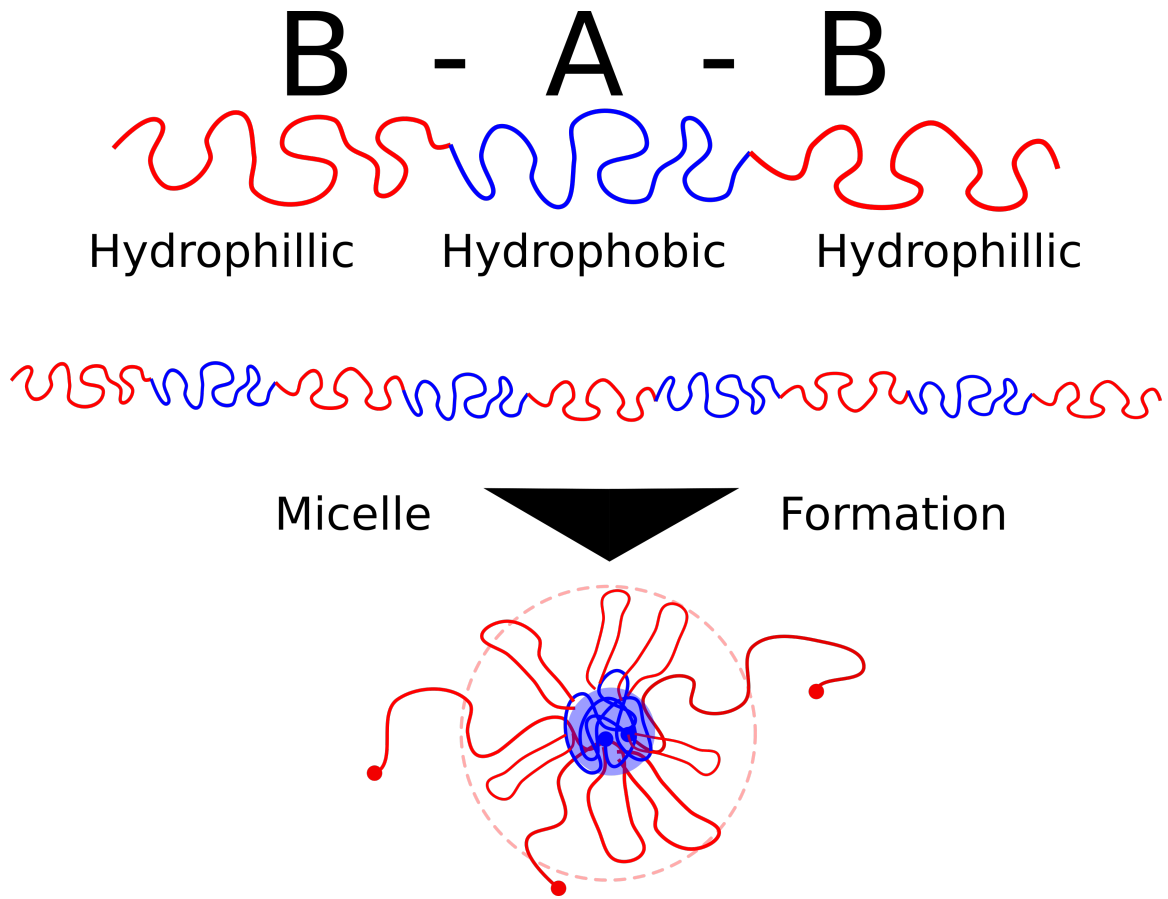


Figure 2.1: Cartoon of BAB-block copolymer. Hydrophobic and hydrophilic blocks in the polymer chain respond to the solvent by forming micelles.

avoid contact with the surrounding fluid. Meanwhile, because the B-type blocks prefer water, they are pushed outward forming a corona around the core. The resulting structure resembles a flower in two dimensions and is called a micelle. Figure 2.1 shows a cartoon representation of this description. Micelle formation is well studied for a variety of polymers [42, 45, 34, 4].

Precise measures at the molecular level for block copolymers can be challenging to obtain. In the case of the telechelic polymer, hydrophobically modified ethoxylated urethane (HEUR) with a backbone of polyethylene oxide (PEO), there are several factors which affect aggregate size, such as temperature, concentration and molecular weight. In one study by Kadam et al. using polyethylene oxide as the center of a triblock micelle forming polymer [26], aggregate sizes had a radius of gyration of that

Table 2.1: Experimental measurements for triblock polymers containing PEO. All measurements were taken at 20°C. ^aData from Kadam et al. [26]. ^bData from Zhao et al. [67] with reported relative error: M_w , $\pm 5\%$; R_h , $\pm 2\%$; R_g , $\pm 8\%$.

Copolymer	Concentration	M_w (g/mol)	R_h (nm)	R_g (nm)
PMEA-PEO-PMEA _a	1 g/L	3.60×10^5	13	-
PMEA-PEO-PMEA _a	2 g/L	3.80×10^5	14	-
PMEA-PEO-PMEA _a	4 g/L	5.90×10^5	17	-
PMEA-PEO-PMEA _a	8 g/L	4.61×10^6	55	65
PMEA-PEO-PMEA _a	10 g/L	1.48×10^7	74	103
PMEA-PEO-PMEA _a	12 g/L	2.85×10^7	95	144
PCL-PEO-PCL _b	2.74×10^{-6} g/mL	4.51×10^6	52	39
PCL-PEO-PCL _b	2.74×10^{-6} g/mL	1.04×10^7	53	49
PCL-PEO-PCL _b	2.74×10^{-6} g/mL	3.03×10^7	56	54

ranged from 65 nm to 144 nm while the hydrodynamic radius ranged from 13 nm to 95 nm. In another study by Zhao et al. they find radius of the formed micelles shrink as the temperature increases [67]. Moreover, they measure a radius of gyration from 54 nm to 39 nm and a hydrodynamic radius from 56 nm to 52 nm with errors of $\pm 5\%$, $\pm 8\%$ and $\pm 2\%$ respectively. The table 2.1 contains complete measurements from these works.

In concentrations above the CMC, networks form as micelles come into increasing contact with one another and entangle. The focus of our model is at these concentrations, where micelle network attachment and detachment play a role in the mechanic response of the fluid. The progression of our model representation is illustrated in figure 2.2. On the far left is an example polymer network from Nykänen et al. [37]. The center illustration shows a cartoon version, with micelles displaying three features: 1) entanglements with other micelles; 2) dangling polymer chains, where one end is embedded in the micelle core and the other end explores the surrounding fluid; and 3) looping chains where both ends embed in the same micelle core. In our model, these three types of segments are classified as active (bridges), dangling and looped species types. On the right is a network diagram of the cartoon. In this diagram

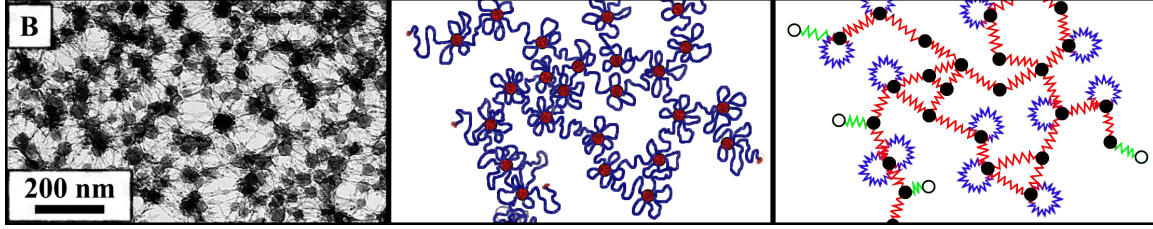


Figure 2.2: Visual representation of the model conceptualization process; from experimental form (*left*), cartoon representation (*center*), to network diagram (*right*). *Left*. Image of a block copolymer hydrogel sample from Nykänen et al. [37]. *Center*. Cartoon representation of a polymer network showing fully formed micelles connected by polymer chains, as well as dangling and looped segments. *Right*. Network diagram containing the three species types used in the model: active (red), dangling (green), and looped (blue).

each segment is clearly represented and color coded by species. Each segment is represented as a dumbbell with two endpoints connected by a spring. The endpoints are considering sticking points, where attaching and detaching to other nodes is possible. Endpoints can be micelle cores or the end of a free dangling polymer chain.

Our model will focus on tracking segment configuration dynamics and species type. Because fluid stress is a force per unit of area, and we consider all the parts of our network to be within sufficient proximity to one another to avoid unique considerations, we make the modelling assumption that is it not necessary to track the position of each segment in the network in order to resolve overall fluid stress in the cell. Using this, we approximate network attachments, detachments and looping with stochastic functions of the dumbbell length. Therefore the main mathematical concerns of our approach are an equation to track segment configuration (length and orientation but not position) and species transition probability functions. This focus allows for each segment to be evolved over time independently of the behavior of other dumbbells and results in gains in computational efficiency through parallel calculation. However, it also presents a challenging conceptual issue—a network model with no position.

There are several other modelling assumptions worth mentioning. First, hydrody-

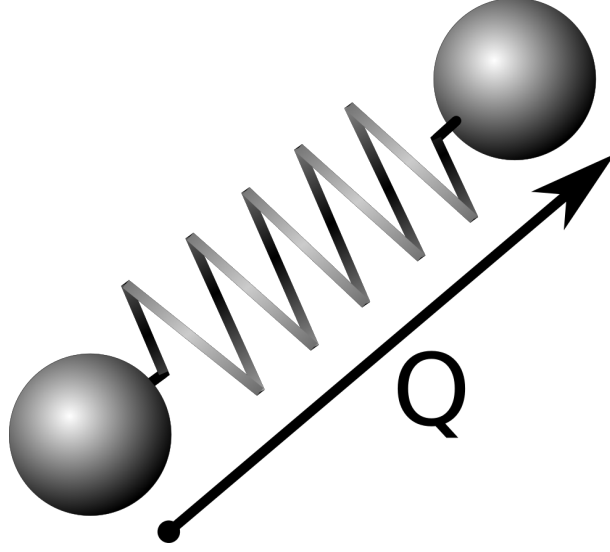


Figure 2.3: Elastic dumbbell. Dumbbells represent each, endpoint-edge-endpoint, segment of the polymer network. Notice that \mathbf{Q} tracks only the configuration (length and orientation) and not the location of the segment.

dynamic interactions with the solvent are neglected. Second, we assume a free draining polymer network. That is, the dumbbells themselves do not impede the movement of the Brownian particles. Third, there are no boundaries. Therefore the model assumes the fluid cell being simulated is a sufficient distance from any wall, so that special boundary conditions are a non-factor.

2.2 DUMBELL EVOLUTION EQUATION

The stochastic differential equation (SDE) describing the evolution of each dumbbell is,

$$\mathbf{Q}(t+\Delta t) = \mathbf{Q}(t) + \boldsymbol{\kappa} \cdot \mathbf{Q}(t) \Delta t - \left(\frac{\zeta_i + \zeta_j}{\zeta_i \zeta_j} \right) \mathbf{F}(\mathbf{Q}) \Delta t + \sqrt{2k_B T \left(\frac{\zeta_i + \zeta_j}{\zeta_i \zeta_j} \right)} \Delta \mathbf{W}(t). \quad (2.1)$$

Here \mathbf{Q} is a vector that represents the end-to-end length and angle (or configuration) of a single dumbbell, $\boldsymbol{\kappa}$ is the fluid velocity tensor, $\mathbf{F}(\mathbf{Q})$ is the FENE spring force, k_B is the Boltzmann constant and T is the temperature. The term $\mathbf{W}(t)$ is a Wiener process representing Brownian motion as a result of particle-solvent inter-

actions at the ends of the dumbbell. Equations for active and dangling species type differ by the assigned drag terms. For active dumbbells, $\zeta_i = \zeta_j = \zeta_{node}$ and for dangling dumbbells, $\zeta_i = \zeta_{node}$ and $\zeta_j = \zeta_{free}$. Dumbbells in the looped state are considered to have negligible interactions with the fluid, and thus their configuration does not change until they return to a dangling state.

2.3 ATTACHED, DANGLING AND LOOPED TRANSITION PROBABILITY FUNCTIONS

Three species types represent different states of a polymer chain under consideration. Attached dumbbells represent a BAB polymer chain where each sticky end (A-block) is attached to separate micelle cores. The dangling type describes a polymer chain, where a single sticky end is embedded in a micelle core, and rest of the polymer chain dangles freely in the solution. A looped type describes the state where the polymer chain has both ends embedded in its own micelle core; looping back upon itself. Each dumbbell evaluates its species type once per simulated time step, and changes according to the map,

$$\text{Active} \leftrightarrow \text{Dangling} \leftrightarrow \text{Looped}.$$

The active to dangling species transition models the situation where a polymer chain bridging two micelle cores separates from one core. A dangling to active transition represents the free end of a dangling chain embedding into the micelle core of another (unspecified) micelle core. The dangling to looped transition occurs when the free end of a polymer chain loops back upon itself. The looped to dangling transition indicates a single end of a looped chain breaking out of the micelle core to dangle freely in the solvent.

In simulation, each dumbbell species type follows a prescribed evolution equation according to the characteristics of its current state. After evolving orientation and

length forward in time, transitions between species states occur according to dynamics unique to each type and are determined via stochastic comparison. First, a transition probability function that may depend on the length of the dumbbell, determines the likelihood of a transition occurring. Then random variables are generated and compared to the values from the transition functions. If the transition probability function value is higher than the generated uniform random variable, a species transition occurs. The following subsections describe the transition probability functions in greater detail.

2.3.1 ACTIVE DUMBBELLS

The active-to-dangling ($A \rightarrow D$) state transition function models the process of two micelles separating through the detachment of a molecular chain. The approach taken here arose out of a combined analysis of the methods used in Hernández Cifre et al. [22] and Sing et al. [44, 43]. In Hernández Cifre et al., they model the attractive force between the chemical bonds as a potential well with the shape of a parabola. By balancing the energy to escape the well with the FENE force of the spring, they derive the expression given here in nondimensional form,

$$P_{A \rightarrow D} = 1 - \exp \left[- \frac{2\Delta t}{\tau_{fund} \exp(U_0) \exp \left(- \frac{d^2}{U_0} \frac{Q^2}{(1-Q^2/Q_{max}^2)^2} \right)} \right]. \quad (2.2)$$

On the other hand, Sing et al, cites Bell's law [5] for the rate of dissociation. This approach is derived from reaction rates and the lifetime of a bond from the kinetic theory of solids [68]. Together Bell's approach relates the rate of bond breakage to the strength of the force between potential bonding sites. In Sing et al, the rate of dissociation is presented as,

$$R_{\text{bridge dissociation}} = k_d \exp \left(B \left| \frac{Q}{1 - Q^2/Q_{max}^2} \right| \right) \quad (2.3)$$

By converting Eq. 2.3 to a probability and rearranging Eq. 2.2 we can compare the two probability transition functions as,

$$1 - \exp \left[-k_d \exp \left(B \left| \frac{Q}{1 - Q^2/Q_{max}^2} \right| \right) \Delta t \right] \quad (2.4)$$

and,

$$= 1 - \exp \left[-\frac{2}{\tau_{fund} \exp(U_0)} \exp \left(\frac{d^2}{U_0} \frac{Q^2}{(1 - Q^2/Q_{max}^2)^2} \right) \Delta t \right] \quad (2.5)$$

for the Sing et al. and Hernández Cifre et al. approaches, respectively. In this form we can see that these two approaches are similar but irreconcilable due to the squared FENE force dependence in Eq. 2.5 versus a non-squared dependence in Eq. 2.4.

For our model we chose to go with the expression from Sing et al. The dimensionless characteristic bond length, B , was set to 0.0325 to create transition probability curves similar to those using the approach and default parameters in Hernández Cifre et al. The parameter β is used to adjust overall rates of dissociation. Thus the probability transition function used in our simulations is,

$$P_{A \rightarrow D} = 1 - \exp \left[-\beta \exp \left(B \left| \frac{Q}{1 - Q^2/Q_{max}^2} \right| \right) \Delta t \right]. \quad (2.6)$$

2.3.2 DANGLING DUMBBELLS

Dangling dumbbells can transition to the active (A) or (L) looped types. Due to this added complexity, a multistep process was used to determine the proper form of each transition probability function. First, transition probability functions for the two transitions, dangling-to-active and dangling-to-looped were considered independently. An asterisk, *, is used to denote these functions. Then these probabilities were combined using a two random variable scheme.

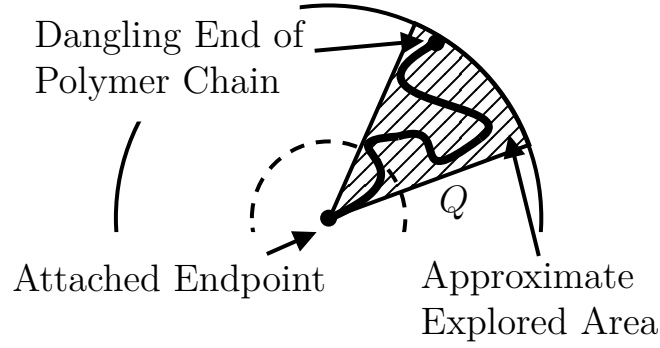


Figure 2.4: Diagram of a polymer chain with one attached end, and one free or dangling end. We model the area explored by the dangling end as the volume of a cone, thus leading to a αQ^2 dependence on the length in the probability of attachment.

Considering only the behavior of a dangling dumbbell transitioning to an active dumbbell we write,

$$P_{D \rightarrow A}^* = 1 - \exp \left[-\frac{\alpha Q^2}{1 - Q^2/Q_{max}^2} \Delta t \right]. \quad (2.7)$$

With this construction the probability of association increases with the length of the dumbbell. In addition, it follows the argument in Hernández Cifre et al. that states this probability should relate to the space explored by a sticky end as it retracts through the solvent. However, because the volume explored by the retracting dangling chain should grow with the same proportionality of the volume of a cone with height the length of the chain, αQ^2 is used for the numerator. Indeed, figure 2.4 illustrates this point.

To simulate the species transition from dangling to looped, a novel probability transition function is proposed. Considering the dynamics of micelle network formation, it is reasonable to assume dumbbells whose lengths tend toward zero have a higher likelihood of becoming loops, while longer dumbbells should have a very low probability of looping. This is because chains dangling from a micelle core should

be more likely to self-embed forming loops if they are close to their core. Moreover, these characteristics align with features of the dangling-to-looped approach used in Sing et al. The probability transition function for this is,

$$P_{D \rightarrow L}^* = 1 - \exp \left[-\frac{\chi Q(Q_{max} - Q)^2}{1 - (Q_{max} - Q)^2/Q_{max}^2} \Delta t \right]. \quad (2.8)$$

This formulation for the transition from a dangling to looped species closely mirrors the dangling-to-active transition making shorter dumbbells more likely to form loops and stretched dumbbells very unlikely to loop. Exactly mirroring the dangling-to-active transition calls for asymptotic growth as a dumbbell tends towards zero length. This was found to create too many loops in simulation and limited the dynamic behavior of the modelled polymer. To address this, the additional Q term was added. This term smooths the growth of the probability transition function as it tends towards zero and allows the maximum value to be adjusted through the parameter χ . We found that this construction allows for a wide range in the persistent number of loops present in simulations.

To accommodate all the possible outcomes for a dangling dumbbell we combine these two probability functions in the following scheme. Two random variables, X_1 and X_2 are drawn at each time step. Then they are compared to the computed probability values, $P_{D \rightarrow A}^*$ and $P_{D \rightarrow L}^*$ in the following way:

If $P_{D \rightarrow A}^* > X_1 \wedge P_{D \rightarrow L}^* < X_2$, then dangling species becomes active,

If $P_{D \rightarrow A}^* < X_1 \wedge P_{D \rightarrow L}^* > X_2$, then dangling species becomes looped,

else, remain dangling.

Formulating the approach in this way has the benefit of maintaining the underlying physical equations driving the creation of loops and active dumbbells segments.

2.3.3 LOOPED DUMBBELLS

Dumbbells in the looped state are given special consideration. In the looped state, the dumbbell does not change length or orientation as interactions with the fluid are considered negligibly small. Therefore, the only dynamic considered is the thermodynamically driven bond breakage that leads to a change in state to a dangling dumbbell ($L \rightarrow D$). Considering this, the transition probability function Eq. 2.6 describing bond detachment, simplifies to the expression,

$$P_{L \rightarrow D} = 1 - \exp[-\beta \Delta t]. \quad (2.9)$$

The parameter β governs the rate of dissociation of a polymer chain from a micelle core and is the same parameter used in the probability transition function for the transition from active to dangling. This construction matches the approach taken in Sing et al.

2.3.4 ADDITIONAL SPECIES TRANSITIONS REPRESENTATIONS

A visual representation is helpful for understanding how the transition probability functions affect each dumbbell. Figure 2.5 provides an illustration of the probability functions for $\alpha = 1.7$, $\beta = 8.7$, $\chi = 1.0$, $Q_{\max} = 33.3334$ and $\Delta t = 5e - 3$. In each plot, the x-axis is the spring length and the y-axis represents the probability of the shaded transition occurring. For example, looking at the center plot we see a dangling dumbbell with length 5, has roughly a 20% chance of becoming looped, a 70% chance of staying dangling, and a 10% chance of attaching to become active.

A single left stochastic matrix [18] can be used to represent all the species changes. First consider the following simplified representation of the above transition probability functions. Notice, that every term but the third, depends on the length of the dumbbell Q .

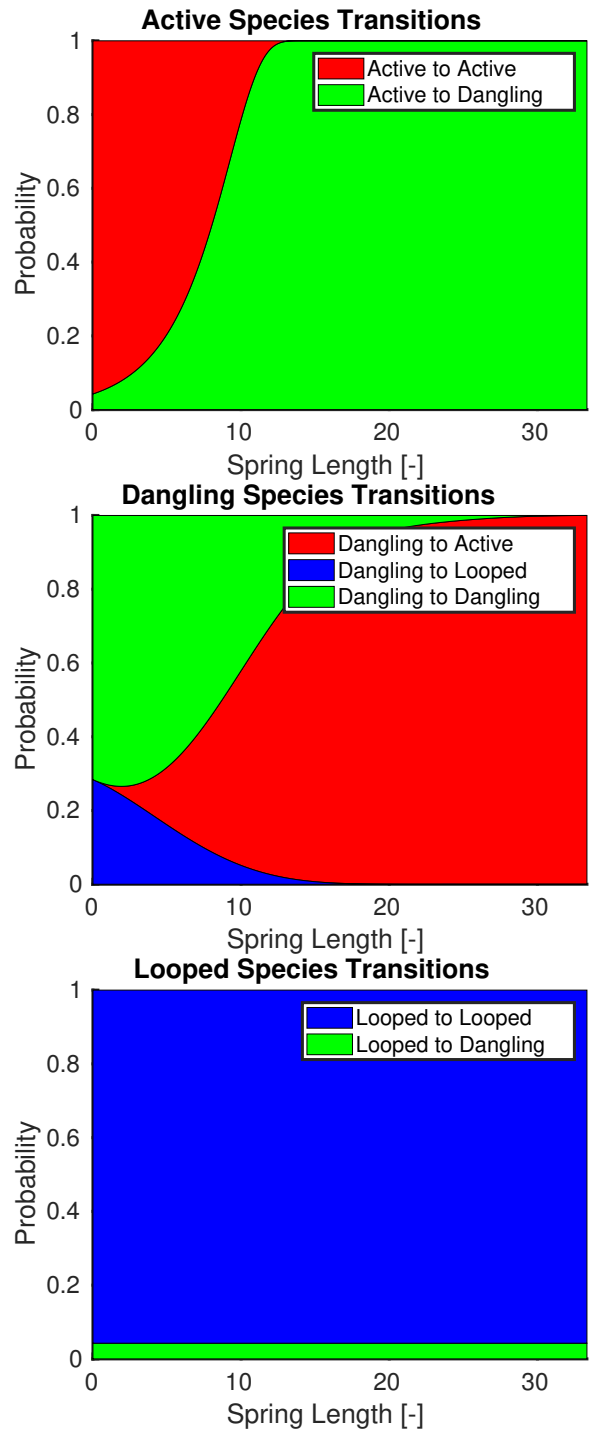


Figure 2.5: Transition probability functions. *Top*. Probability of transitioning from an active to dangling species type. *Center*. Probability of transitioning from a dangling species to either an active or looped type. *Bottom*. Probability of transitioning from a looped to dangling species type. *All*. Parameters used for the plots are $\alpha = 1.7$, $\beta = 8.7$, $\chi = 1.0$, $Q_{\max} = 33.3334$ and $\Delta t = 5e - 3$.

$$\alpha(Q) = \frac{\alpha Q^2}{1 - Q^2/Q_{max}^2} \quad (2.10)$$

$$\beta_A(Q) = \beta \exp \left(0.0325 \left| \frac{Q}{1 - Q^2/Q_{max}^2} \right| \right) \quad (2.11)$$

$$\beta_L(Q) = \beta \quad (2.12)$$

$$\chi(Q) = \frac{\chi Q(Q_{max} - Q)^2}{1 - (Q_{max} - Q)^2/Q_{max}^2} \quad (2.13)$$

Putting these expressions into a 3×3 matrix, we have

	Active	Dangling	Looped
Active	$e^{-\beta_A \Delta t}$	$(1 - e^{-\alpha \Delta t}) e^{-\chi \Delta t}$	0
Dangling	$1 - e^{-\beta_A \Delta t}$	$(1 - e^{-\alpha \Delta t}) (1 - e^{-\chi \Delta t})$ $+ e^{-\chi \Delta t} e^{-\alpha \Delta t}$	$1 - e^{-\beta_L \Delta t}$
Looped	0	$e^{-\alpha \Delta t} (1 - e^{-\chi \Delta t})$	$e^{-\beta_L \Delta t}$

The species along the top row indicate the current state, the column down the left side represents a transition to the named species. By the laws of probability, each column should sum to 1. For active and looped dumbbells, this is straight forward. For dangling dumbbells,

$$\begin{aligned} & (1 - e^{-\alpha \Delta t}) e^{-\chi \Delta t} + (1 - e^{-\alpha \Delta t}) (1 - e^{-\chi \Delta t}) + e^{-\chi \Delta t} e^{-\alpha \Delta t} + e^{-\alpha \Delta t} (1 - e^{-\chi \Delta t}) \\ &= e^{-\chi \Delta t} - e^{-(\alpha+\chi)\Delta t} + 1 - e^{-\alpha \Delta t} - e^{-\chi \Delta t} + 2e^{-(\alpha+\chi)\Delta t} + e^{-\alpha \Delta t} - e^{-(\alpha+\chi)\Delta t} \\ &= 1. \end{aligned}$$

2.4 ADDITIONAL EQUATIONS

The drag on an attached segment should differ from a segment with one end dangling freely. The proportionality constant, Z , serves this purpose. In contrast with

Hernández Cifre, we make no connection between state of the overall dumbbell population and this term as they found it had little influence on the viscosity curve. The approach we present here simplifies computational complexity and maximizes the potential for parallel computation. The result is,

$$\zeta_{node} = Z\zeta_{free}. \quad (2.14)$$

The total stress from the polymer chain network on the solvent is determined by Kramer's type expression [6]. Looped dumbbells are not considered to contribute to the fluid stress because they do not carry tension in the looped state [28]. However, their presence effects the number density of the chains in the solution, and therefore they are included in the count for the total number of dumbbells, N , in the simulation. This is in line with the approach taken by Sing et al. in [44]. The stress contribution σ is nondimensionalized by $k_B T n$, where n is the number density of polymer chains [15]. In non-dimensional form it is given by,

$$\sigma_{ij} = -\frac{2}{N} \left(\sum_{active} F(Q_i) Q_j + \sum_{dangling} F(Q_i) Q_j \right). \quad (2.15)$$

We follow viscosity, η and the first normal stress coefficient, Ψ_1 , as defined in [35]:

$$\eta = \frac{\sigma_{xy}}{\dot{\gamma}} \quad \Psi_1 = \frac{\sigma_{xx} - \sigma_{yy}}{\dot{\gamma}^2}.$$

2.4.1 NONDIMENSIONALIZATION

Equations are made nondimensional by the variables:

$$\tilde{t} = t \frac{\zeta_{free}}{4H} \quad \tilde{Q} = Q \sqrt{\frac{2k_B T}{H}} \quad \tilde{\sigma} = n k_B T \sigma.$$

Table 2.2: Model Parameters: Description and Values.

Parameter	Description	Simulated Values
α	Alters probability of attachment in the dangling to active species transition.	0.1-1000
β	Alters probability of detachment, from active to dangling, and looped to dangling species.	0.1-100
χ	Alters probability of looping attachment in dangling to looped species transition.	0.01-0.00015
B	Dimensionless characteristic bond length.	0.0325
Z	Balances the difference in drag between active and dangling dumbbells.	30
Q_{\max}	Maximum dumbbell length.	33.3334
ζ_{free}	Drag of a free dumbbell.	12
H	Spring Constant.	3

2.5 MODEL PARAMETERS

Although our model interpretation is straight forward it contains many parameters. Many of these parameters are representative of physical quantities and their values can thus be guided by measurement [23]. In this work, we focus on the default values used in Hernández Cifre [22] for Z , Q_{\max} , ζ_{free} and H . The choice of the value of B is discussed above in section 2.3.1. Some parameters, such as those modifying the attachment detachment and looping probabilities, are more abstract in nature and are explored in our results. Descriptions and values for each parameter are listed in table 2.2.

CHAPTER 3

SIMULATION METHOD

3.1 BRIEF OVERVIEW

Each dumbbell's configuration and state are computed in parallel on graphical processing units (GPUs). A semi-implicit first order method evolves the stochastic differential equation 2.1 ensuring that dumbbells do not exceed their maximum length [40]. At each time step, dumbbell configurations evolve according the SDE and species type, probability transition values are computed and species types are altered appropriately. At regular intervals the configuration and type are used to calculate the fluid stress response. All simulations presented in this work contain 1024000 dumbbells. Simulations are run until a steady state is achieved which was determined by a combination of visual and analytical inspection. For simple shear flow, the final value is a mean over the steady state time period. For oscillatory flows, viscous and elastic coefficients are fitted to the steady state period using MATLAB's fit functions. For large amplitude oscillatory flow, the software MITLaos [17] is used to determine the dynamic moduli and higher harmonics present in nonlinear rheological measurements. Based on the Fourier transform spectrum, a technique described in [58, 59, 27], valid harmonics are identified from stochastic noise, and higher harmonics are filtered to improve clarity.

3.2 CODING FOR THE HIGH PERFORMANCE COMPUTING ENVIRONMENT

The programming scope of this project and fits squarely into the realm of Big Data. Big Data is defined as, “Information assets characterized by such a high volume, velocity and variety to require specific technology and analytical methods for its transformation into value”[13]. In this project, over one million dumbbells are simulated to provide clear results from the stochastic differential equations describing them; fulfilling the volume requirement. Second, in order to do this efficiently, parallel computation is written in CUDA C. This involves developing an understanding of the memory and executable hardware architecture [11]. Moreover, the scale necessitates moving to a high performance computing (HPC) cluster where GPU accelerators and file storage systems can process and store the large amounts of data produced. These are the specific technological requirements. Finally, a second set of MATLAB codes is used to analyze the data and produce useful information. Together these tools form the complex workflow necessary for Big Data. Indeed, the results achieved in this project are not currently possible with routine coding methods and computation platforms.

The simulation code consists of about 3400 lines of CUDA C. The cuRAND library is used to generate random numbers on the GPU [36]. Beyond this however, no special packages or libraries are employed. The main execution code follows a macro-micro loop design, macro for the CPU and micro for the GPU (See Figure 3.1). The main execution loop is as follows: Code on the CPU sends a full set of the dumbbell data to the GPU to be evolved for a set number of time steps; The GPU evolves each dumbbell the set amount of times in parallel and then returns the data back to the CPU; The new configuration is recorded by the CPU and the old is updated; The loop repeats until the desired time is reached. At the end of the simulation only the configurations recorded on the CPU are written to the csv file for output. The upshot of this arrangement is that it avoids sending large amounts of data between

the CPU and GPU allowing for efficient computation. However, the downside is that configuration changes on the GPU are not recorded.

In certain configurations the simulation code can quickly produce large amount of data. At 20 bytes of data per dumbbell per time step its easy to see how 102400 dumbbells quickly add-up over the course of simulations which have an average of 10^8 time steps (That's 2048T of data from a single run). The macro-micro loop itself helps to limit the data size, however, it alone is not enough. In order to manage and derive information from the output much of the analysis revolves around metadata, such as the calculated stress, average lengths, average angle variance, etc. These results are stored in the output csv file. When the configuration of every dumbbell is needed, this is done at specific intervals and over time periods of interest, such as the steady state. This type of data was used to create figures such as the dumbbell configuration histograms in figure 4.15 for example. It is also possible to track every change of a single dumbbell as is displayed in figure 4.16. Enabling these features results in a bin file which is produced concurrently with the csv output.

Simulations where run in batches on multi-code nodes with Nvidia Tesla M2090, K80 and P100 GPU Accelerators. Since the memory footprint on the GPU is small, and the CPU core is usually fully utilized multiple simulations were run simultaneously depending on the environment. The table 3.1 lists the CPU-GPU combinations used in this work. Simulations were found to run significantly faster when writing to local storage. For certain file systems, not writing to local storage was enough to slow down a large cluster, and therefore care should be exercised if this is the case. Computation time ranges from mins to days depending on simulation parameters, with low flow rate steady shear flow and high frequency SAOS requiring the most time. Improving code performance beyond usable runtimes was not the primary concern of this work, and thus there are many areas for improvement.

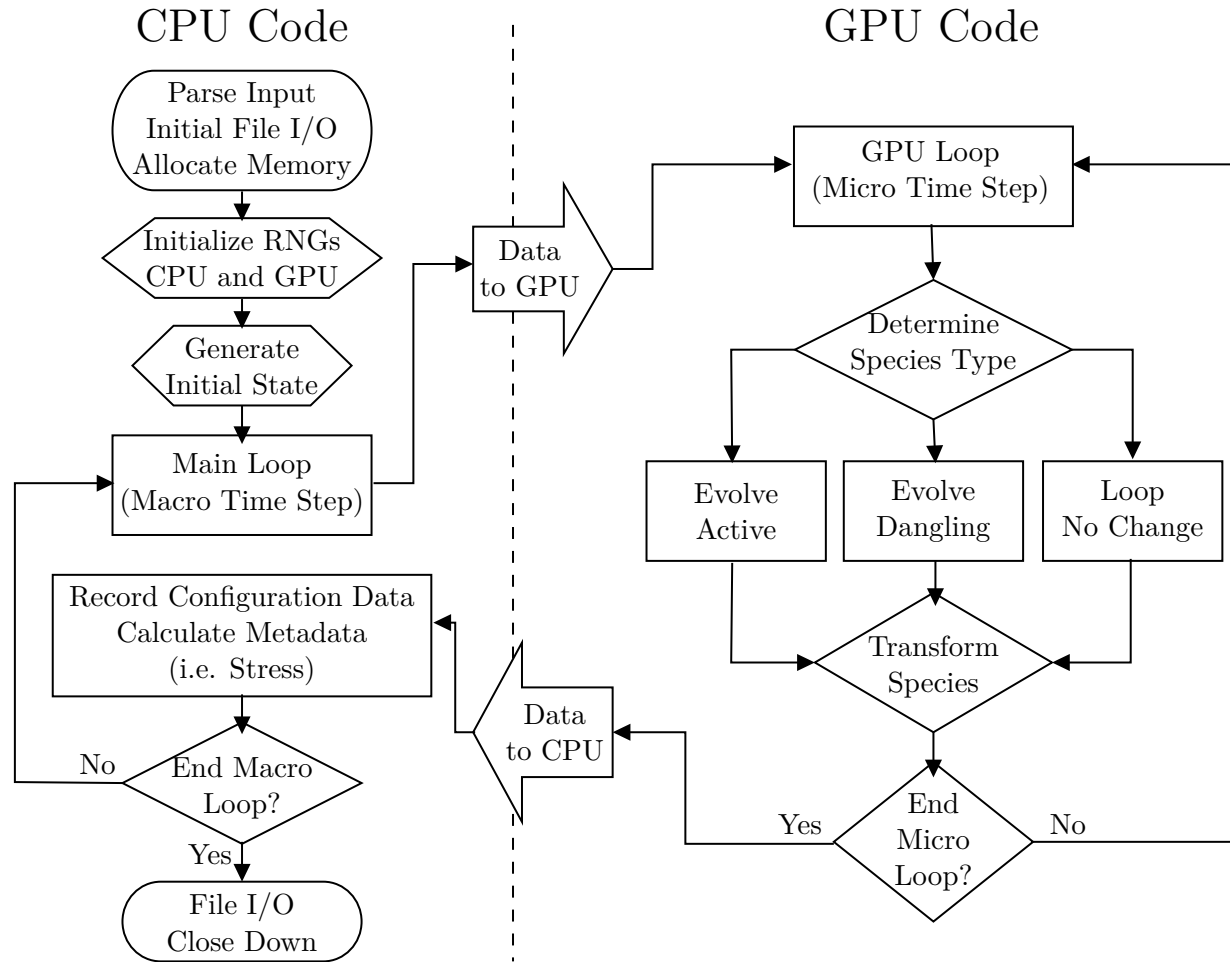


Figure 3.1: Code flow chart. The design of the code can be divided into CPU (left) and GPU (right) parts. Sending data between the CPU and GPU is a time intensive operation. The loop on the GPU represents a single thread and is run independently for each of the 1024000 dumbbells in the simulation. The term ‘RNG’ refers to random number generator.

Table 3.1: Table of computation environments and run combinations. The code has a small memory footprint on the GPU but fully utilizes the CPU core. Therefore, to saturate the hardware, multiple runs were executed simultaneously.

CPU	GPU	Number of Simultaneous Simulations
Intel Xeon X5660 @2.8GHz	Nvidia Tesla M2090	1
Intel Xeon E5-2620 v3 @2.4GHz	Nvidia Tesla K80	4 (2 per GPU core)
Intel Xeon E5-2680 v4 @2.4Ghz	Nvidia Tesla P100	3

3.3 STRAIN SIMULATIONS

The main body of this work is concerned with modelling two small strain experiments used in rheology; both of which are well established [31, 6, 35]. The first is steady shear flow. In steady shear flow simulations, a shear rate proportional to the vertical displacement imposes a force on each dumbbell. This simulates strain imposed via drag on the polymer network by the fluid flow that results from a sliding top plate moving in a single direction. For each steady shear flow simulation, the system is allowed to equilibrate at zero shear rate flow for 100s of non-dimensional time. Then the shear rate is imposed at the prescribed rate. This protocol was followed for each run although in practice it was not shown to affect the steady state stress response. The measured stress values used in the simulations are the result of an average taken over the final period of the steady state that was verified visually; typically the last 10% of simulated flow time. Figure 3.2 shows the output from a steady shear simulation.

The second simulated type of flow is small amplitude oscillatory shear (SAOS).

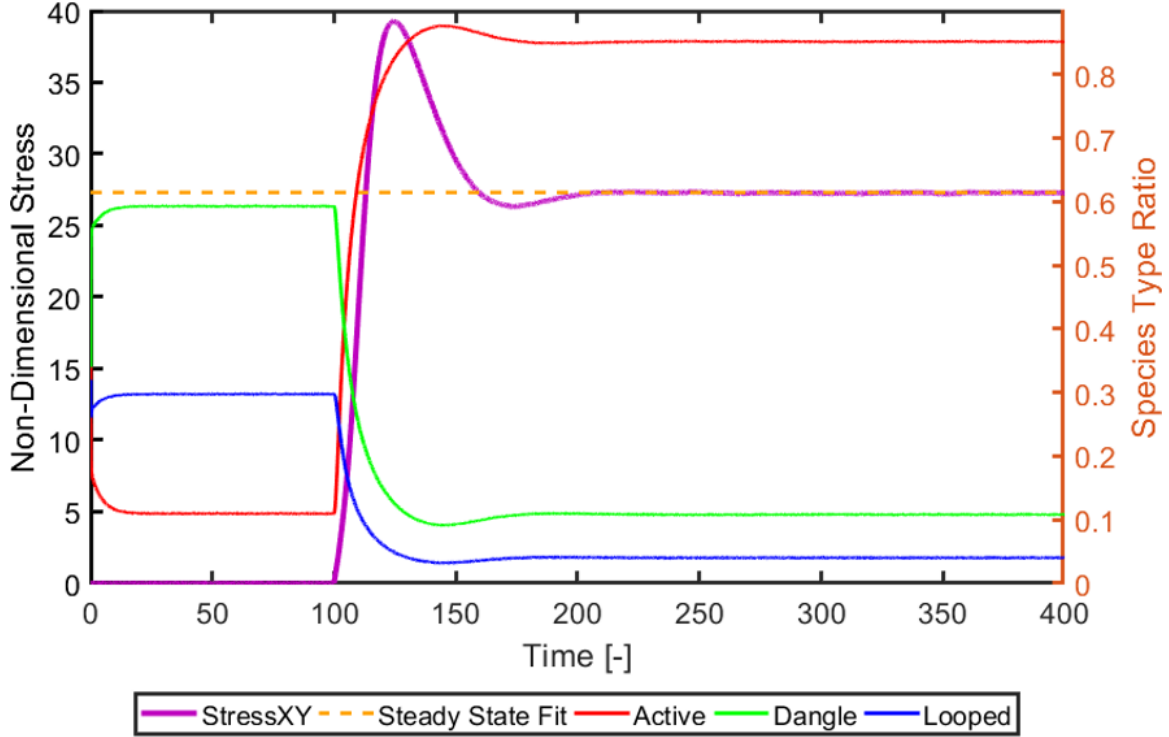


Figure 3.2: Plot of a typical steady shear flow simulation. The left axis shows the stress response, σ_{xy} , versus time. The right axis indicates the fraction of each species type. The system is allowed to equilibrate with zero flow until $t = 100$ then the flow is imposed. The dashed line indicates the steady state stress value measured as an average over the last 10% of simulated flow time.

Small amplitude oscillatory shear differs from steady shear in that imposed strain varies sinusoidally in time. This imposed strain is written as $\gamma = \gamma_0 \sin(\omega t)$, where ω is in radians per second. In these simulations, the viscoelastic moduli are calculated from the stress over a range of oscillation frequencies ω for a fixed strain amplitude, γ_0 . The stress response is decomposed into in-phase and out-of-phase components, $G'(\omega)$ and $G''(\omega)$, the storage or elastic modulus and the loss or viscous modulus, respectively. In our simulations, these coefficients are determined by fitting the steady state period (typically the last 25%) to the expression, $G' \gamma_0 \sin(\omega t) + G'' \gamma_0 \cos(\omega t)$, using the default fit routine in MATLAB. Figure 3.3 illustrates the performance of the curve fitting. The value of γ_0 is often described vaguely as “small enough” or $\gamma_0 \ll 1$ [31]. Based on Ewoldt [16], we use $\gamma_0 = 0.5$, and verify visually that the ratio

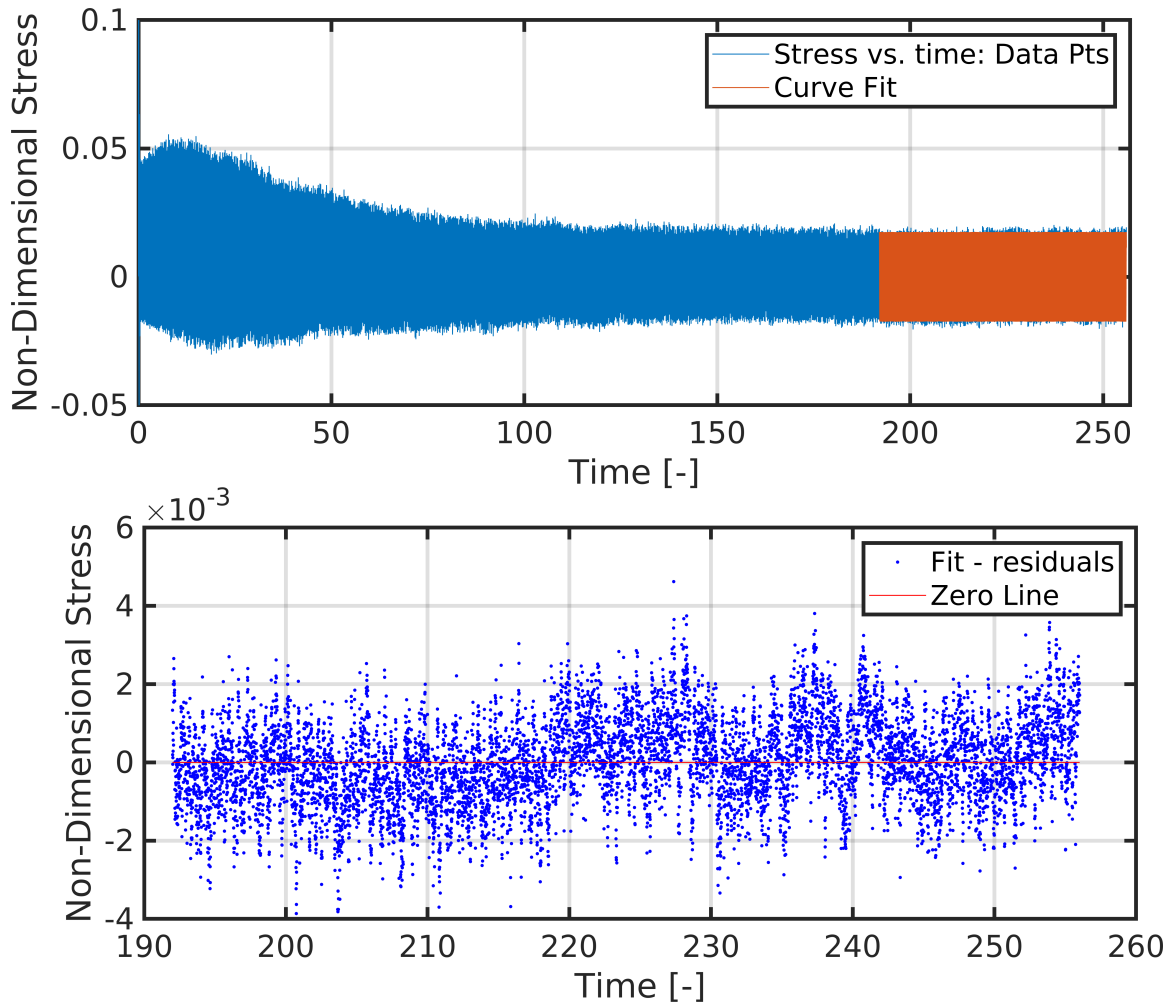


Figure 3.3: Figure illustrating the fitting of the coefficients of $G'\gamma_0 \sin(\omega t) + G''\gamma_0 \cos(\omega t)$ to the stress response of a SAOS simulation. The top plot shows the simulated stress response. The red curve is the fitted expression over the steady state period. The lower plot indicates the error between each data point and the computed curve.

of the third harmonic to the first is much less than one ($e_3/e_1 \ll 1$, in their notation) to ensure simulations are within the linear regime and thus qualify as small strain. This was visually verified for each SAOS simulation output using the plot seen in figure 3.4 that shows the Fourier transform of the stress from the steady state of a SAOS simulation.

Large amplitude oscillatory shear (LAOS) simulations differ from SAOS in only that the strain amplitude γ_0 is increased. For large enough γ_0 the stress signature

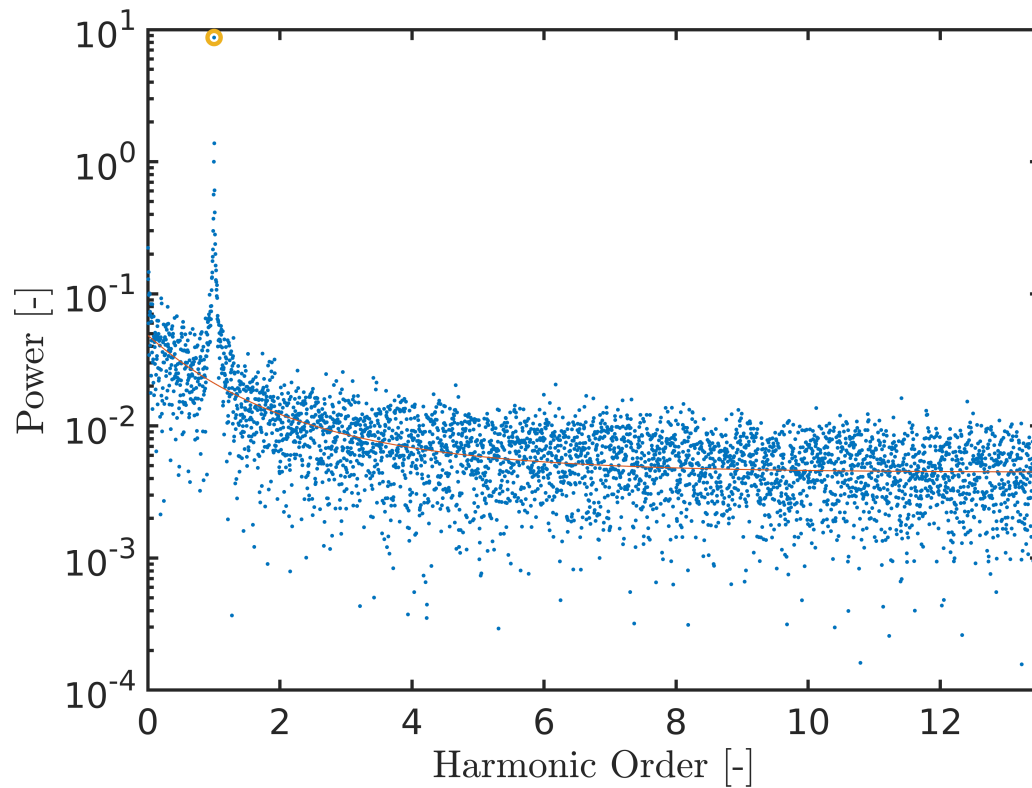


Figure 3.4: Plot showing the Fourier transform of the stress response from a SAOS simulation. The single peak at 1 indicates there is only a clear first harmonic present and thus this response should be considered within the linear regime.

contains multiple harmonics indicating entrance into the nonlinear viscoelastic regime [16]. A plot showing the multiple harmonics can be see in figure 3.5. A short MATLAB routine automatically identifies the largest harmonic and feeds the information to the MITLaos software where higher harmonics are filtered to smooth the output. The yellow circles indicate harmonics identified by the routine. Output from the steady state of LAOS simulations is analyzed via the MITLaos software [17]. MITLaos was used to construct the viscous and elastic Lissajous-Bowditch curves used in the Pipkin diagrams in figures 4.19 and 4.20 in section 4.4.

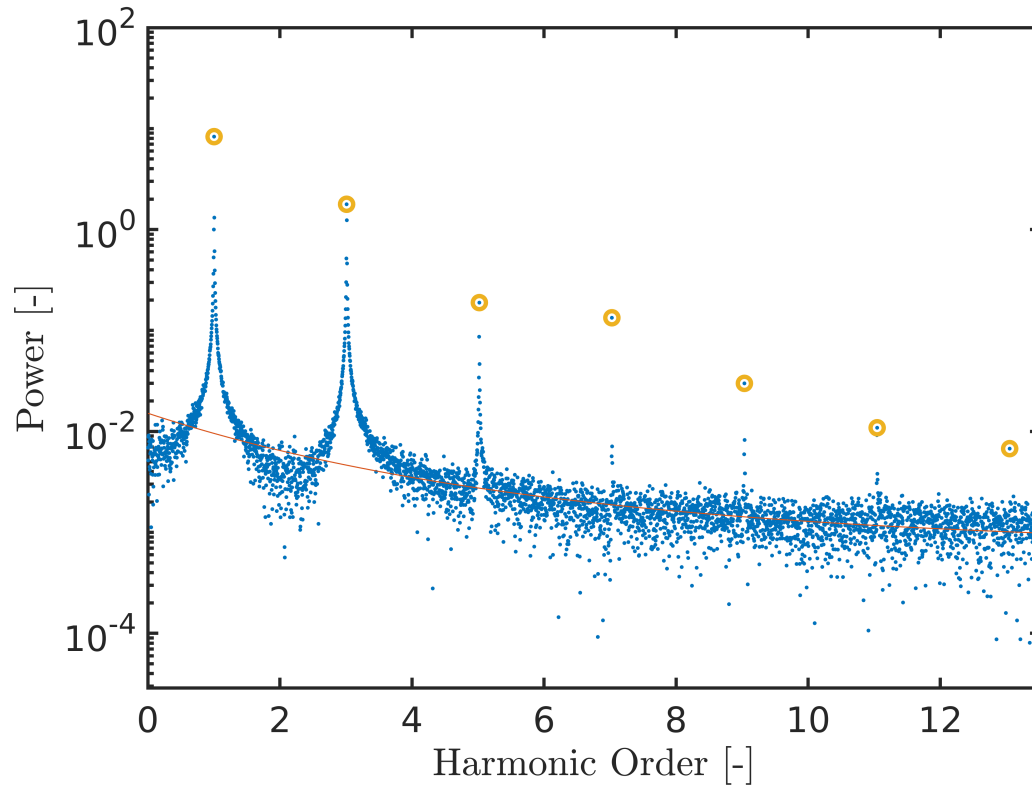


Figure 3.5: Plot showing the Fourier transform of the simulated stress response from a LAOS plot. The multiple peaks indicate additional harmonics present in the stress response. Harmonics automatically identified by the MATLAB routine are identified with a yellow circle.

3.4 UNCERTAINTY QUANTIFICATION

In stochastic simulation, it is best practice to indicate uncertainty in simulated values and provide an explanation of the “error bar” representation employed [21, 7]. However, the simulated values in the results section of this work do not contain error bars. The reason is that in our statistic simulations, the variation between runs was small enough that including representations of the uncertainty did not add to understanding in the presentation. The purpose of this section is therefore to accurately represent the uncertainty in our simulated values with analysis and figures purposed for the task.

Two example analyses of uncertainty in simulated values are included here; one

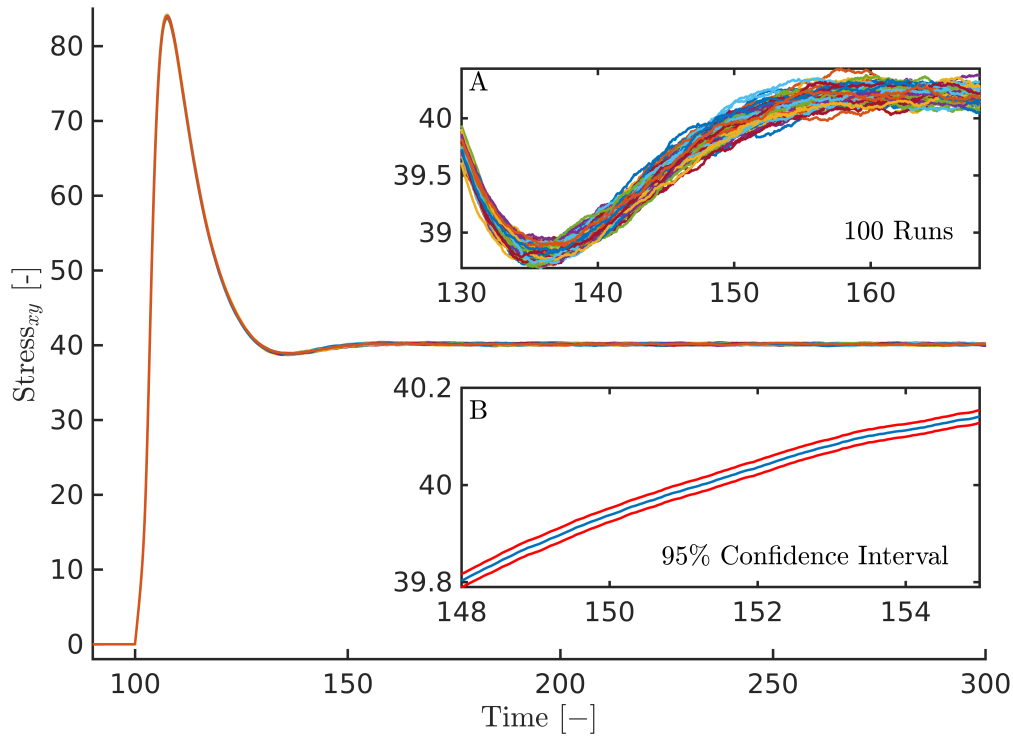


Figure 3.6: Figure showing the stress response from 100 steady shear simulations. The largest plot shows the full runtime of a collection of 100 simulations. Insert A is an enlarged view of the transient period where variations are largest. Insert B is a plot of the 95% confidence interval. These areas were enlarged to highlight the variation between simulations.

for steady shear and one for SAOS flow. Each example includes 100 runs with randomly generated initial states. The initial state consists of x and y lengths of each dumbbell randomly chosen from a normal distribution. Dumbbells assigned lengths longer than the maximum were reinitialized. Time was used to seed random number generation and efforts were made to avoid running multiple simulations at the same time. Confidence intervals (95%) were computed via established methods [21] and are illustrated in figures 3.6 and 3.7. It is important to note that while transient behavior is examined in these figures, only steady state measures were used elsewhere in this work. The uncertainty of these measures as it pertains to these two examples is described in table 3.2.

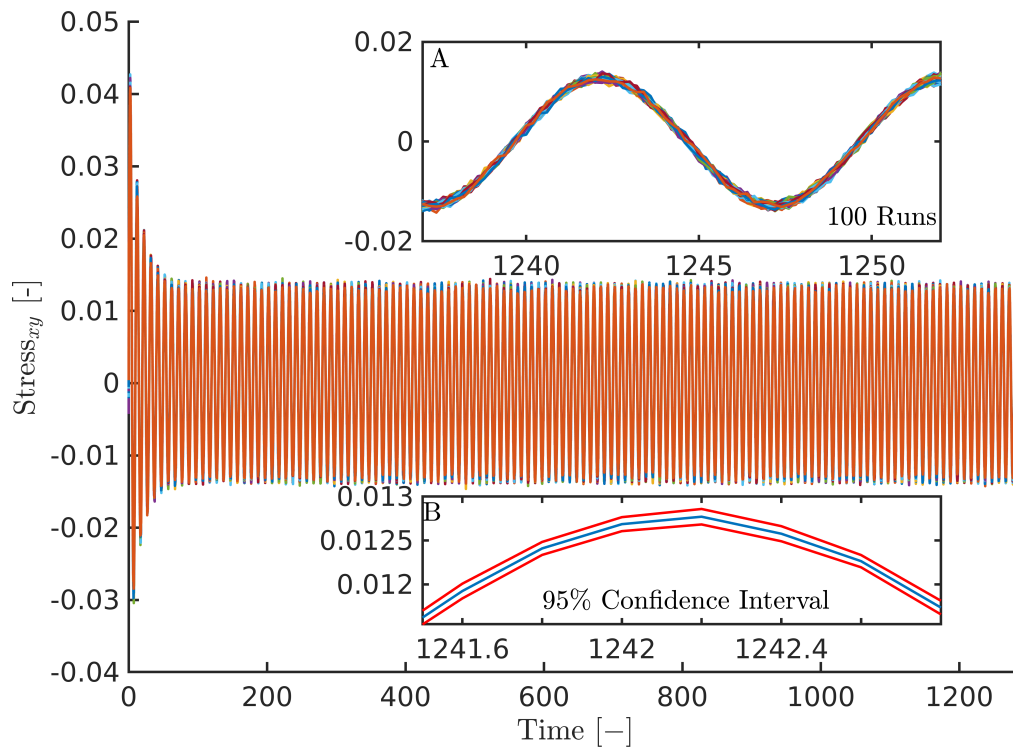


Figure 3.7: Figure showing the stress response from 100 SAOS simulations. The largest plot shows the full runtime of a collection of 100 simulations. Insert A is an enlarged view of a selected time period. Insert B is a plot of the 95% confidence interval. These areas were enlarged to highlight the variation between simulations.

By examining the figures and data above we can draw a few conclusions about the significance of simulated values from the model. Transient behavior was included in these examples because it is expected to show larger variations since the modelled system is out of equilibrium. However, both figures show that every simulation captured important features such as ringing in steady shear, decreasing stress amplitude in SAOS, and similar start times to the steady state period. Moreover, the quantitative difference in these features was small, indicating that there is very good agreement between multiple runs of the same simulation parameters. For the more robust steady state measures used in the results section, such as stress in the xy direction (σ_{xy}) and G' and G'' , variation between runs was even more diminished. The small size of the confidence intervals indicates that computed values are close to

Table 3.2: Uncertainty in the steady state values from examples seen in figures 3.6 and 3.7.

Simulation	Computed Quantity	Mean	95% Confidence Interval	Standard Deviation	Figure
Steady Shear	σ_{xy}	40.1427	± 0.0062	0.0313	3.6
SAOS	G'	0.0250	$\pm 8.5167 \times 10^{-6}$	4.2922×10^{-5}	3.7
SAOS	G''	0.0053	$\pm 7.7415 \times 10^{-6}$	3.9015×10^{-5}	3.7

what would be expected in large systems of polymer chains. The standard deviation gives an estimate of how close we can expect the computed value from a single run to be to the mean of multiple runs. Indeed, the standard deviations for these values are small enough that we can be confident in the qualitative conclusions drawn from single runs in this work.

CHAPTER 4

RESULTS

This chapters presents results obtained using the model. This includes two and three species simulations for steady shear flows. A comparison of SAOS output with two and three species. In addition, two methods for determining the configuration of a dangling dumbbell after being looped are compared. Finally, results from LAOS simulations are showcased.

4.1 SIMPLE SHEAR

Simple shear experiments introduce a deformation flow parallel to the bottom of the fluid cell at a steady rate. This type of flow is also referred to as steady shear, sliding plate or Couette shearing flow. The velocity gradient is prescribed as,

$$\nabla v = \begin{bmatrix} 0 & 0 \\ \dot{\gamma}_0 & 0 \end{bmatrix} \quad (4.1)$$

In the presentation herein, we set $\kappa = (\nabla v)^T$. For each experiment the system is given time to equilibrate before flow starts. Then viscosity and the first normal stress coefficient are measured once a steady state is achieved.

Complex fluids can be categorized by their fluid response. In pure viscous fluids, the stress response decreases with increasing flow rate. This phenomena is called shear thinning. In an elastic material, the stress response increases with increasing shear deformation. Fluids that increases their stress response with increasing shear rate are called shear-thickening. The focus of this work is simulating the fluid response of

a viscoelastic fluid, where a combination of shear thinning and shear thickening can be present.

Another method of categorizing complex fluids is to separate Newtonian and non-Newtonian. Two important characteristics of the latter fluid are; the fluid's viscosity does not increase proportionally with the rate of shear strain, and a positive normal stress coefficient. The non-Newtonian category incorporates viscoelastic fluids that exhibit shear thinning or shear thickening, and thus could be used to describe the scope of fluids simulated by this model as well.

In simple shear experiments, parameters describing individual dumbbell properties adopt the default values listed in table 2.2. Parameters that alter the species transition behavior (α, β, χ) were varied, and viscosity was examined.

4.1.1 TWO SPECIES SIMPLE SHEAR

In a two species simulation, containing only active and dangling dumbbells, we find that shear thickening or shear thinning behavior can be altered by modifying either or both attachment or detachment mechanics. Consider the plot for $\alpha = 10$ and $\beta = 10$ in the center of Figure 4.1. By increasing the probability of attachment so that $\alpha = 100$ and $\beta = 10$, we can see from the run in the left plot, that the amount of shear thickening decreases and the amount of shear thinning increases. Conversely, if we increase the detachment parameter so that $\alpha = 10$ and $\beta = 100$, we find in the plot on the right that the amount of shear thickening increases. These two parameters can be combined into a ratio which determines the fluid response as shown in 4.1.

Our simulations indicate that shear thickening and shear thinning behavior is caused by the interplay of attached and dangling network segments. These are shown in the species fraction plots in 4.2. At low flow rates when number attachments in the network is high relative to the number of dangling, less shear thickening occurs as the flow rate increases. This is because the length of active dumbbells increases

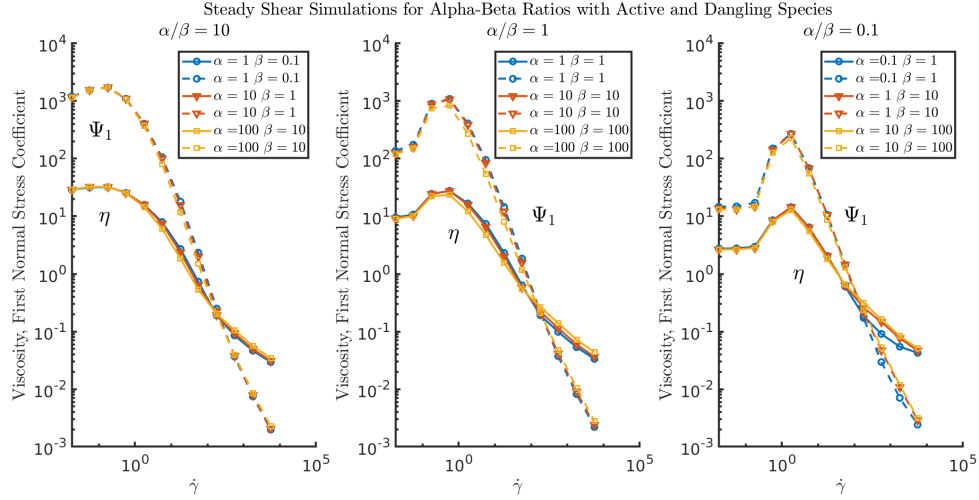


Figure 4.1: Viscosity η and First Normal Stress Coefficient Ψ_1 for steady shear flow simulations of a two species model. Each plot contains a single α/β ratio.

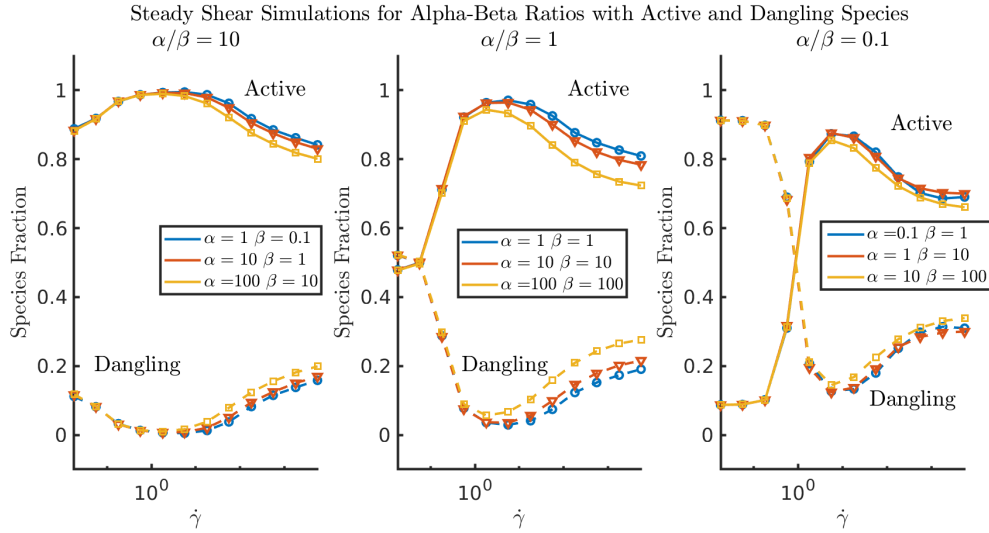


Figure 4.2: Species fractions in shear flow. Plots show the steady state species fraction of each type, active and dangling, for the simple shear simulations in 4.1.

proportionately with the flow rate. Therefore, when a large number of segments are already attached, their length grows and few species changes occur. The period of shear thinning that follows, is the result of length growing and dumbbells detaching to a dangling state where they are more likely to reduce length. This behavior is the result of having a detachment probability that depends on the length of the dumbbell.

Shear thickening is achieved in the model by our choice of attachment probability.

For simulations where the ratio of alpha to beta is near 1, there are a number of dangling segments available to attach at low flow rates. As flow rates increase, they lengthen and as a result of the form of the dangling-to-attached probability function, increasing numbers of dangling dumbbells change species to active and remain in an extended state. When the flow rate increases to the point where active dumbbells extend and break, transitioning back to dangling dumbbells, shear thinning appears.

A short mathematical analysis provides some insight into the α/β ratio control over shear thickening and shear thinning. To more easily make sense of the complex dynamics, let $F(Q)$ be an arbitrary function of the spring length and consider the simplified representation of the transition probability functions:

$$P_{Dangling \rightarrow Active} = 1 - \exp(-\alpha F(Q) \Delta t) \quad (4.2)$$

$$P_{Active \rightarrow Dangling} = 1 - \exp(-\beta F(Q) \Delta t) \quad (4.3)$$

For each length of spring Q the function of $F(Q)$ has a fixed value. After choosing values for α , β and Δt the value of the transition probability functions are fixed as well. In this way, the probability of being in one state or the other is set. Now, because the dumbbells transition from active to dangling and dangling to active, altering either α or β , shifts this preference. Therefore, the ratio $\frac{\alpha}{\beta}$ describes the relative difference in preference at any dumbbell length. Considering all the dumbbells in the simulation we see the ratios influences the species fractions of active and dangling species which thus influences the amount of shear thinning and shear thickening seen in the simulations.

Traditional network theory has placed a lot of focus on the attachment and detachment probabilities [51]. Many approaches are based on the Leonard-Jones electric potential in bond forming and breaking. Indeed, in Hernández Cifre, the association energy affects both the attachment and detachment of dumbbells. In our approach,

we posit that the probability of dumbbell attachment has more to do with the physical space explored by an unattached end, then the electro-chemical potential of the bond to be formed. For detachment, we reason that overcoming the energy barrier to break the bond is a greater factor. In combination, we show that these two mechanics are each individually able to influence shear-thinning and shear-thickening behavior in steady shear flow. By delinking these processes, we give our model the ability to better simulate tunable polymer experiments that modify bond attachment and detachment independently, such as in several recent works [26, 10].

4.1.2 THREE SPECIES SIMPLE SHEAR

In three species simple shear simulations we incorporate a third dumbbell species—loops. This looped species is assumed to have negligible interaction with the fluid flow and does not contribute to the stress. Including the third species, however, modifies the amount of shear thickening and shear thinning and thus breaks the α/β ratio symmetry seen in the two species simulations.

In three species simulations we find the behavior of the viscosity and the first normal stress coefficient is controlled by the two ratios, α/β and χ/β . In figure 4.3, these correspond with changes in the vertical direction and changes in the horizontal direction respectively. We see that increasing the looping ratio, χ/β , leads to increased shear thickening when there are a moderate number of active dumbbells. The number of active dumbbells in the simulation increases with a larger attachment ratio, α/β , and leads to less shear thickening and more shear thinning. At low flow rates, a higher fraction of active dumbbells increases the fluid stress response. As flow rates increase, the amount of shear thickening depends on how many loops are in the system. When flow rates increase over a rate of $\dot{\gamma} > 1.8$ all simulations show shear thinning.

By examining figure 4.3 we can identify several trends in the model. Starting

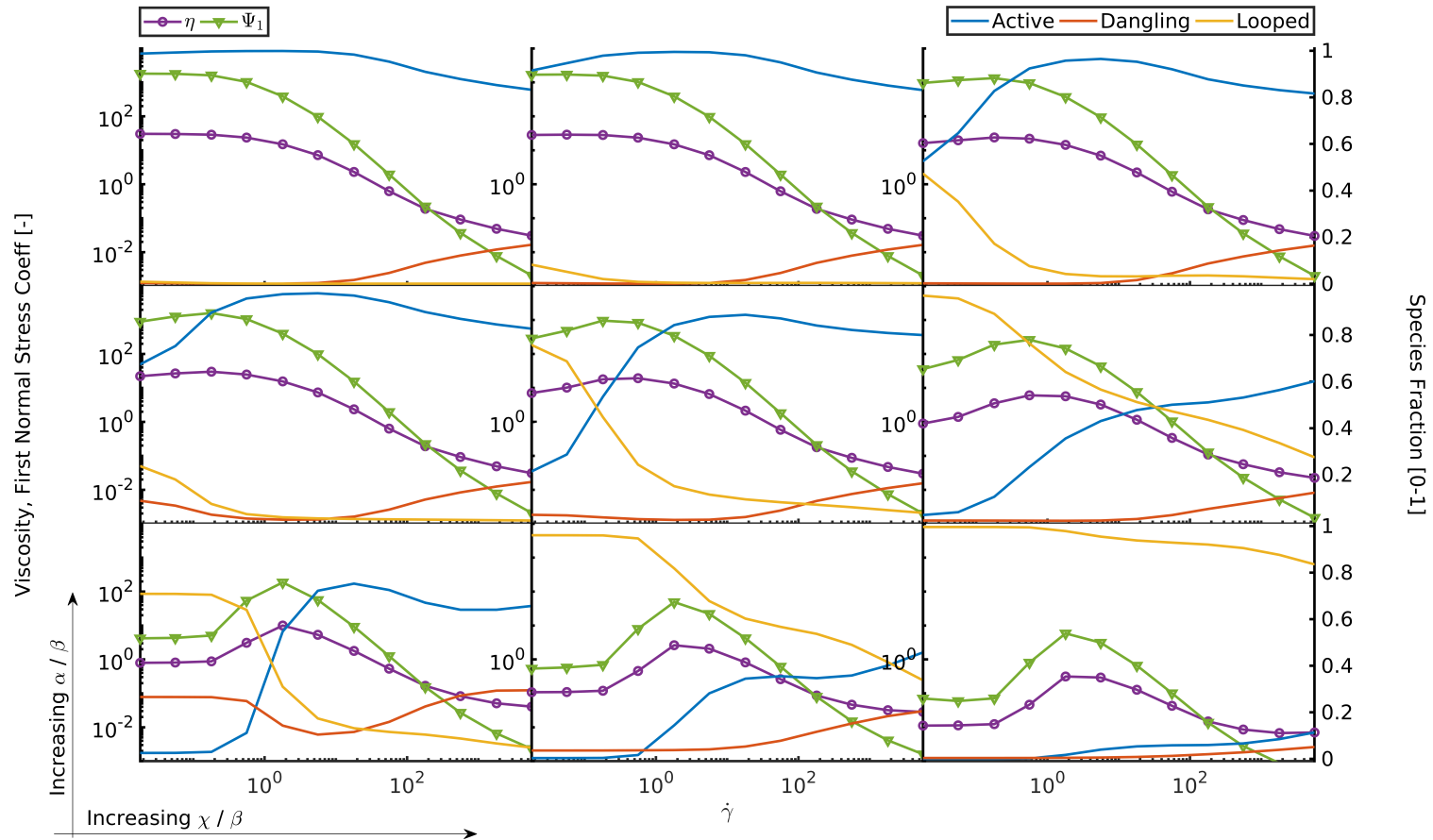


Figure 4.3: Three species steady shear flow simulations. Plot shows steady state viscosity η and first normal coefficient Ψ_1 , organized by attachment, α/β , and looping, β/χ , ratios. The α/β ratio increases in the upward direction and the β/χ ratio increases left to right.

with the plot in the top left, there are a large amount of bridged segments and fewer dangling and looped. We could say that this is a polymer network with many interconnections and few loops. When flow rates increase the model shows shear-thinning with flow increase. For the plot in lower right, we have a large number of loops occurring in the network. The model shows a much reduced stress response, but still has shear thickening followed by shear thinning. Indeed, we see that as the flow rate increases, there are more dangling and active chains. This would correspond to the loops breaking out of the micelle formation and dangling or forming connections. Then because the rate of attachment is low, the amount of stress from dangling and active dumbbells extending with the fluid does not increase linearly.

On the other two extremes, we have the example in the top right. This shows a large number of attachments and loops in the network, but few dangling dumbbells that would form connections. In this case, any loops are quickly transitioning to active dumbbells as the flow increases. The result is a shear-thinning response. In the lower left, we see that the looped dumbbells enhanced the shear-thickening response. Without loops, the increase in flow rate and shift between active and dangling dumbbells is enough to generate shear thickening. When loops are added, they lower the fluid stress at low flow rates even further. Then like dangling dumbbells, the number of loops drops due to fluid extension. In contrast to dangling dumbbells, loops however do not again increase as chains extend and break in high rate flow.

THREE SPECIES DISSYMMETRY

In the two species model presented in 4.1.1, the fluid response was controlled by the ratio α/β . This is also true for χ/β when only looping and dangling species are present, as is shown in figure 4.4. However, when these two are combined into one three species model the symmetries are broken. The diagram in figure 4.5 provides a visual guide to the dynamics that lead to this phenomenon. Each circle in the diagram

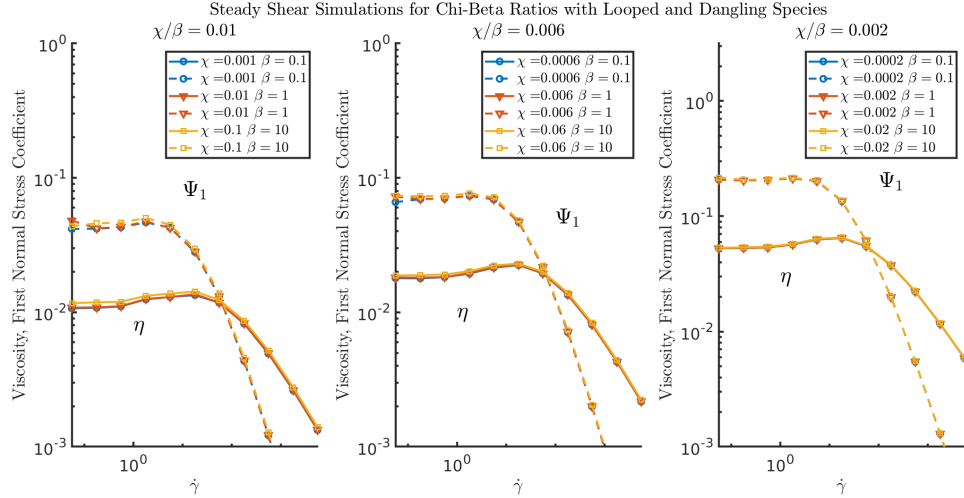


Figure 4.4: Two species, dangling and looped, steady shear flow simulations. Plots show the viscosity η and first normal stress coefficient Ψ_1 . Each plot shows the result of three data sets with the same χ/β ratio.

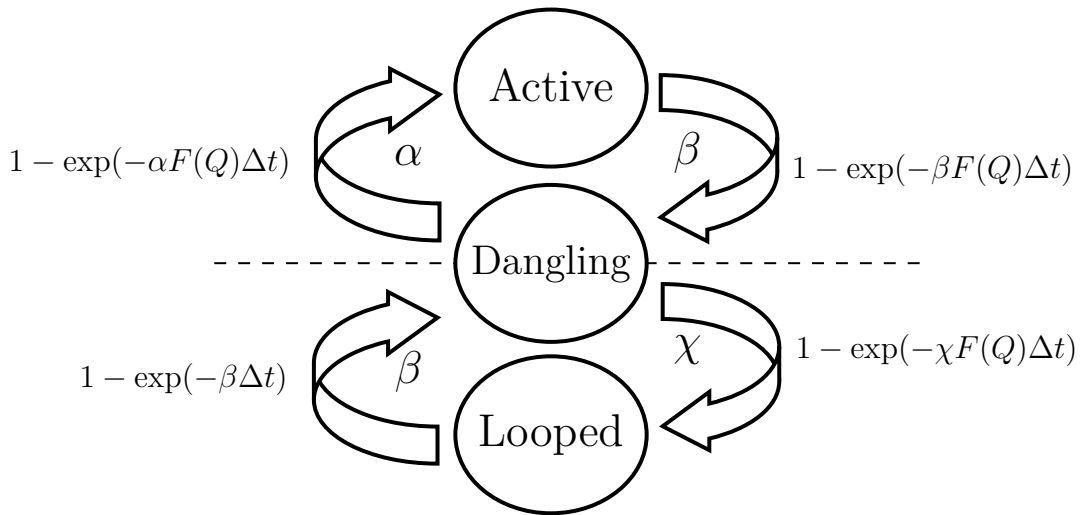


Figure 4.5: Dumbbell species transition diagram. Equations are simplified in that $F(Q)$ represents different functions of the length of a dumbbell, Q . Each ellipse represents a species type. Each arrow represents a species transition and is labeled with the parameter that affects the transition probability. In the two species model, only the area above the dashed line is considered. In the three-species model, the entire diagram is considered.

represents a species type, dumbbell transitions are indicated by arrows between them, the equations on the side are simplified representations of the transition probabilities functions and the parameter is the one associated with each transition.

In steady state, we found species fractions remain constant. Therefore, there are

a balanced number of dumbbells entering and exiting each species type. In the two species model, this balance exists between the active and dangling dumbbells and thus between the parameters α and β . This is also true for χ and β . When the two two species models are combined into a three model, because species fractions are constant in the steady state, there must be a balance between all three types. Since the dumbbells are now distributed among three types, and dangling dumbbells transition to active or loops, the original balances are upset.

These effects can be clearly seen by comparing the two species model to the behavior of the active and dangling dumbbells in the three species model as is done in figure refDissymmetry. Each plot in the figure has the same alpha-beta ratio. The top row does not contain loops, and therefore the flow curves show very similar behavior. Introducing loops with $\chi = 0.001$ immediately breaks the symmetry across the second row. This is because the beta-chi ratios are different.

By construction, only dangling dumbbells form loops in the simulation. This behavior means that the inclusion of loops has different effects on the fluid response depending on the fraction of dangling dumbbells in the simulation. Therefore, when flow rates are low dumbbells are less extended and we find an abundance of dangling dumbbells. Because there are more dangling dumbbells at shorter lengths, there are more dumbbells that will become looped. The presence of a higher fraction of loops in the simulation leads to lower overall fluid stresses. As the flow rate increases, dumbbells extend and fewer dangling dumbbells become looped. The overall effect is that shear thickening is more pronounced when loops are included.

In general, we find that by adjusting the likelihood of bridging in relation to the likelihood of disassociating via the α/β ratio, it is possible to control the fluid response. In addition, the ratio between the likelihood of looping and breaking out of the looped state enhances the nonlinear response. In this sense, in a polymer where loops are largely present, and endgroups are reluctant to disassociate we should see

Transition Function Parameter Dissymmetry in Three Species Model

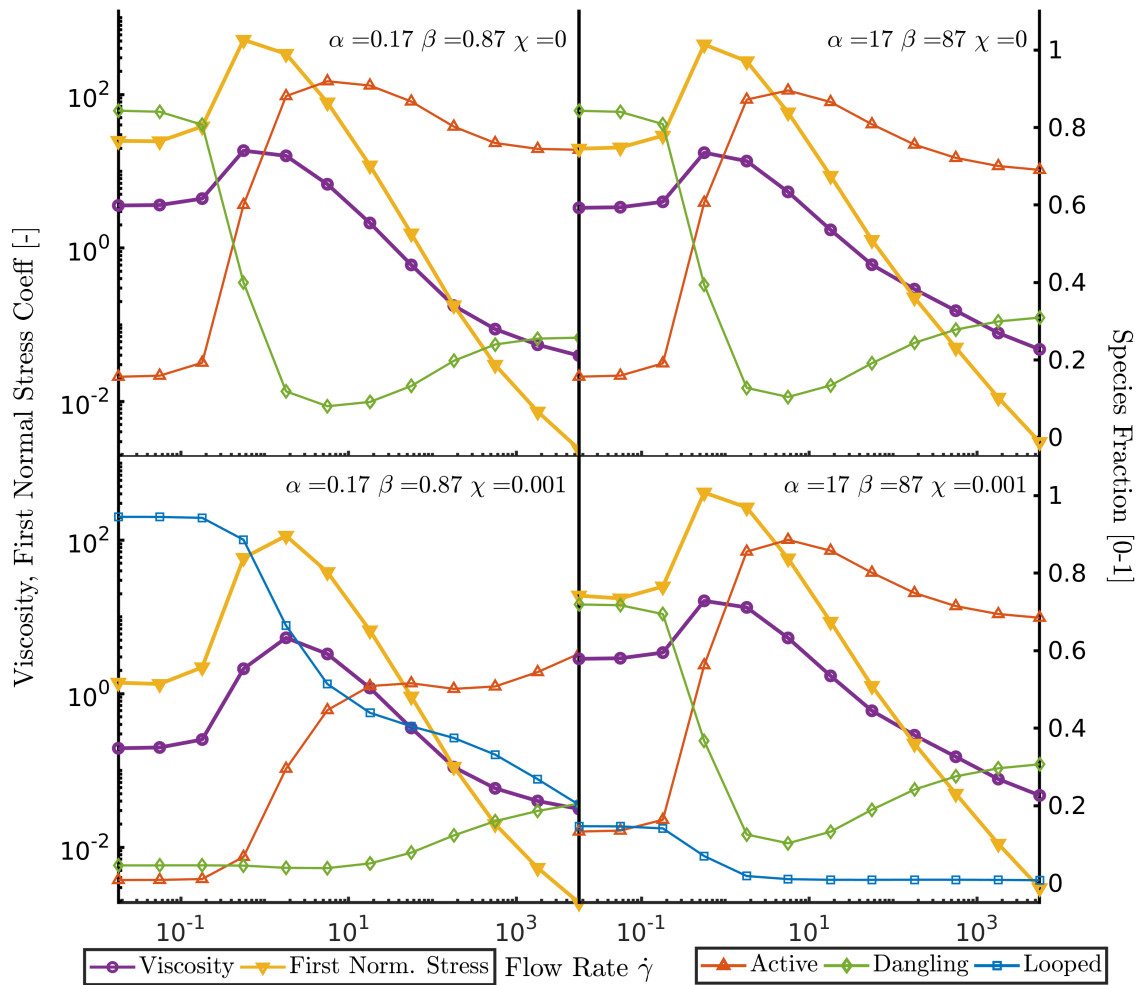


Figure 4.6: Transition function parameter dissymmetry in the three species model. Steady shear plots of viscous and first normal stress coefficient on the left axis. On the right axis, are species fractions. Plots on the first row include only active and dangling species. Plots on the second row also include loops.

greater shear thickening and shear thinning. On the other hand, in a polymer network consisting of mostly bridged networks and less loops, we expect to see higher stresses at low flow rates, followed by less shear thickening before giving way to shear thinning.

Our results compliment the conclusions Sing et al. [44] achieved with their reaction-diffusion Smoluchowski approach. In their work they conclude that the inclusion of loops enhances non-monotonic fluid responses. In examining results across our two and three species models, we too see that it is possible to generate non-monotonic behavior with only two species. However, adding loops enhances the non-monotonicities while lowering overall stress. These effects are most visible when the probability of attachment is not high.

4.2 SMALL AMPLITUDE OSCILLATORY SHEAR

Small amplitude oscillatory shear (SAOS) measures the stress response to an oscillating shear flow to separate out-of-phase viscous and in-phase elastic forces. The shear flow is kept small in order to measure the properties the material without large disruptions to the structure [31]. In this type of simulation, the direction of shear flow is constantly changing at increasingly rapid rates, therefore the stress response has a larger dependence on the dumbbell orientation. In this section we compare SAOS simulations for two and three species models. Figure 4.7 illustrates the characteristics of each simulation across several metrics. In addition, figure 4.8 represents species fractions in terms of only the species that contribute to the fluid response, thereby providing insight into the effects that including the third looping species has on the behavior of the other two.

At low frequency oscillations, dumbbell extension in active and dangling types is similar among the two simulations implying that loops do not on average affect dumbbell length at low frequencies. Instead, the looping dynamic prevents a portion of the dumbbells from contributing to the overall stress calculation. This results in

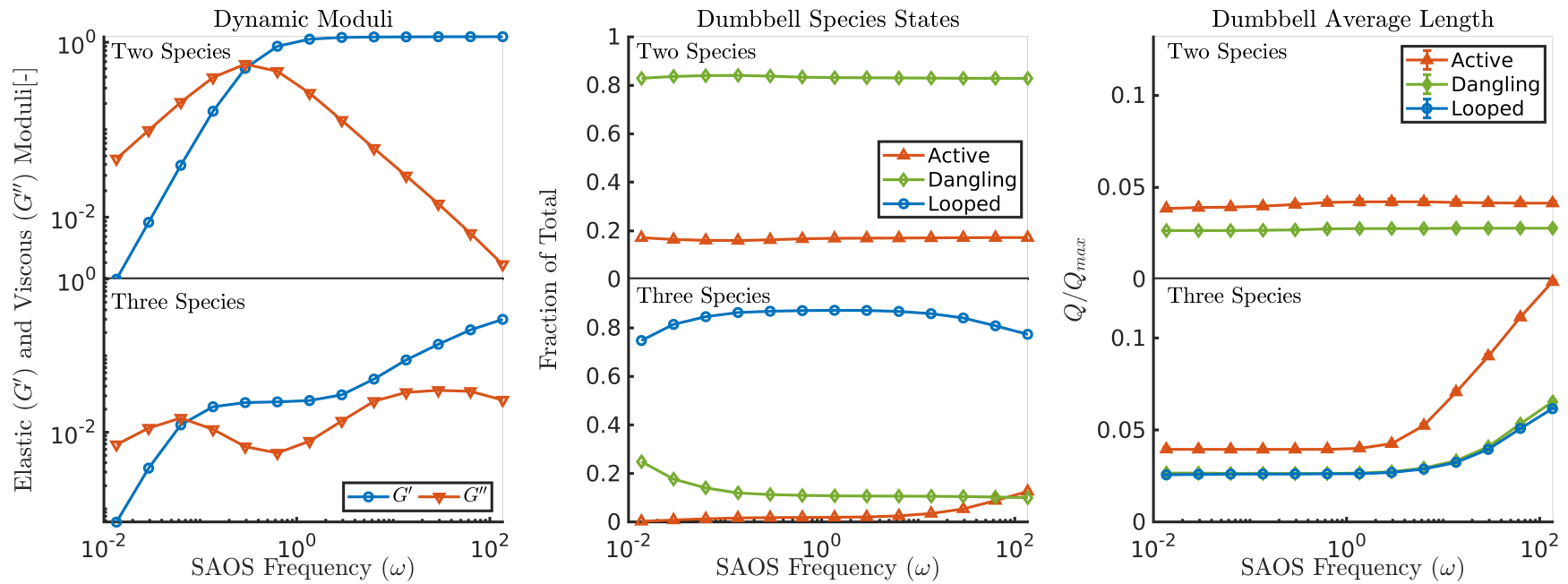


Figure 4.7: Three measurements from a two species and three species SAOS simulation. (Left) Dynamic moduli plots indicate the strength of the network response, and describe elastic-like and viscous-like behavior of the fluid. (Center) Species fraction separated by state. (Right) Average normed length of dumbbell segments.

smaller values for both dynamic moduli in the three-species model. The effect is more dramatic at lower frequencies because the dangling-to-looped transition probability is significantly higher than the dangling-to-active transition probability at shorter lengths. Thus, the correspondence with a drop in the fraction of active dumbbells among species contributing to the stress. In terms of physical behavior this implies that micelle looping stores the potential for greater increases in stress contributions, both viscous and elastic, for when the fluid is under a higher strain rate.

At middle frequencies, we begin to see the effect of incorporating loops on the shape of the dynamic moduli diminish. The reason is that as dumbbells increase in length the difference in transition probability between dangling-to-active and dangling-to-looping shrinks. By inspecting the ratios of species contributing to stress we see that it closely follows that of the two species simulation. Therefore, we can conclude that dumbbells going into the looping state are not demonstrating a length preference beyond what is seen in the two-species case. If they were, their inclusion would disproportionately affect the ratios of one species more than another. Instead, their inclusion effects the other species evenly. This is what leads to the similarities seen in the dynamic moduli characteristics –flat elastic curve and declining viscosity– at lower overall stress levels. In physical terms, this stage of the simulation represents a range of strain rates where loops are not playing a large role in the fluid response. Instead, it is the attachments and detachments of dangling chains in the network that are driving the fluid response.

At higher frequencies, dumbbell extension and orientation become the major factors in stress generation. In the three species model, active dumbbells are captured in an extended and aligned configuration greatly increasing the amount of stress they generate. In addition, the larger flow gradient and subsequent length cause the dangling dumbbells to transition to active more quickly. Meanwhile, dumbbells out of alignment with the fluid flow have shorter length and therefore follow similar loop-

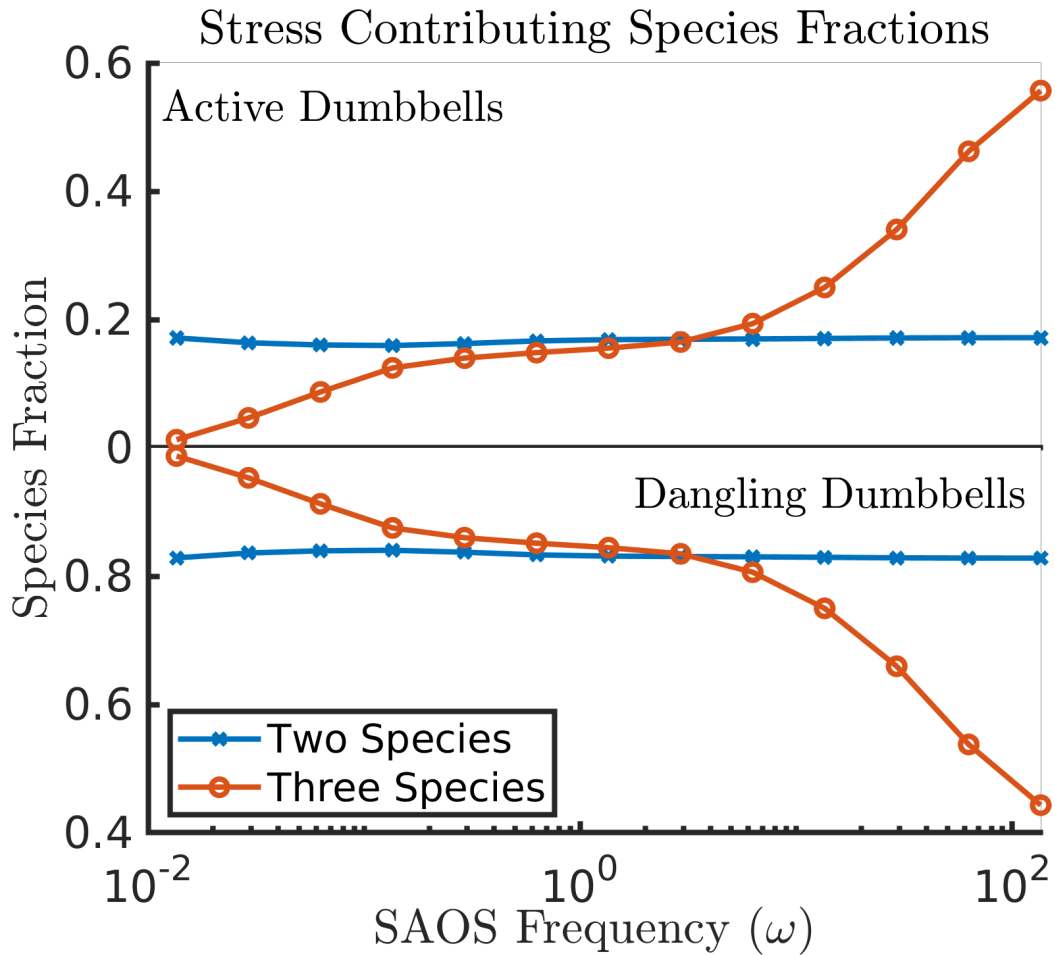


Figure 4.8: Stress contributing species fractions. Plots show the ratio of active (top) and dangling (bottom) dumbbells to active and dangling combined. Three distinct regions in the three species model are apparent; A low frequency region where including loops decreases the ratio of active dumbbells and increase the ratio of dangling. A mid-frequency region, where both models show similar ratios. A high frequency region, where the three species models shows increasing numbers of active dumbbells and decreasing numbers of dangling dumbbells.

dangling transition dynamics. These three factors combine to create a stronger fluid response that causes both moduli to turn upwards, a quality that compares favorably with experimental data the telechelic associative polymer, hydrophobically modified ethoxylated urethane (HEUR) [46, 52, 47].

Figure 4.9, compares model output to experimental data for HEUR measured by Suzuki et al. [46]. The experimental data in the figure is the result of multiple measurements superimposed to create a single master curve using time-temperature superposition [14]. The curves for each temperature show a plateau in the elastic modulus (G') after the relaxation time –where the curves for the moduli cross. In addition, after the relaxation point the loss modulus (G'') decreases before curling up. At this point no more data is provided. The model output matches both these features well with a plateau after the relaxation time in the elastic modulus and a similar drop and curl in the loss modulus. The filled symbols in the figure indicate this area of similarity. The unfilled symbols are included to show the behavior of the model at higher frequencies. The beginning of the unfilled section contains an upward curve at the end of the G' plateau that matches previously reported data for HEUR from Uneyama et al. [52].

Figures 4.10 through 4.15 show the intracycle behavior of the two and three species models. Each plot shows normalized intracycle stress and strain and species ratios on the top left. Numbers on the curve indicate the correspondence with the dumbbell configuration histograms on the right. The SAOS plot bottom left indicates the frequency from which the data is taken. On the right, dumbbell configuration histograms represent the amount of dumbbells at a specific length and orientation if one end is fixed at the origin. Dumbbell positions are not tracked so dumbbells oriented in the quadrants I and III, have the same contribution to the stress as dumbbells oriented in quadrants II and IV. Therefore, the configuration histograms are represented as a half circle.

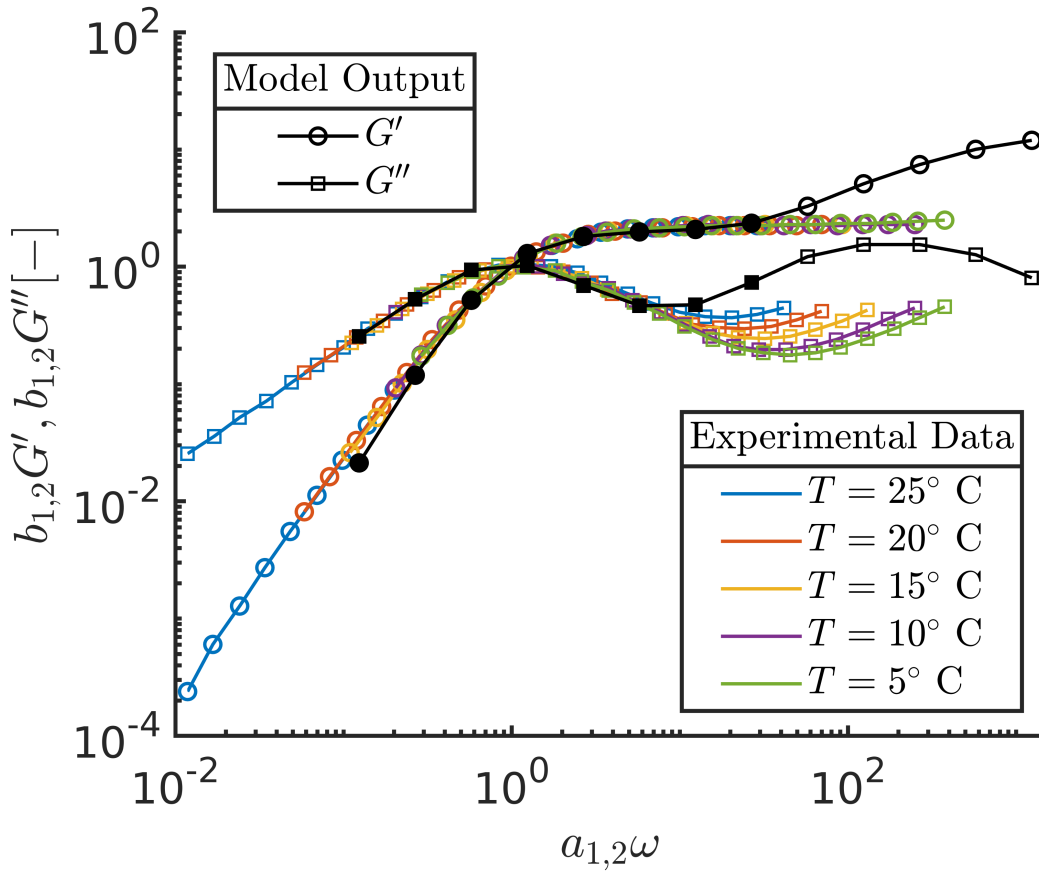


Figure 4.9: Figure showing the dynamic moduli from the model and experimental data for hydrophobically modified ethoxylated urethane. Experimental data and model values have been shifted by constant multiples to align relaxation points. Model parameters were set to $\alpha = 1.7$ $\beta = 8.7$ $\chi = 0.002$ for this simulation. Filled symbols indicate the frequency range with the best match to the data. Unfilled symbols indicate values without experimental data for qualitative comparison.

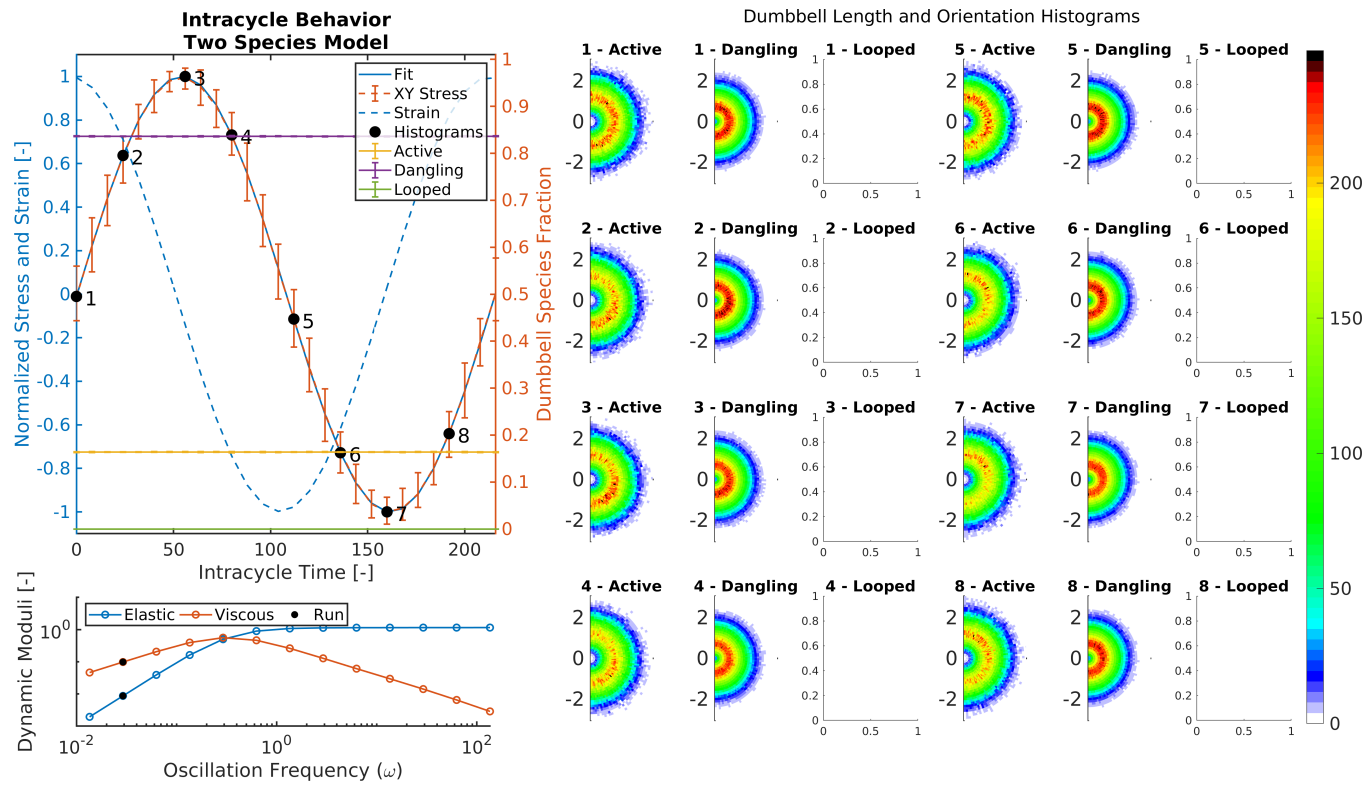


Figure 4.10: Intracycle analysis of a low frequency two species SAOS simulation. *Upper Left* Normalized σ_{xy} stress, strain, curve fit and species fractions over a single cycle. Error bars indicate the range of data over the steady state. Fit refers to the curve generated by fitting σ_{xy} to the function $A\cos\omega t + B\sin\omega t$. The right axis shows the species fractions over the cycle. Error bars indicate variation over the steady state. The numbered dots indicate the corresponding time in the cycle where the corresponding dumbbell configuration histogram is taken. *Right* Dumbbell configuration histograms. To generate the histograms, one end of the dumbbell is fixed at the origin. The placement of the other end is used to for the histogram. Colors represent the number of dumbbell ends in the bin. *Bottom Left* Dynamic moduli for the batch of runs from which the current data is taken. Dots indicate the frequency currently under examination.

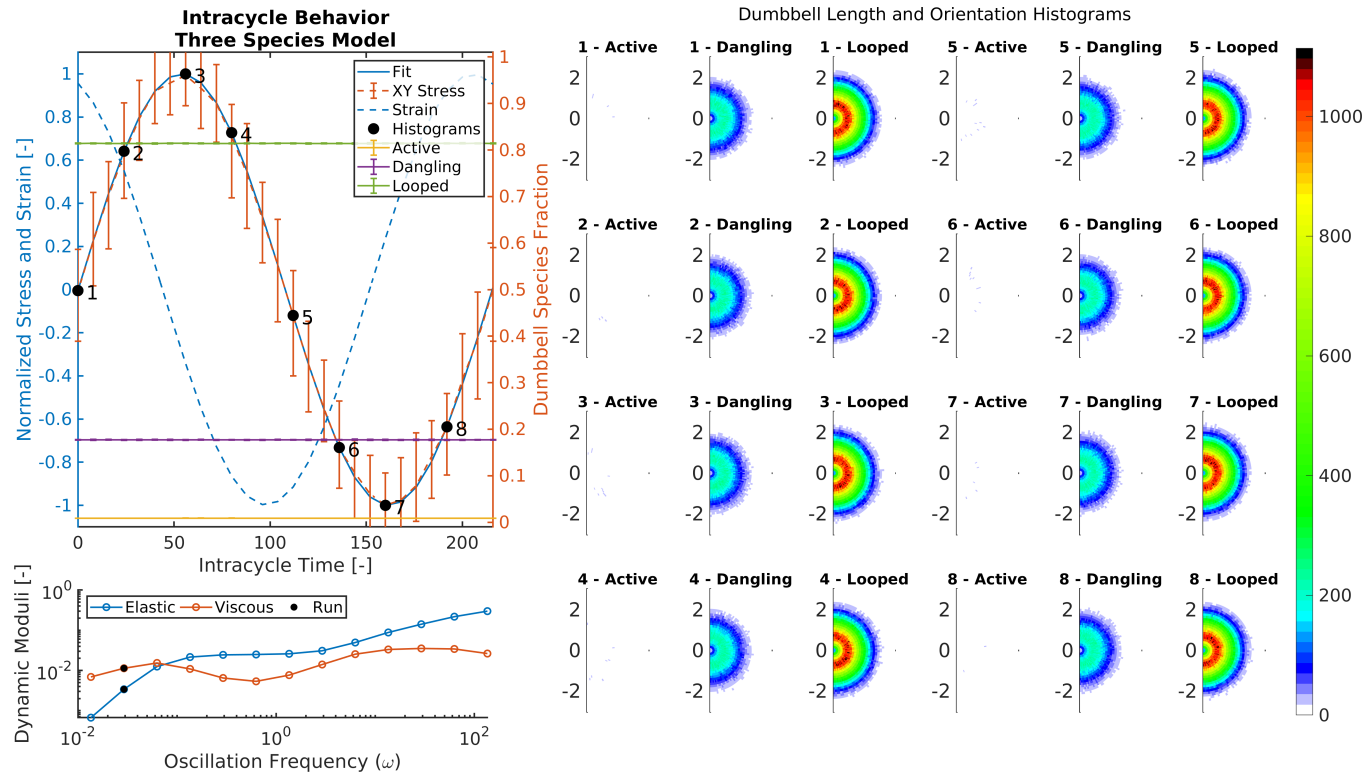


Figure 4.11: Intracycle analysis of a low frequency three species SAOS simulation. *Upper Left* Normalized σ_{xy} stress, strain, curve fit and species fractions over a single cycle. Error bars indicate the range of data over the steady state. Fit refers to the curve generated by fitting σ_{xy} to the function $A\cos\omega t + B\sin\omega t$. The right axis shows the species fractions over the cycle. Error bars indicate variation over the steady state. The numbered dots indicate the corresponding time in the cycle where the corresponding dumbbell configuration histogram is taken. *Right* Dumbbell configuration histograms. To generate the histograms, one end of the dumbbell is fixed at the origin. The placement of the other end is used to for the histogram. Colors represent the number of dumbbell ends in the bin. *Bottom Left* Dynamic moduli for the batch of runs from which the current data is taken. Dots indicate the frequency currently under examination.

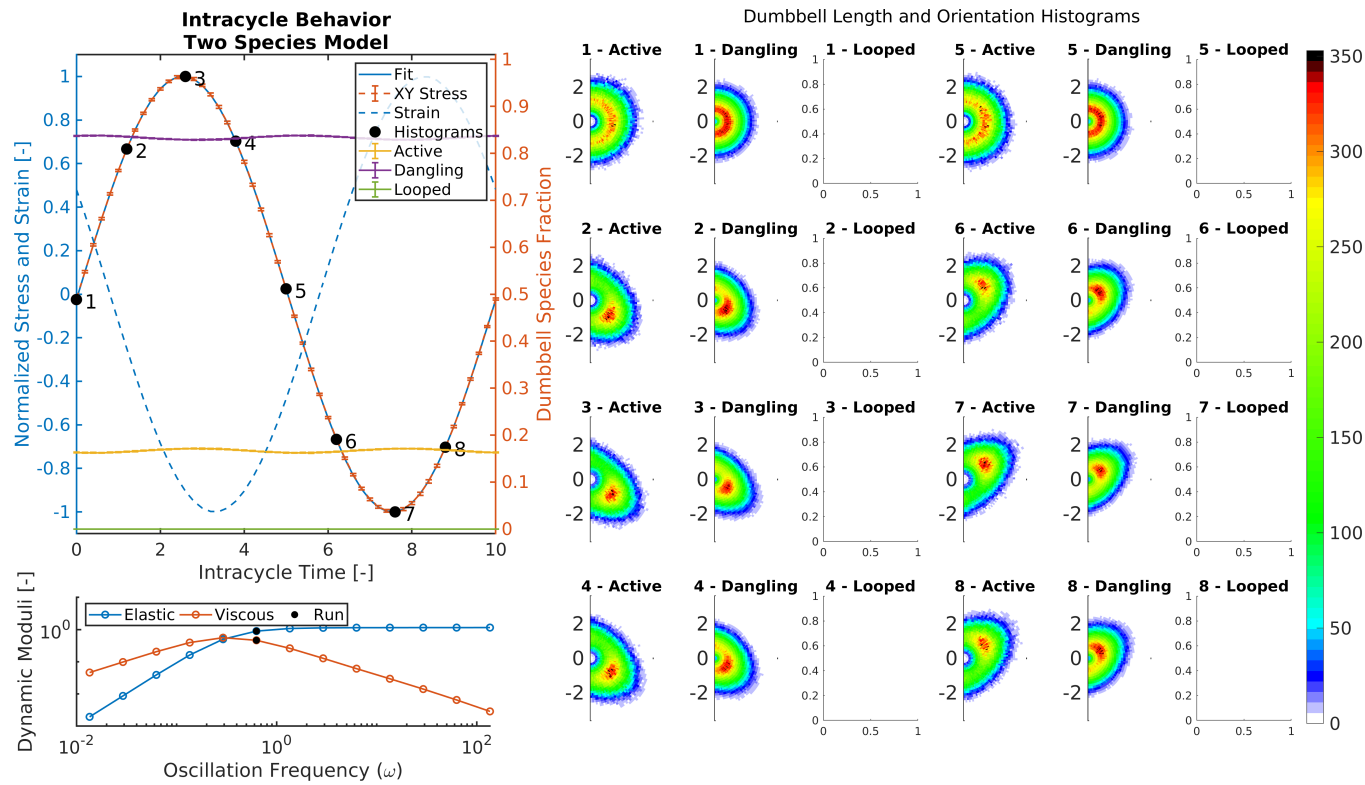


Figure 4.12: Intracycle analysis of a mid-frequency two species SAOS simulation. *Upper Left* Normalized σ_{xy} stress, strain, curve fit and species fractions over a single cycle. Error bars indicate the range of data over the steady state. Fit refers to the curve generated by fitting σ_{xy} to the function $A\cos\omega t + B\sin\omega t$. The right axis shows the species fractions over the cycle. Error bars indicate variation over the steady state. The numbered dots indicate the corresponding time in the cycle where the corresponding dumbbell configuration histogram is taken. *Right* Dumbbell configuration histograms. To generate the histograms, one end of the dumbbell is fixed at the origin. The placement of the other end is used to for the histogram. Colors represent the number of dumbbell ends in the bin. *Bottom Left* Dynamic moduli for the batch of runs from which the current data is taken. Dots indicate the frequency currently under examination.

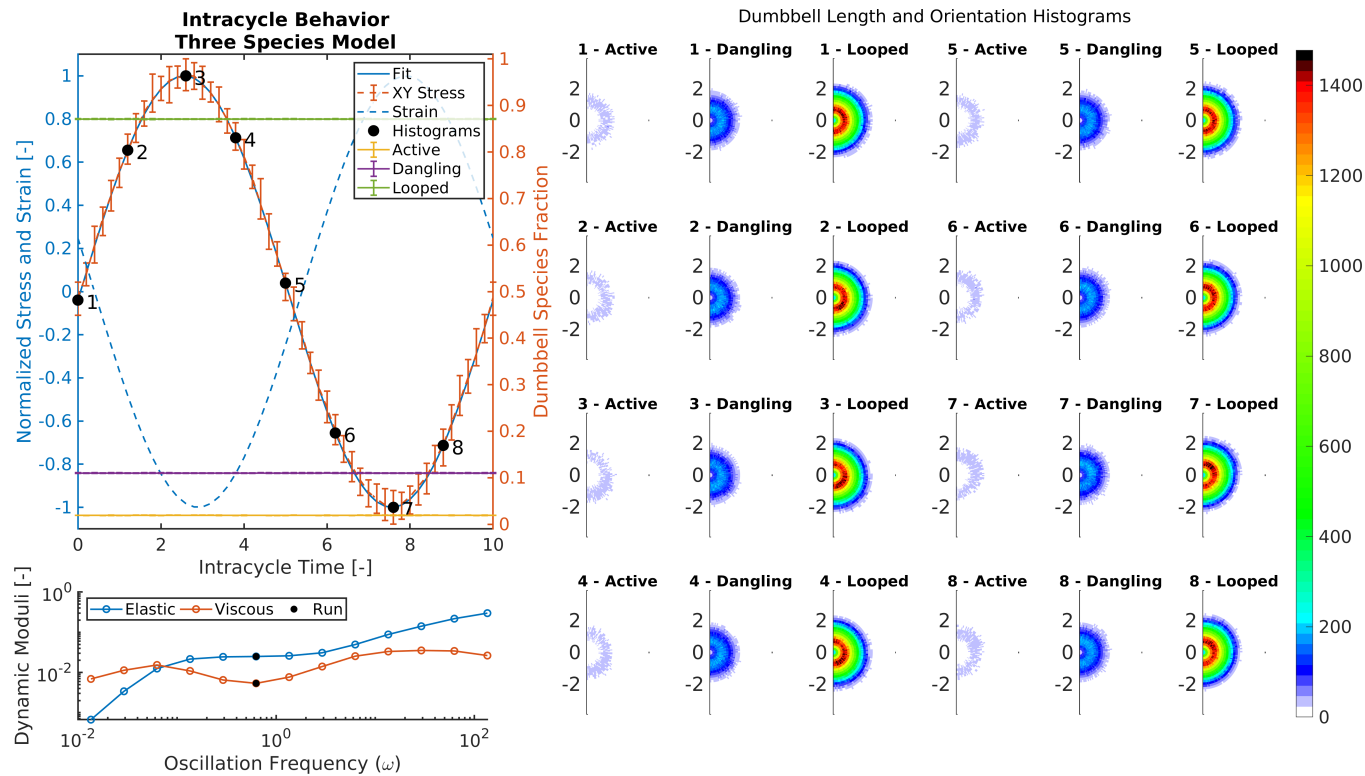


Figure 4.13: Intracycle analysis of a mid-frequency three species SAOS simulation. *Upper Left* Normalized σ_{xy} stress, strain, curve fit and species fractions over a single cycle. Error bars indicate the range of data over the steady state. Fit refers to the curve generated by fitting σ_{xy} to the function $A\cos\omega t + B\sin\omega t$. The right axis shows the species fractions over the cycle. Error bars indicate variation over the steady state. The numbered dots indicate the corresponding time in the cycle where the corresponding dumbbell configuration histogram is taken. *Right* Dumbbell configuration histograms. To generate the histograms, one end of the dumbbell is fixed at the origin. The placement of the other end is used to for the histogram. Colors represent the number of dumbbell ends in the bin. *Bottom Left* Dynamic moduli for the batch of runs from which the current data is taken. Dots indicate the frequency currently under examination.

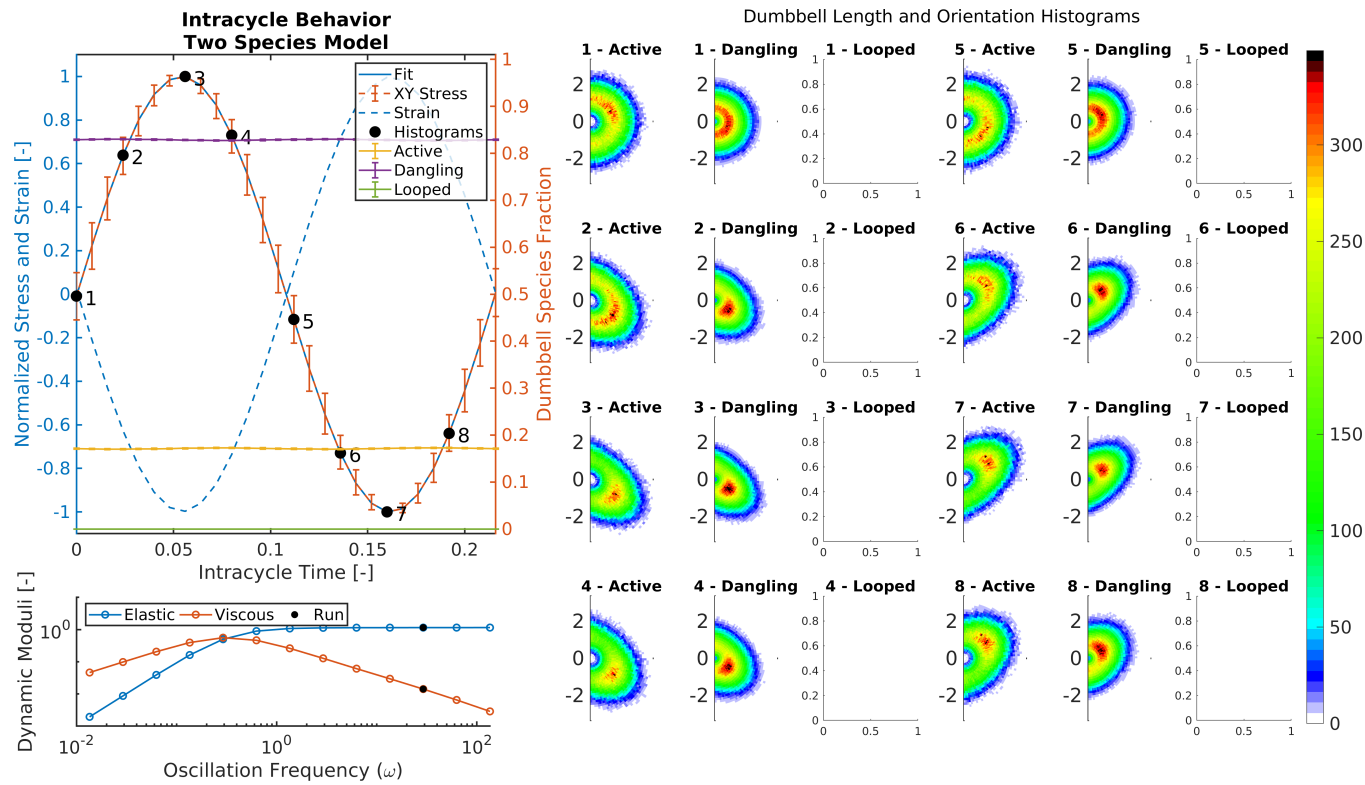


Figure 4.14: Intracycle analysis of a high frequency two species SAOS simulation. *Upper Left* Normalized σ_{xy} stress, strain, curve fit and species fractions over a single cycle. Error bars indicate the range of data over the steady state. Fit refers to the curve generated by fitting σ_{xy} to the function $A\cos\omega t + B\sin\omega t$. The right axis shows the species fractions over the cycle. Error bars indicate variation over the steady state. The numbered dots indicate the corresponding time in the cycle where the corresponding dumbbell configuration histogram is taken. *Right* Dumbbell configuration histograms. To generate the histograms, one end of the dumbbell is fixed at the origin. The placement of the other end is used to for the histogram. Colors represent the number of dumbbell ends in the bin. *Bottom Left* Dynamic moduli for the batch of runs from which the current data is taken. Dots indicate the frequency currently under examination.

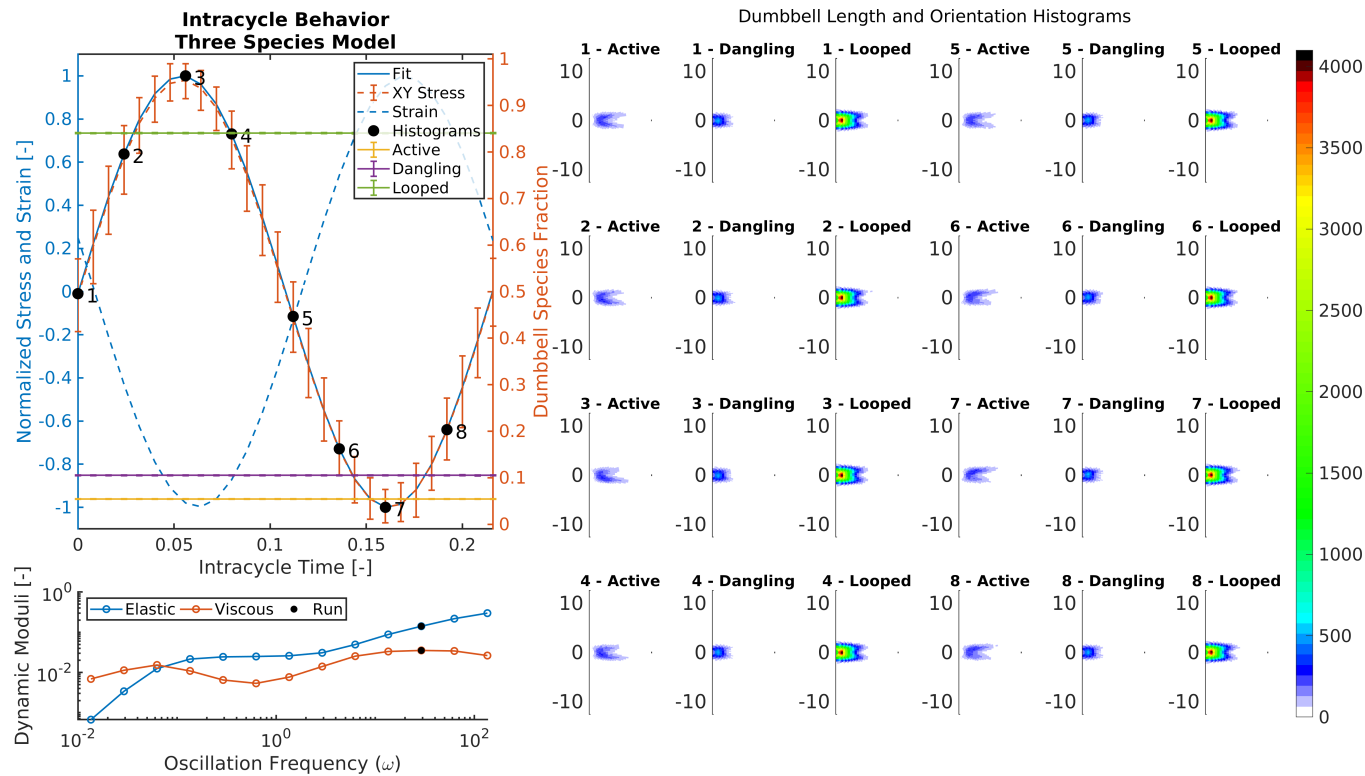


Figure 4.15: Intracycle analysis of a high frequency three species SAOS simulation. *Upper Left* Normalized σ_{xy} stress, strain, curve fit and species fractions over a single cycle. Error bars indicate the range of data over the steady state. Fit refers to the curve generated by fitting σ_{xy} to the function $A\cos\omega t + B\sin\omega t$. The right axis shows the species fractions over the cycle. Error bars indicate variation over the steady state. The numbered dots indicate the corresponding time in the cycle where the corresponding dumbbell configuration histogram is taken. *Right* Dumbbell configuration histograms. To generate the histograms, one end of the dumbbell is fixed at the origin. The placement of the other end is used for the histogram. Colors represent the number of dumbbell ends in the bin. *Bottom Left* Dynamic moduli for the batch of runs from which the current data is taken. Dots indicate the frequency currently under examination.

Dumbbell configuration plots give insight in the effect of flow on dumbbell orientation. For example, we see in figures 4.10 and 4.11, that dumbbells show little orientation at low frequencies. Mid-range frequency results are shown in figures 4.12 and 4.13. In these plots we began to see the beginning of dumbbells orienting with the flow. At higher frequencies the three species simulation shown in figure 4.15 and the two species in figure 4.14 show different behavior. The two species dumbbell configurations show dumbbells moving with oscillations in the fluid flow. The three species dumbbell configuration shows active dumbbells captured an extended V-shape.

There are two factors behind the V-shape formation found in the configuration histograms for the three species model. One is the competing effects of the spring force and imposed solvent flow, which is also present in the two species model, and results in a preferred orientation angle for most stretched dumbbells. The balance between these forces is further explored mathematically in the following section. The second factor is the length and orientation assigned to a dumbbell after it transitions from the looped to dangling state. For example, when a dangling dumbbell extends in the direction of the flow and becomes looped, it retains that configuration when it transitions back to a dangling dumbbell later. If these dynamics coincide with the oscillations of the fluid flow, a dumbbell becomes looped for the time period where the fluid flow would cause it to retract had it stayed in the dangling state. Moreover, if it reenters as a dangling dumbbell when the flow is moving in the same direction, it will extend further than it would have otherwise. Figure 4.16 shows these dynamics occur in our simulations.

The topological interpretation of the inclusion of this looping behavior depends on the oscillation frequency. At lower frequencies, shorter dumbbells are forming loops correspondent with the lower force of the fluid flow that should accompany less micelle attachments and dangling chains. At mid-level flow force, the effect of loops decreases as dumbbells extend further in the dangling state and make more network

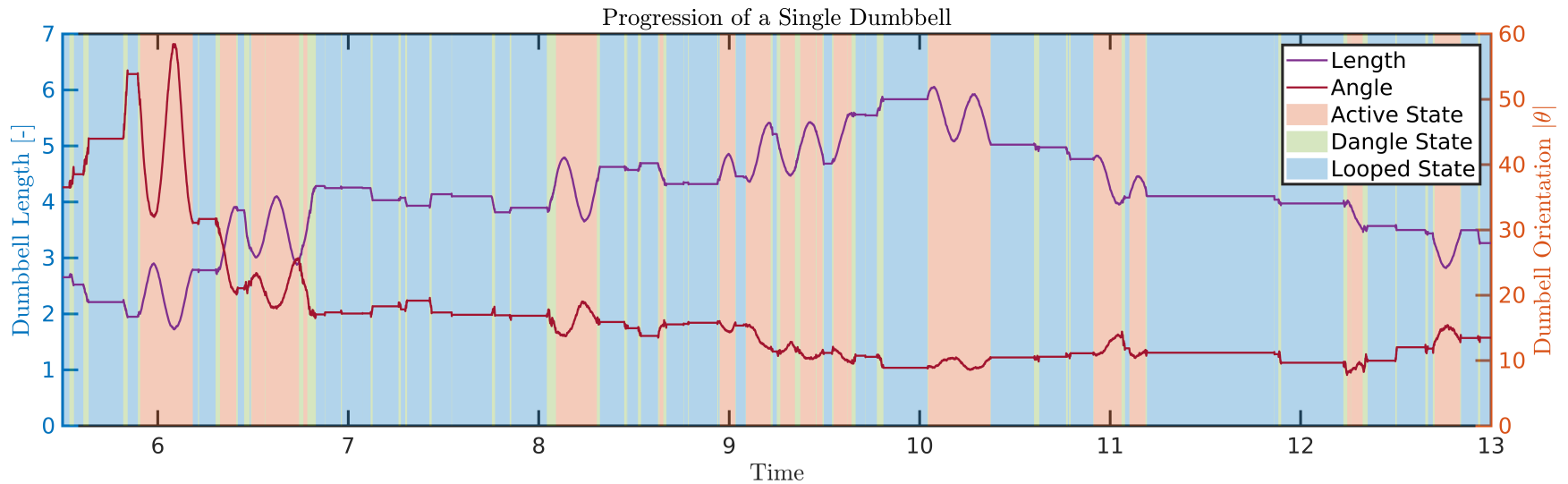


Figure 4.16: Progression of a single dumbbell. Plot shows the length and angle of a single dumbbell in the three species SAOS simulation. The background colors indicate the species state of the dumbbell. Oscillations occur in both directions when the dumbbell is not in the looped state. However, entering and exiting the looped state at opportune times allows the dumbbell to progressively extend in length.

attachments. At higher frequencies the role of loops is to impede movement with the flow in a one direction and increase the potential for extension in length when the flow reverses. The physical scenario that justifies this behavior is the case when a dangling dumbbell which is pushed back towards its micelle core by the oscillating flow causing it to fold back on itself and loop. In this situation, the dumbbell is unable to follow the fluid flow. However, when the flow reverses and the dumbbell breaks out of its looped state it forms a longer dangling dumbbell that extends further with the fluid flow, thus enhancing its effect on the stress response. This line of reasoning follows suggestions that loops or micelles could hinder the relaxation of chains made in previous work [38]. Together we see that a consistent physical interpretation of including a looping species, as we have, depends on a consideration for the dynamics imposed by the movement of the fluid. The merits of this approach are discussed further in the Loop Reentry Methods section.

4.2.1 MATHEMATICAL ANALYSIS FOR OSCILLATORY SHEAR FLOW

A mathematical analysis of the dumbbell evolution equation provides insight into these dynamics. The non-dimensional form of an explicit computation time step is given by,

$$Q(t + \Delta t) = Q(t) + \kappa \cdot Q(t)\Delta t - \zeta F(Q)\Delta t + \sqrt{\zeta \Delta t} dW \quad (4.4)$$

The constant ζ differs for active and dangling dumbbells and varies with the value of Z in the case of active dumbbells. The function $F(Q)$ is the FENE spring force function. The main terms that affect dumbbell length at the flow rate term, and the spring force term. The Brownian motion term plays a role, but its influence on average is small. The flow rate term for SAOS flow is know precisely. Out of the three terms, the FENE force is the only asymptotic term and therefore has the potential for the greatest impact. However, in our SAOS simulations most springs spend little

Table 4.1: Dumbbell configuration term approximations.

Purpose	Flow Rate	FENE Spring
Term	$\kappa \cdot Q(t)\Delta t$	$\zeta F(Q)\Delta t$
Approximation	$\begin{bmatrix} \gamma_0\omega Q_y(t) \Delta t \\ 0 \end{bmatrix}$	$-1.5\zeta Q(t) \Delta t$
Description	Accounts for the effects of the oscillating fluid flow. Notice, that the shearing motion only changes a dumbbell's x length based on the y length.	Approximates the spring force for dumbbells of moderate length ($Q < 10$). As dumbbells grow in length, the FENE spring force grows asymptotically and would therefore dominate over any other acting forces.

time in the asymptotic growth region. The nonlinear force in the FENE term, can thus be estimated as $F(Q) \approx 1.5|Q|$ for values of Q from 0 to 20. These terms are summarized in table 4.1.

By comparing the values for different orientation angles and flows, we can determine whether the flow force or the FENE spring force plays a more dominant role. This is illustrated by the figure 4.17. The plot contains three sections. In one section the orientation is such that for smaller oscillation rates, the spring force is more responsible for changing the dumbbell configuration. In the other extreme, the flow rate dominates the behavior of the spring. In the middle, it depends on the species of the dumbbell. The lines are estimated by the reasoning above and are not hard boundaries, but instead indicate a balance of forces.

By examining whether the spring force or fluid flow behavior dominates the change in spring configuration, we can clearly distinguish between the phenomena witness in the simulation data. For example, in SAOS simulations at low frequencies, $\omega\gamma_0$

Term influence on dumbbell by orientation

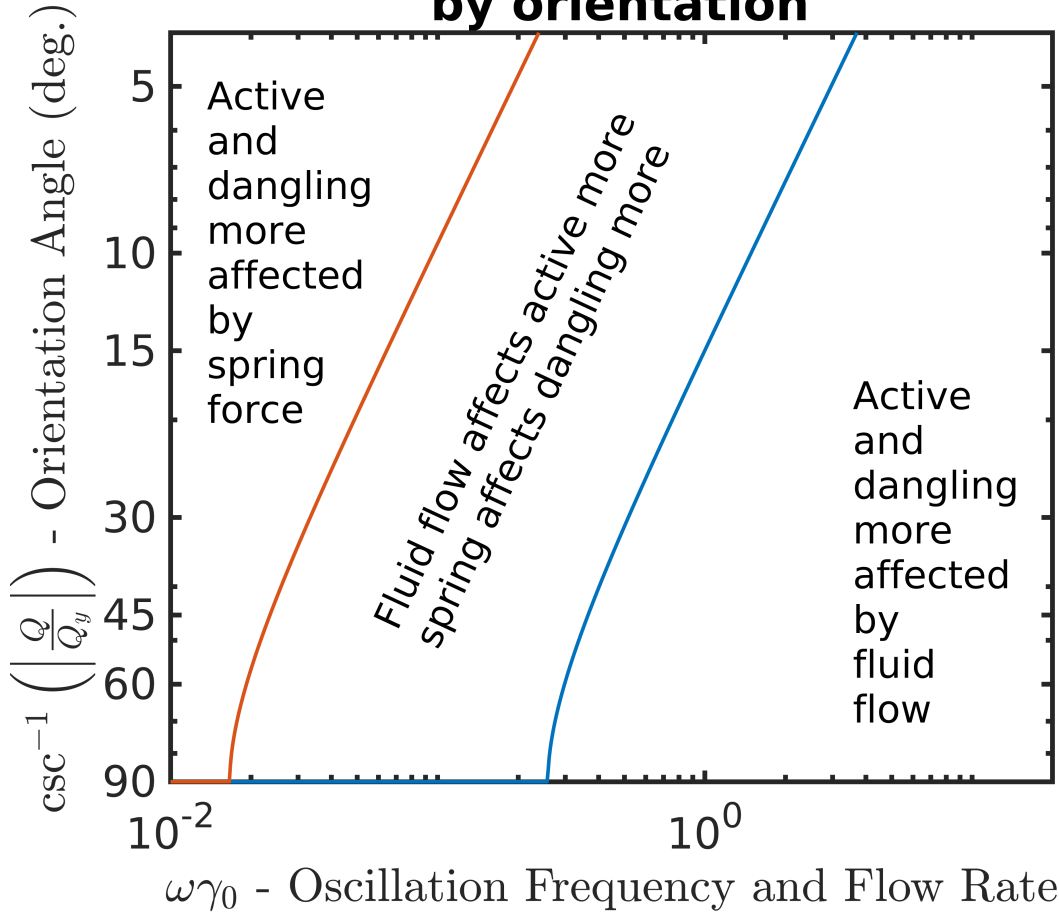


Figure 4.17: Orientation angle versus oscillation frequency and flow rate. There are three regions; a left region where the spring force is the largest factor influencing change in dumbbell configuration, a right region where frequency and flow rate are the larger factor, and a middle region where it depends on the dumbbell species type. Slope and position of dividing lines depend on the value of Z .

is small, and therefore spring behavior is dominated by the FENE force for all orientations. Because the FENE force is isotropic, springs show little alignment in a specific direction. In our simulations, all runs with $\omega \leq 10$ exhibit little alignment. At middle frequencies, springs show more alignment with the flow, however, there is still a large amount of springs randomly aligned. At high frequencies, the flow orients and stretches active springs. As active dumbbells break and become dangling, the spring force dominates and causes the dumbbell to retract.

In the three species model its common for active dumbbells to reach a length and angle where the movement of the fluid flow is not enough to move the dumbbell out of the region where flow is more influential nor is the flow strong enough to cause a breaking transition to the dangling species as they stretch. Instead, the extended dumbbells persist in the angle of their orientation and simply extend and retract with the change in shear direction. The result of this behavior can be seen in the V-shape that appears in the configuration histograms in figure 4.15.

4.3 LOOP-TO-DANGLING TRANSITION METHODS

In the SAOS simulations we see that the method of reincorporating loops plays a significant role in the characteristics of the dynamic moduli. In this section, we highlight this difference by comparing two loop re-entry methods. This first method is the one presented in the previous section. In this approach when a dangling dumbbell transitions to the looped species, its length and orientation remain unchanged. When the loops transition back to dangling dumbbells and reenter the stress calculations, they regain their previous configuration. In this way, longer loops form longer dangling dumbbells and shorter loops form shorter dangling dumbbells when they transition species type. Moreover, this type of jumping from coiled to partial stretched state has been seen in other work examining polymer behavior [1]. On the other hand, the concern of this method is that it allows a dumbbell in the looped state to transition

to the dangling state with a length and orientation out of phase with the fluid flow. However, the impact of this behavior is overwhelmed by the behavior of the flow itself. This is why we find dumbbells well aligned in the horizontal direction in steady shear flow simulations. Moreover, because the re-entry length and orientation are chosen from a position that resulted from the same type of flow, this method can only be said to be enhancing characteristics already present in the dumbbell population as a result of oscillating shear flow.

In this second method, loops are assigned random lengths chosen from a normal distribution when they transition back to dangling dumbbells. The results of this simulation are shown in figure 4.18. The normal distribution is truncated to ensure dumbbells do not exceed the maximum length prescribed by the FENE condition. This approach can be said to replicate the equilibrium behavior of the dumbbells under no flow conditions. The main difference in this approach is that the transition from looped to dangling states causes the resulting dangling dumbbell to be shorter. Choosing from a normal distribution diminishes the impact of the shorter length and allows for differences arising from Brownian fluctuations in the fluid. The drawback of this approach is that the configuration the loops take on when they transition from loop to dangling is disconnected from the fluid flow. In this way, the resulting after-transition configuration is the same even for drastically different fluid flows, such as steady shear and oscillating shear.

In a comparison of simulations using the two methods we see that they lead to significantly different behavior. The looping behavior in the first simulation enhances the effect of oscillating shear flow on the dumbbell configuration. This results in longer dangling and active dumbbells that adapt a V-shape in the configuration histograms. The V-shape also corresponds with increases in both the dynamic moduli. In the second simulation, the looping reentry choice diminishes the effects of the imposed fluid flow because reentry configurations are the same at zero and non-zero flow. The

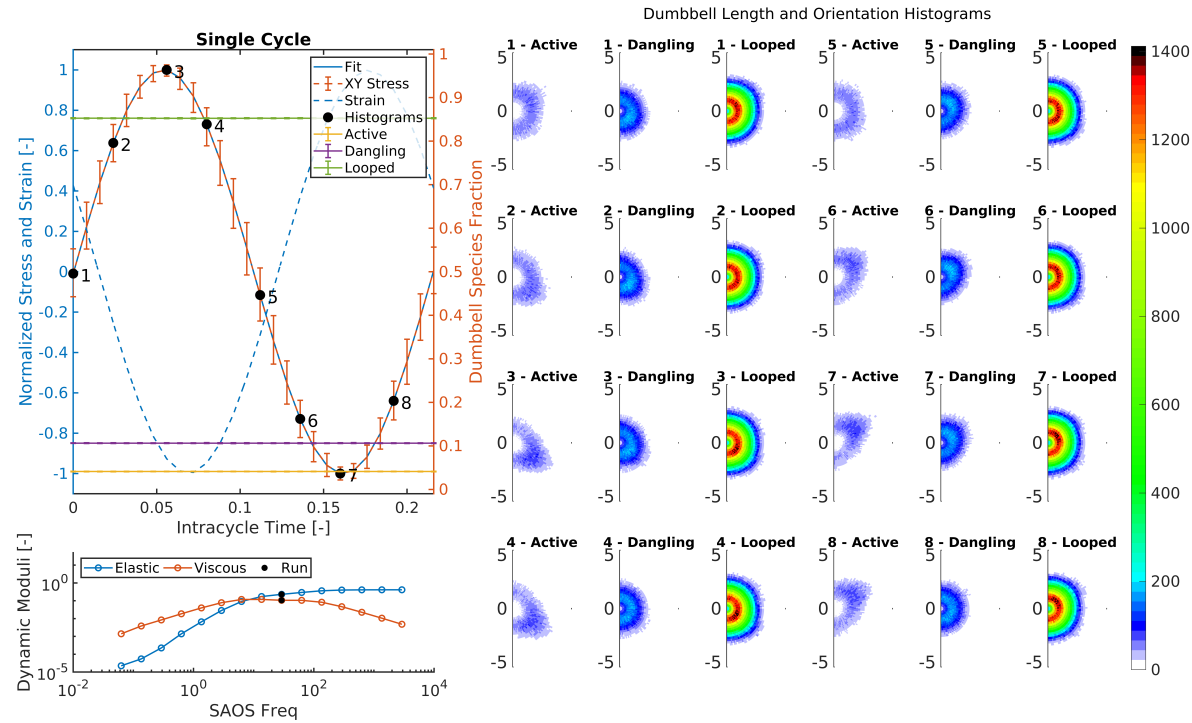


Figure 4.18: Intracycle behavior from a three species SAOS simulation where loops transition to dangling with length draw from a normal distribution. In these simulations, the looped-to-dangling dumbbells take configurations based on a truncated normal distribution. (Upper left) Plot showing intracycle stress, strain and species fractions. (Lower left) Dynamic moduli across a range of frequencies. The intra-cycle is taken from the run indicated by the black dot. (Right) Dumbbell configuration histograms separated by type and intracycle time.

result is that all three species types show more rounded distributions that have less alignment in any specific directions. In addition, the relaxation point shows a marked shift to higher frequencies, indicating the diminished influence of the oscillating shear flow.

On the whole, our simulations show that the method used to transition loops to dangling dumbbells has a significant effect on the dynamic moduli measured in SAOS flows. For both methods, there exists reasonable physical arguments for and against their implementation. However, we chose to focus our efforts on the first method due to the unique behaviors it exhibits and its similarities to experiment. Although comprehensive examination of loop reentry dynamics is beyond the scope of the current work, the results present herein show that it is an area worthy of further study.

4.4 LARGE AMPLITUDE OSCILLATORY SHEAR

In comparison to SAOS, large amplitude oscillatory shear (LAOS) studies have become common place only recently with the advent of more sensitive transducers in commercially available rheometers [41]. LAOS studies go beyond SAOS, using larger deformations to probe nonlinear rheology, whereas the linear viscoelastic theory behind SAOS is only valid for small deformations. In most processing operations polymer deformation is both rapid and large and thus LAOS simulations are necessary for a complete understanding [25]. In light of the significance of this emerging field, we simulated LAOS deformations and measured the stress response using our three species model with the same attachment detachment and looping parameter values.

A pipkin diagram provides a rheological fingerprint that illustrates the nonlinear viscoelastic properties of the material response [16]. As with SAOS simulations, the resulting stress from LAOS can be decomposed into the elastic and viscous contributions [12]. For each of these, a pipkin diagram is provided in figure 4.19 for the

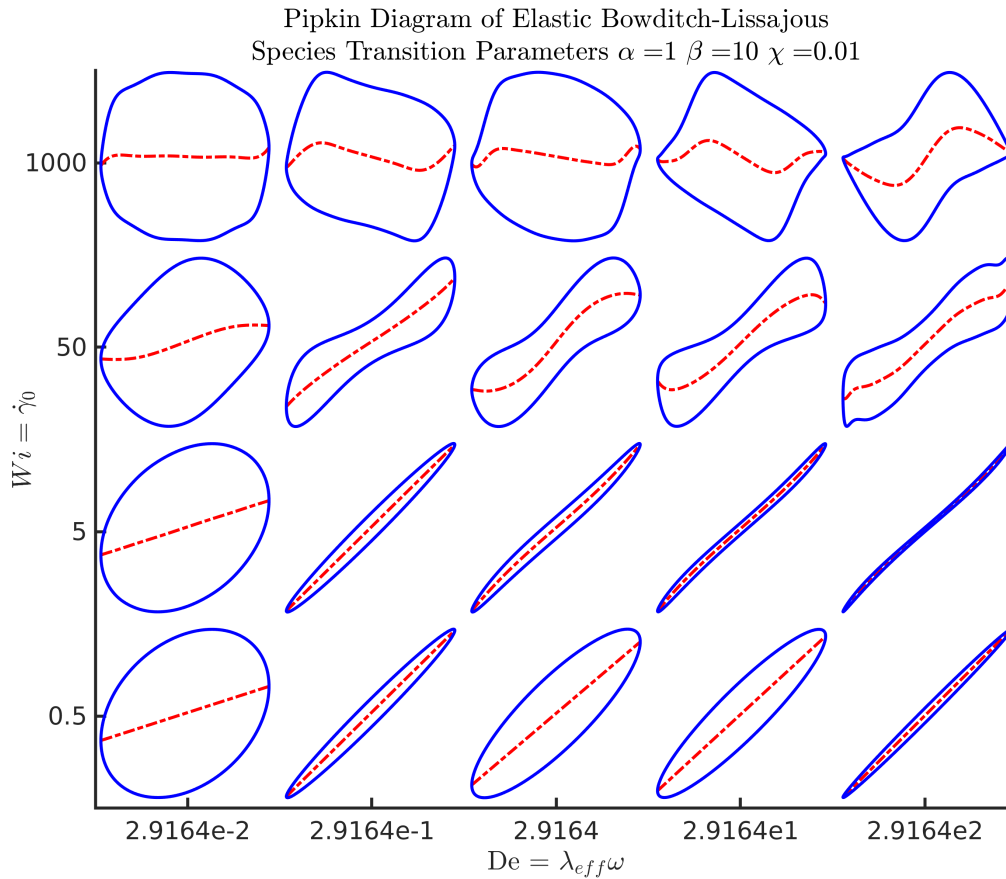


Figure 4.19: Pipkin diagrams showing elastic Bowditch-Lissajou curves form a three species large amplitude oscillatory shear flow simulation. Each simulation was done with parameters $\alpha = 1$, $\beta = 10$ and $\chi = 0.01$. ω is the oscillation frequency, $\lambda_{eff} = 1/\tau = 14.1343$.

elastic component and figure 4.20 for the viscous component. Within each diagram, a grid of Lissajou-Bowditch curves expresses the nature of the nonlinear response at intervals of frequency, ω , and strain amplitude, γ_0 . The dashed line represents the elastic stress contribution for the elastic diagram, and the viscous stress in the viscous diagram. The total stress, including both elastic and viscous, is represented by the solid line [9].

In both figures, the bottom row of curves represents results within the linear regime. In this row, the undistorted ellipse indicates a linear material response (this was also confirmed via Fourier Transform techniques, see section 3.3). In figure 4.19,

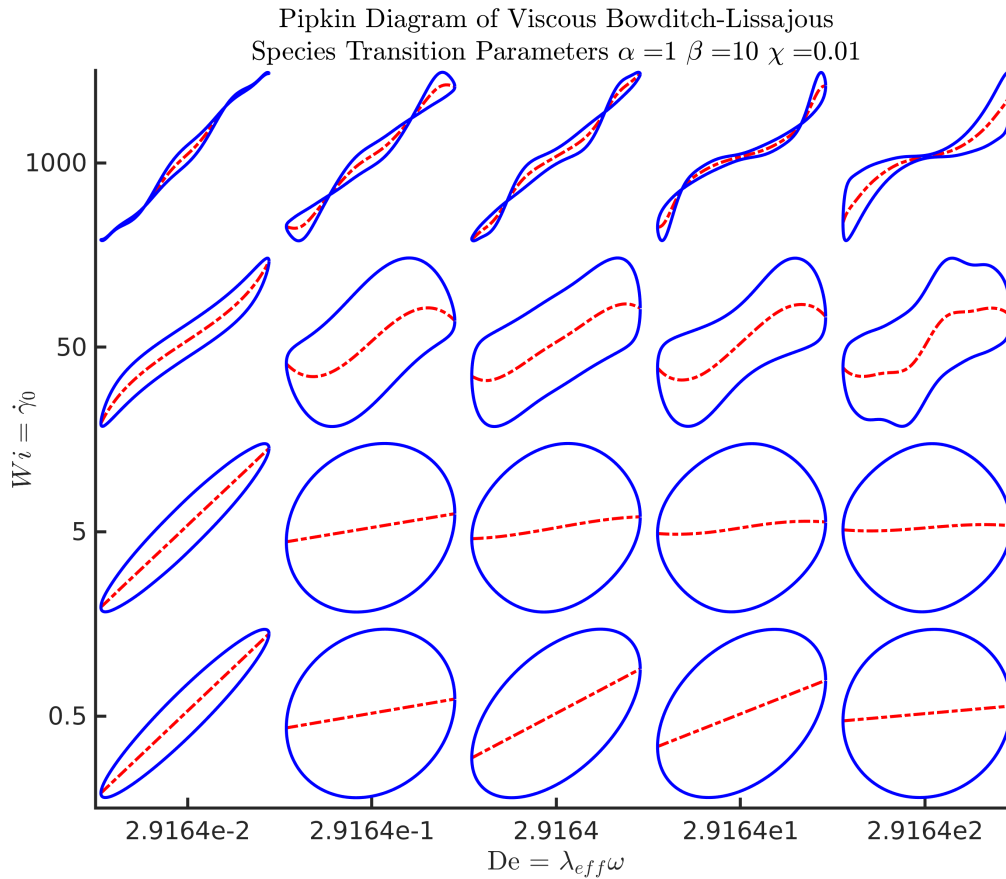


Figure 4.20: Pipkin diagrams showing viscous Bowditch-Lissajou curves from a three species large amplitude oscillatory shear flow simulation. Each simulation was done with parameters $\alpha = 1$, $\beta = 10$ and $\chi = 0.01$. ω is the oscillation frequency, $\lambda_{eff} = 1/\tau = 14.1343$.

a more circular curve indicates a more viscous response. Whereas, a single straight line represents a purely elastic response [16]. Applying this understanding, we see that the Lissajou-Bowditch curves at this strain-amplitude indicate a progression from a viscous response to something more elastic, followed by several more viscous responses, before again shifting back to a more elastic response. This is consistent with results seen in the dynamic moduli plots in figure 4.7 from section 4.2.

As the strain-amplitude increases both diagrams indicate increasing nonlinear responses. By examining the figures column-wise, we see a shift from smooth ellipses to increasingly distorted shapes. This indicates the presence of higher harmonics

in the material response that can be used to provide additional detail about the material response. For example, the strength and sign of the third harmonic can be used to indicate strain stiffening or strain softening in the elastic diagram, or shear thickening or thinning in the viscous diagram [16]. In the first column of figure 4.19, the distortion from a circular ellipse to a rounded rectangle between the second and third rows is largely the result of contributions from the third harmonic and indicates intracycle softening. The additional distortions to the shape on the fourth row are an example of a material response with large contributions from additional harmonics beyond the third.

The purpose of the brief analysis above is not to detail all the intricacies of the non-linear response but to instead demonstrate the potential application to LAOS simulations due to the fidelity of the model. Indeed, generating the figures presented here required no modification to the model or oscillatory shear simulation code. Instead, they represent the result of increasing the strain-amplitude parameter and analyzing the results via the MITLaos software [17]. Through this natural extension our model shows the ability to simulate the additional harmonics of the material response found in LAOS simulations. By demonstrating this, we hope to lay the groundwork for a more detailed analysis to appear in future work.

CHAPTER 5

CONCLUSION

In this article we present an extension of the Brownian Dynamics approach inspired by the work of Hernández Cifre et al. We incorporate recent developments in the probability of network bridge destruction and offer a new form for the probability of bridge creation. We also include a third species type, looped dumbbells, and offer novel methods of incorporating them into the Brownian dynamics structure previously established. Furthermore, our work employs an efficient parallel computational scheme using GPUs that allows for accurate Brownian dynamics simulations under complex conditions.

Steady shear flow simulations show the ability of our scheme to generate shear-thickening and shear-thinning behavior by independently adjusting bridging and detaching parameters. This distinction demonstrates the added flexibility in the basis of our model which will allow it to be more readily adapted to additional complexities in the future. In three species simulations, we find that including looping dumbbells lowered overall stress and strengthened the nonlinear response. This was largely the result of the looping species regulating the number of dangling and active dumbbells contributing to the stress; a function, that decreased with increasing flow rate.

This work also presents the results of small amplitude oscillatory shear flow with ensembles of 1024000 dumbbells spanning a wide frequency spectrum. In these simulations, including a third looping species makes a clear impact across the frequency spectrum. The most notable portion being an upward turn in both dynamic moduli at medium-to-high frequency oscillations that is not found in two species simulations.

Moreover, we plot configuration histograms which show the existence of a V-shape distribution in the steady state that results from including looping dynamics. This V-shape corresponds to the unique upward turn in the dynamic moduli.

We further examine two separate approaches to the dynamics of the looped-to-dangling species transition. In the first, we allow dumbbells to take on their previous configuration when transitioning from looped to dangling. In the second, the dumbbells are assigned lengths according to a Gaussian distribution truncated to fit within the maximum dumbbell length. A comparison of these two approaches makes it clear that these dynamics play a significant role in the fluid response. Therefore, we identify this aspect of the model as an area important to future research.

To demonstrate the range of fluid flow simulations that our code platform is capable of modeling, we include elastic and viscous Bowditch-Lissajous plots from large amplitude oscillatory shear simulations. Together this work makes a strong case for revisiting the Brownian dynamics approach to simulating complex rheology modelled with FENE dumbbells. Three reasons are the straight forward equations used to describe the molecular motion, the wide range of flow types that can be simulated, and the ease with which multiple species dynamics can be incorporated. Each of these advantages are the result of the mean-field approach which allows the independent simulation of dumbbells to approximate overall network influence on the fluid. Moreover, because our approach can be updated easily, as scientific understanding of micro-rheology in telechelic polymers advances, the capability of this code platform will increase with it.

BIBLIOGRAPHY

- [1] US Agarwal, Rohit Bhargava, and RA Mashelkar. “Brownian dynamics simulation of a polymer molecule in solution under elongational flow”. In: *The Journal of chemical physics* 108.4 (1998), pp. 1610–1617.
- [2] Carolina de las Heras Alarcón, Sivanand Pennadam, and Cameron Alexander. “Stimuli responsive polymers for biomedical applications”. In: *Chem. Soc. Rev.* 34 (3 2005), pp. 276–285. DOI: 10.1039/B406727D. URL: <http://dx.doi.org/10.1039/B406727D>.
- [3] Arlette RC Baljon, Danny Flynn, and David Krawzsenek. “Numerical study of the gel transition in reversible associating polymers”. In: *The Journal of chemical physics* 126.4 (2007), p. 044907.
- [4] NP Balsara, M Tirrell, and TP Lodge. “Micelle formation of BAB triblock copolymers in solvents that preferentially dissolve the A block”. In: *Macromolecules* 24.8 (1991), pp. 1975–1986.
- [5] George I. Bell. “Models for the Specific Adhesion of Cells to Cells”. In: *Science* 200.4342 (1978), pp. 618–627. ISSN: 00368075, 10959203. URL: <http://www.jstor.org/stable/1746930>.
- [6] R. B. Bird et al. *Dynamics of polymeric liquids*. John Wiley & Sons, 1987.
- [7] Andrew H Briggs et al. “Model parameter estimation and uncertainty: a report of the ISPOR-SMDM Modeling Good Research Practices Task Force-6”. In: *Value in Health* 15.6 (2012), pp. 835–842.
- [8] B.H.A.A van den Brule and P.J Hoogerbrugge. “Brownian Dynamics simulation of reversible polymeric networks”. In: *Journal of Non-Newtonian Fluid Mechanics* 60.2 (1995), pp. 303–334. ISSN: 0377-0257. DOI: [https://doi.org/10.1016/0377-0257\(95\)01378-4](https://doi.org/10.1016/0377-0257(95)01378-4). URL: <http://www.sciencedirect.com/science/article/pii/0377025795013784>.
- [9] Roger W Chan. “Nonlinear viscoelastic characterization of human vocal fold tissues under large-amplitude oscillatory shear (LAOS)”. In: *Journal of rheology* 62.3 (2018), pp. 695–712.

- [10] Céline Charbonneau et al. “Controlling the dynamics of self-assembled triblock copolymer networks via the pH”. In: *Macromolecules* 44.11 (2011), pp. 4487–4495.
- [11] John Cheng, Max Grossman, and Ty McKercher. *Professional Cuda C Programming*. John Wiley & Sons, 2014.
- [12] Kwang Soo Cho et al. “A geometrical interpretation of large amplitude oscillatory shear response”. In: *Journal of rheology* 49.3 (2005), pp. 747–758.
- [13] Andrea De Mauro, Marco Greco, and Michele Grimaldi. “What is big data? A consensual definition and a review of key research topics”. In: *AIP conference proceedings*. Vol. 1644. 1. AIP. 2015, pp. 97–104.
- [14] John Dealy and Don Plazek. “Time-temperature superposition—a users guide”. In: *Rheology Bulletin* 78.2 (2009).
- [15] Patrick S Doyle, Eric SG Shaqfeh, and Alice P Gast. “Dynamic simulation of freely draining flexible polymers in steady linear flows”. In: *Journal of Fluid Mechanics* 334 (1997), pp. 251–291.
- [16] Randy H Ewoldt, AE Hosoi, and Gareth H McKinley. “New measures for characterizing nonlinear viscoelasticity in large amplitude oscillatory shear”. In: *Journal of Rheology* 52.6 (2008), pp. 1427–1458.
- [17] RH Ewoldt, P Winter, and GH McKinley. “MITlaos version 2.1 Beta for MATLAB”. In: *Cambridge, MA, self-published: MATLAB-based data analysis software for characterizing nonlinear viscoelastic responses to oscillatory shear strain* (2007).
- [18] Paul A Gagniuc. *Markov Chains: From Theory to Implementation and Experimentation*. John Wiley & Sons, 2017.
- [19] M. S. Green and A. V. Tobolsky. “A New Approach to the Theory of Relaxing Polymeric Media”. In: *The Journal of Chemical Physics* 14.2 (1946), pp. 80–92. DOI: 10.1063/1.1724109. eprint: <https://doi.org/10.1063/1.1724109>. URL: <https://doi.org/10.1063/1.1724109>.
- [20] Gary S Grest and Kurt Kremer. “Molecular dynamics simulation for polymers in the presence of a heat bath”. In: *Physical Review A* 33.5 (1986), p. 3628.
- [21] Alan Grossfield et al. “Best Practices for Quantification of Uncertainty and Sampling Quality in Molecular Simulations [Article v1. 0]”. In: *Living journal of computational molecular science* 1.1 (2018).

- [22] J G Hernández-Cifre et al. “Brownian dynamics simulation of reversible polymer networks under shear using a non-interacting dumbbell model”. In: *Journal of Non-Newtonian Fluid Mechanics* 113.2 (2003), pp. 73–96. ISSN: 0377-0257. DOI: [https://doi.org/10.1016/S0377-0257\(03\)00063-6](https://doi.org/10.1016/S0377-0257(03)00063-6). URL: <http://www.sciencedirect.com/science/article/pii/S0377025703000636>.
- [23] J G Hernández-Cifre et al. “Brownian dynamics simulation of reversible polymer networks using a non-interacting bead-and-spring chain model”. In: *Journal of Non-Newtonian Fluid Mechanics* 146.1 (2007). 3rd Annual European Rheology Conference, pp. 3–10. ISSN: 0377-0257. DOI: <https://doi.org/10.1016/j.jnnfm.2006.08.010>. URL: <http://www.sciencedirect.com/science/article/pii/S0377025706002102>.
- [24] Allan S Hoffman. “Hydrogels for biomedical applications”. In: *Advanced drug delivery reviews* 64 (2012), pp. 18–23.
- [25] Kyu Hyun et al. “Progress in Polymer Science A review of nonlinear oscillatory shear tests : Analysis and application of large amplitude oscillatory shear (LAOS)”. In: *Progress in Polymer Science* 36.12 (2011), pp. 1697–1753. ISSN: 0079-6700. DOI: 10.1016/j.progpolymsci.2011.02.002. URL: <http://dx.doi.org/10.1016/j.progpolymsci.2011.02.002>.
- [26] Vijay Kadam et al. “Structure and Rheology of Self-Assembled Telechelic Associative Polymers in Aqueous Solution before and after Photo-Cross-Linking”. In: *Macromolecules* 44.20 (2011), pp. 8225–8232.
- [27] Stefan Kallus et al. “Characterization of polymer dispersions by Fourier transform rheology”. In: *Rheologica acta* 40.6 (2001), pp. 552–559.
- [28] H A Kramers. “The Behavior of Macromolecules in Inhomogeneous Flow”. In: 415 (1946). DOI: 10.1063/1.1724163.
- [29] Kurt Kremer and Gary S Grest. “Dynamics of entangled linear polymer melts: A molecular-dynamics simulation”. In: *The Journal of Chemical Physics* 92.8 (1990), pp. 5057–5086.
- [30] Werner Kuhn. “Über die gestalt fadenförmiger moleküle in lösungen”. In: *Kolloid-Zeitschrift* 68.1 (1934), pp. 2–15.
- [31] Ronald G Larson. *The structure and rheology of complex fluids*. Oxford University Press, 1999.
- [32] Claude Le Bris and Tony Lelievre. “Multiscale modelling of complex fluids: a mathematical initiation”. In: *Multiscale modeling and simulation in science*. Springer, 2009, pp. 49–137.

- [33] Don S Lemons and Paul Langevin. *An introduction to stochastic processes in physics*. JHU Press, 2002.
- [34] Kevin Letchford and Helen Burt. “A review of the formation and classification of amphiphilic block copolymer nanoparticulate structures: micelles, nanospheres, nanocapsules and polymersomes”. In: *European Journal of Pharmaceutics and Biopharmaceutics* 65.3 (2007). Drug delivery: a Canadian perspective, pp. 259–269. ISSN: 0939-6411. DOI: <https://doi.org/10.1016/j.ejpb.2006.11.009>. URL: <http://www.sciencedirect.com/science/article/pii/S0939641106003316>.
- [35] Christopher W Macosko and Ronald G Larson. “Rheology: principles, measurements, and applications”. In: (1994).
- [36] Markus Manssen, Martin Weigel, and Alexander K Hartmann. “Random number generators for massively parallel simulations on GPU”. In: *The European Physical Journal Special Topics* 210.1 (2012), pp. 53–71.
- [37] Antti Nykänen et al. “Direct Imaging of Nanoscopic Plastic Deformation below Bulk T_g and Chain Stretching in Temperature-Responsive Block Copolymer Hydrogels by Cryo-TEM”. In: (2008), pp. 3243–3249.
- [38] Linda Pellens et al. “Evaluation of a transient network model for telechelic associative polymers”. In: 121 (2004), pp. 87–100. DOI: 10.1016/j.jnnfm.2004.05.002.
- [39] E.A.J.F. Peters. “Polymers in flow — modelling and simulation”. PhD thesis. Sept. 2000. ISBN: 9037001831.
- [40] E.A.J.F. Peters and Th.M.A.O.M. Barenbrug. “Efficient Brownian dynamics simulation of particles near walls. I. Reflecting and absorbing walls”. In: *Phys. Rev. E* 66 (5 Nov. 2002), p. 056701. DOI: 10.1103/PhysRevE.66.056701. URL: <https://link.aps.org/doi/10.1103/PhysRevE.66.056701>.
- [41] Simon Rogers. “Large amplitude oscillatory shear: simple to describe, hard to interpret”. In: *Physics Today* 71.7 (2018), pp. 34–40.
- [42] Y Séréro et al. “Associating polymers: from “flowers” to transient networks”. In: *Physical Review Letters* 81.25 (1998), p. 5584.
- [43] Michelle K Sing, Jorge Ramírez, and Bradley D Olsen. “Mechanical response of transient telechelic networks with many-part stickers”. In: *The Journal of chemical physics* 147.19 (2017), p. 194902.

- [44] Michelle K Sing et al. “Celebrating Soft Matter’s 10th Anniversary : Chain configuration and rate-dependent mechanical properties in transient networks”. In: *Soft Matter* 11 (2015), pp. 2085–2096. ISSN: 1744-683X. DOI: 10.1039/C4SM02181A. URL: <http://dx.doi.org/10.1039/C4SM02181A>.
- [45] Ecole Nationale Supé. “Micellization of block copolymers”. In: 28 (2003), pp. 1107–1170. DOI: 10.1016/S0079-6700(03)00015-7.
- [46] Shinya Suzuki et al. “Nonlinear rheology of telechelic associative polymer networks: Shear thickening and thinning behavior of hydrophobically modified ethoxylated urethane (HEUR) in aqueous solution”. In: *Macromolecules* 45.2 (2012), pp. 888–898.
- [47] KC Tam et al. “A structural model of hydrophobically modified urethane-ethoxylate (HEUR) associative polymers in shear flows”. In: *Macromolecules* 31.13 (1998), pp. 4149–4159.
- [48] F Tanaka and SF Edwards. “Viscoelastic properties of physically crosslinked networks: Part 1. Non-linear stationary viscoelasticity”. In: *Journal of Non-Newtonian Fluid Mechanics* 43.2-3 (1992), pp. 247–271.
- [49] F Tanaka and SF Edwards. “Viscoelastic properties of physically crosslinked networks: Part 2. Dynamic mechanical moduli”. In: *Journal of non-newtonian fluid mechanics* 43.2-3 (1992), pp. 273–288.
- [50] F Tanaka and SF Edwards. “Viscoelastic properties of physically crosslinked networks: Part 3. Time-dependent phenomena”. In: *Journal of non-newtonian fluid mechanics* 43.2-3 (1992), pp. 289–309.
- [51] Anubhav Tripathi, Kam C Tam, and Gareth H Mckinley. “Rheology and Dynamics of Associative Polymers in Shear and Extension : Theory and Experiment”. In: 05 (2006), pp. 1981–1999. DOI: 10.1021/ma051614x.
- [52] Takashi Uneyama, Shinya Suzuki, and Hiroshi Watanabe. “Concentration dependence of rheological properties of telechelic associative polymer solutions”. In: *Physical Review E* 86.3 (2012), p. 031802.
- [53] A Vaccaro and G Marrucci. “A model for the nonlinear rheology of associating polymers”. In: 92.December 1999 (2000), pp. 261–273.
- [54] Rui Wang et al. “Classical Challenges in the Physical Chemistry of Polymer Networks and the Design of New Materials”. In: *Accounts of Chemical Research* 49.12 (2016), pp. 2786–2795. ISSN: 15204898. DOI: 10.1021/acs.accounts.6b00454.

- [55] Shi Qing Wang. “Transient network theory for shear-thickening fluids and physically crosslinked networks”. In: *Macromolecules* 25.25 (1992), pp. 7003–7010.
- [56] Shihu Wang and Ronald G Larson. “Multiple relaxation modes in suspensions of colloidal particles bridged by telechelic polymers”. In: *Journal of Rheology* 62.2 (2018), pp. 477–490.
- [57] Harold R Warner Jr. “Kinetic theory and rheology of dilute suspensions of finitely extendible dumbbells”. In: *Industrial & Engineering Chemistry Fundamentals* 11.3 (1972), pp. 379–387.
- [58] Manfred Wilhelm, Pierre Reinheimer, and Martin Ortseifer. “High sensitivity Fourier-transform rheology”. In: *Rheologica Acta* 38.4 (Oct. 1999), pp. 349–356. ISSN: 1435-1528. DOI: 10.1007/s003970050185. URL: <https://doi.org/10.1007/s003970050185>.
- [59] Manfred Wilhelm et al. “The crossover between linear and non-linear mechanical behaviour in polymer solutions as detected by Fourier-transform rheology”. In: *Rheologica Acta* 39.3 (2000), pp. 241–246.
- [60] Mark Wilson, Avinoam Rabinovitch, and Arlette RC Baljon. “Computational study of the structure and rheological properties of self-associating polymer networks”. In: *Macromolecules* 48.17 (2015), pp. 6313–6320.
- [61] Hans M Wyss et al. “Strain-rate frequency superposition: A rheological probe of structural relaxation in soft materials”. In: *Physical review letters* 98.23 (2007), p. 238303.
- [62] Misazo Yamamoto. “The visco-elastic properties of network structure I. General formalism”. In: *Journal of the physical society of Japan* 11.4 (1956), pp. 413–421.
- [63] Misazo Yamamoto. “The visco-elastic properties of network structure II. Structural viscosity”. In: *Journal of the physical society of Japan* 12.10 (1957), pp. 1148–1158.
- [64] Misazo Yamamoto. “The visco-elastic properties of network structure III. Normal stress effect (Weissenberg effect)”. In: *Journal of the physical society of Japan* 13.10 (1958), pp. 1200–1211.
- [65] Takehiro Yamamoto and Nobuhiro Kanda. “Brownian Dynamics Simulation for Shear Flow of Entangled Polymer Systems Using a Reversible Network Model”. In: *Nihonkikaigakkai ronbun-shū B-hen* 79.802 (2013), pp. 1072–1080. DOI: 10.1299/kikaib.79.1072.

- [66] Takehiro Yamamoto and Nobuhiro Kanda. “Computational model for Brownian dynamics simulation of polymer/clay nanocomposites under flow”. In: *Journal of Non-Newtonian Fluid Mechanics* 181-182 (2012), pp. 1–10. ISSN: 0377-0257. DOI: <https://doi.org/10.1016/j.jnnfm.2012.06.005>. URL: <http://www.sciencedirect.com/science/article/pii/S0377025712001139>.
- [67] Yue Zhao et al. “Self-assembly of poly (caprolactone-b-ethylene oxide-b-caprolactone) via a microphase inversion in water”. In: *The Journal of Physical Chemistry B* 105.4 (2001), pp. 848–851.
- [68] SN Zhurkov. “Kinetic concept of the strength of solids”. In: *International Journal of Fracture* 26.4 (1984), pp. 295–307.

APPENDIX A

DERIVATION OF THE DUMBBELL EQUATION

In the elastic bead-spring or dumbbell model [30] a macromolecule is idealized as an “elastic dumbbell”. Each endpoint of the dumbbell undergoes drag from two sources. The first is due to movement of the endpoint itself. The second is due to the flow of fluid around it. Endpoint collisions with molecules in the solvent lead to Brownian motion. The edge between each endpoint represents a molecular chain which has a maximum length and a resistance to stretching due to a preferred configuration in the solution. Therefore, a FENE spring force [57] is employed. In the model interpretation we assume the inertial forces to be considered negligible in comparison to other forces in the model, as is convention [6]. Collecting these factors in a force balance equation yields a mathematical expression for the behavior of a single endpoint.

$$\sum F_i = \text{Movement Drag} + \text{Fluid Flow Drag} + \text{Spring Force} + \text{Brownian Motion} \quad (\text{A.1})$$

Using Newton’s second law $\sum F = ma$, expressions for the forces, and assuming negligible inertia $ma = 0$, we then get,

$$0 = -\frac{1}{\zeta} d\mathbf{x}_i + \mathbf{F}_{Spring}(\mathbf{x}_i)dt + \frac{1}{\zeta} \mathbf{v}_i dt + \sqrt{\frac{k_B T}{\zeta}} dt d\mathbf{W} \quad (\text{A.2})$$

$$d\mathbf{x}_i = \zeta \mathbf{F}_{Spring}(\mathbf{x}_i)dt + \mathbf{v} dt + \sqrt{k_B T \zeta} dt d\mathbf{W}. \quad (\text{A.3})$$

Now let \mathbf{Q} be the edge connecting the two end points so that $\mathbf{Q} = \mathbf{x}_2 - \mathbf{x}_1$. The conceptualization of \mathbf{Q} shown in figure 2.3 and is the source of the term ‘Elastic Dumbbell’. Then,

$$d(\mathbf{x}_2 - \mathbf{x}_1) = -\zeta \mathbf{F}_{Spring}(\mathbf{x}_2 - \mathbf{x}_1)dt + (\mathbf{v}_2 - \mathbf{v}_1) dt + \sqrt{k_B T \zeta dt} (d\mathbf{W}_2 - d\mathbf{W}_1) \quad (\text{A.4})$$

$$d(\mathbf{Q}) = -\zeta \mathbf{F}_{Spring}(\mathbf{Q})dt + (\nabla \mathbf{v}) dt + \sqrt{k_B T \zeta dt} (d\mathbf{W}_2 - d\mathbf{W}_1). \quad (\text{A.5})$$

By the Normal Sum Theorem [33], $d\mathbf{W}_2 \pm d\mathbf{W}_1 = \sqrt{2}d\mathbf{W}$. In addition, its common to let $\boldsymbol{\kappa} = (\nabla \mathbf{v})^T$. Incorporating these two adjustments leads to,

$$d\mathbf{Q} = -\zeta \mathbf{F}_{Spring}(\mathbf{Q})dt + \boldsymbol{\kappa} \cdot \mathbf{Q}dt + \sqrt{2k_B T \zeta dt} d\mathbf{W}. \quad (\text{A.6})$$

This equation is what is used to simulate the polymer segment behavior.

APPENDIX B

NUMERICAL SCHEME

A semi-implicit absolutely stable numerical scheme evolves the dumbbells over time. Put forth by E.A.L.F, Peters in [39], the scheme is only first order accurate. However, the value of the approach comes from the relative computational cost of each step. Due to the stochastic nature of the simulation, a large number of realizations must be computed to lower noise in the model. Under this consideration, the ability to calculate many individual dumbbells quickly is balanced by the need for accuracy in each. More accurate schemes exist, however employing and developing them was not a focus of the current work. The scheme as it applies to this application is derived in full below.

The following equation describes the change in configuration of a single dumbbell,

$$d\mathbf{Q} = \kappa \cdot \mathbf{Q}dt - H\zeta \frac{\mathbf{Q}}{1 - Q^2/Q_{max}^2}dt + \sqrt{2k_B T \zeta} d\mathbf{W}. \quad (\text{B.1})$$

Using the formula,

$$\frac{d}{dt} |\mathbf{Q}|^2 = 2 \left(\frac{d}{dt} \mathbf{Q} \right) \cdot \mathbf{Q}, \quad (\text{B.2})$$

the change in dumbbell length can be found as,

$$d|Q|^2 = 2\mathbf{Q} \cdot \kappa \cdot \mathbf{Q}dt - 2H\zeta \frac{Q^2}{1 - Q^2/Q_{max}^2}dt + 2\mathbf{Q} \cdot \sqrt{2k_B T \zeta} d\mathbf{W}. \quad (\text{B.3})$$

The numerical scheme first calculates changes in the orientation and length due to the flow and Brownian motion in an explicit step. Then the change in length due

to the FENE spring force is added in a second implicit step.

$$\mathbf{Q}_1 = \mathbf{Q} + \kappa \cdot \mathbf{Q} dt + \sqrt{2k_B T \zeta} d\mathbf{W} \quad (\text{B.4})$$

$$Q^2 = |\mathbf{Q}_1|^2 - 2H\zeta \frac{Q^2}{1 - Q^2/Q_{max}^2} \quad (\text{B.5})$$

$$\mathbf{Q} = \sqrt{\frac{Q^2}{Q_1^2}} \mathbf{Q}_1 \quad (\text{B.6})$$

Equation B.5 is quadratic in Q^2 .

$$Q^2 = |\mathbf{Q}_1|^2 - 2H\zeta \frac{Q_{max}^2 Q^2}{Q_{max}^2 - Q^2} dt \quad (\text{B.7})$$

$$(Q_{max}^2 - Q^2) Q^2 = |\mathbf{Q}_1|^2 (Q_{max}^2 - Q^2) - 2H\zeta Q_{max}^2 Q^2 dt \quad (\text{B.8})$$

$$Q^4 + -Q^2 [1 + 2H\zeta dt + |\mathbf{Q}_1|^2 / Q_{max}^2] |\mathbf{Q}_1|^2 = 0 \quad (\text{B.9})$$

This results in two solutions for Q^2 . The solution with $|\mathbf{Q}| < Q_{max}$ is given by the solution:

$$\frac{2Q^2}{Q_{max}^2} = [1 + 2H\zeta dt + |\mathbf{Q}_1|^2 / Q_{max}^2] + \sqrt{[1 + 2H\zeta dt + |\mathbf{Q}_1|^2 / Q_{max}^2]^2 - 4 \frac{|\mathbf{Q}_1|^2}{Q_{max}^2}} \quad (\text{B.10})$$

Multiplying by the conjugate gives,

$$\frac{2Q^2}{Q_{max}^2} = \quad (B.11)$$

$$\frac{[1 + 2H\zeta dt + |\mathbf{Q}_1|^2 / Q_{max}^2]^2 - [1 + 2H\zeta dt + |\mathbf{Q}_1|^2 / Q_{max}^2]^2 + 4|\mathbf{Q}_1|^2 / Q_{max}^2}{[1 + 2H\zeta dt + |\mathbf{Q}_1|^2 / Q_{max}^2] + \sqrt{[1 + 2H\zeta dt + |\mathbf{Q}_1|^2 / Q_{max}^2]^2 - 4|\mathbf{Q}_1|^2 / Q_{max}^2}} \quad (B.12)$$

$$\frac{Q^2}{|\mathbf{Q}_1|^2} = \quad (B.13)$$

$$\frac{Q^2}{|\mathbf{Q}_1|^2} = \frac{Q^2}{2} \frac{1}{[1 + 2H\zeta dt + |\mathbf{Q}_1|^2 / Q_{max}^2] + \sqrt{[1 + 2H\zeta dt + |\mathbf{Q}_1|^2 / Q_{max}^2]^2 - 4|\mathbf{Q}_1|^2 / Q_{max}^2}}. \quad (B.14)$$

APPENDIX C

CUDA C CODE

The CUDA C simulation code is presented below.

```
1 /*
2  * Erik Palmer
3  * 10-22-2015
4  *
5  * Three species dumbbell simulation
6  *
7  * Evolves population of dumbbells over time according to
8  * flow characterists and species switching probabilities.
9  * Produces a measure of the stresses on the fluid.
10 *
11 * To Compile:
12 * nvcc <filename.cu> -lcurand -o <output file>
13 *
14 * GelModel:
15 * Use transistion probabilities from the physical arguments.
16 * Add ifdefs to control SAOS, and other aspects of the model
17 *
18 *
19 * SPECIES GUIDE:
20 * Int | Type
```

```

21  * 0 | Polymer One – Active
22  * 1 | Polymer One – Dangling
23  * 2 | Polymer Two – Active
24  * 3 | Polymer Two – Dangling
25  *
26  *
27  */
28
29
30  #include <stdio.h>
31  //required to compile on windows, must be before math.h
32  #define _USE_MATH_DEFINES
33  #include <math.h>
34  #include <stdlib.h>
35  #include <time.h>
36  #include <string.h>
37  #include <errno.h>
38  #include <ctype.h>
39  #include <stdint.h> //added to use unsigned int32
40
41  #include <cuda.h>
42  #include <curand.h>
43  #include <curand_kernel.h>
44  // #include <math_functions.h>
45  #include <unistd.h> //added to check for file existence
46
47
48
49  //Define Macros for Error handling

```

```

50
51 #define CUDA_CALL(x) do { if((x)!=cudaSuccess) { \
52     printf("Error at %s:%d\n", __FILE__,__LINE__); \
53     return EXIT_FAILURE; }} while(0)
54 #define CURAND_CALL(x) do { if((x)!= CURAND_STATUS_SUCCESS) { \
55     printf("Error at %s:%d\n", __FILE__, __LINE__); \
56     return EXIT_FAILURE; }} while(0)
57 //This one is better because it also outputs the error message
58 #define gpuErrchk(ans) { gpuAssert((ans), __FILE__, __LINE__);}
59 inline void gpuAssert(cudaError_t code, const char *file, int line,
60     bool abort=true)
61 {
62     if (code != cudaSuccess)
63     {
64         fprintf(stderr, "GPUassert: %s %s %d\n", cudaGetErrorString(code), file,
65             line);
66         if (abort) exit(code);
67     }
68 }
69
70 //define maximum filesize for raw data file 5e10 bytes = 50GB
71 #define RAWDATA_MAX_FILESIZE 1e10
72
73 #define MICRODATA_MAX_FILESIZE 2e11
74
75
76 //Define Macro for Histogram debugging
77 #define PRINT_VAR(x) printf(" " #x "\n ")
78

```



```

79 //Debugging Macros
80 #define PRINT_VAR_FLOAT_VALUE(x) printf("#x "=%f\n", x)
81 #define PRINT_VAR_INT_VALUE(x) printf("#x "=%d\n", x)
82 /* Also useful: printf("DEBUG LINE %d\n", __LINE__);
83
84
85 //___velocity field on-off matrix ___
86 // note that this matrix is multiplied by the inputed flowrate value
87 #define U11 0.0
88 #define U12 0.0
89 #define U21 1.0
90 #define U22 0.0
91 //*****
92
93 //__ Name for .csv file ___
94 #define OUTPUT_FILENAME "THREESPECIES"
95
96 /* Name for Raw Output File */
97 #define RAWDATA_FILENAME "RAWDATA"
98
99
100
101 #define INIT_ACT_TO_DNG_RATIO 0.5
102 #define TAO_FUND 5e-6 //Default 5e-6
103 #define ZEE 10.0 //Default 10.0
104 #define CHI 0.03 //Default 0.83
105 #define ALPHA 0.1 //Default 0.17
106 #define BETA 0.1 //Default 0.17
107 #define D_FREE 12.0 //Default 12.0

```

```

108
109 #define A_COEFF 1.2026e6
110 #define B_COEFF 6.4286e-5
111
112 //*****
113
114
115
116 //_____Define Global Variables_____
117 //For GPU
118 __device__ double devStepSizeMicro;
119 __device__ double devFlowRate;
120 __device__ double devMaxSpringLength;
121 __device__ double devFreq;
122
123
124 //For CPU
125 static unsigned int hostNumberOfParticles = 0;
126 static double hostStepSizeMicroFirst = 0;
127 static double hostStepSizeMicroSecon = 0;
128 static unsigned int hostTimeStepsMicro = 0;
129 static unsigned int hostTimeStepsMacro = 0;
130 static double hostFlowRate;
131 static double hostMaxSpringLength;
132 static double hostFreq;
133 static unsigned int hostMacroStepSizeSplitPt = 0;
134
135 //Additional Commandline Arguments
136 //GPU

```

```

137 __device__ double devD_free;
138 __device__ double devZee;
139 __device__ double devChi;
140 __device__ double devAlpha;
141 __device__ double devBeta;
142
143 //CPU
144 static double hostD_free = D_FREE;
145 static double hostZee = ZEE;
146 static double hostChi = CHI;
147 static double hostAlpha = ALPHA;
148 static double hostBeta = BETA;
149
150 static double Init_Active_Ratio;
151 static double Init_Dangle_Ratio;
152
153 #ifdef NO_REPORT
154 /*
155  * This variable wasn't doing anything useful so I hijacked it to
156  * create a period of the simulations where the output is not sent to the
157  * cpu to report it. Instead it stays on the GPU. Seems to speed things
158  * up quite a bit so far.
159  */
160 static unsigned long long hostA_coeff = A_COEFF;
161 #else
162 static double hostA_coeff = A_COEFF;
163 #endif
164
165 static double hostB_coeff = B_COEFF;

```

```

166
167 static int GPU_select;
168 static char RawData_select[256];
169 static char DataFileName[256];
170 //*****
171
172
173 //___ Struct defintions ___
174 typedef struct SpeciesValue {
175     double ActiveLen;
176     double DangleLen;
177     double LoopedLen;
178     double ActiveAng;
179     double DangleAng;
180     double LoopedAng;
181     double ActiveX;
182     double DangleX;
183     double LoopedX;
184     double ActiveY;
185     double DangleY;
186     double LoopedY;
187 } SpeciesValue;
188
189 typedef struct SpeciesCount {
190     int Active;
191     int Dangle;
192     int Looped;
193 } SpeciesCount;
194

```

```

195 typedef struct TwoDimSpring {
196     double x;
197     double y;
198 } TwoDimSpring;
199
200 typedef struct Stress {
201     double XX;
202     double XY;
203     double YY;
204 } Stress;
205
206 typedef struct Dumbbell {
207     int type;
208     double x;
209     double y;
210 } Dumbbell;
211
212 #ifdef SINGLE_MICRO
213 typedef struct DBSpecChng {
214     int type;
215     double time;
216     double x;
217     double y;
218 } DBSpecChng;
219 #endif
220 #ifdef MICRO_RAW
221 typedef struct DBSpecChng {
222     int type;
223     double length;

```

```

224 } DBSpecChng;
225 #endif
226
227 //*****
228
229 //Function: ParseInput
230 //Sorts and examines command line input for inappropriate data
231 int ParseInput(int argc, char *argv[]){
232
233
234     if ( argc > 1 && argc != 22 ){
235         printf("ERROR: Incorrect number of input arguments. 20 required.\n");
236         printf("Format: %s \n [number of dumbbells]\n", argv[0]);
237         printf(" [micro step size stage 1]\n [micro step size stage 2]\n ");
238         printf(" [micro time steps per macro step]\n ");
239         printf(" [total steps macro]\n ");
240         printf(" [number of macro steps with micro step size stage 1]\n ");
241         printf(" [flow rate]\n [Maximum Spring Length]\n");
242         printf(" [SAOS frequency]\n [Drag Coefficient]\n [Z]\n"
243             "[Alpha0]\n [Alpha1]\n");
244         printf(" [Beta]\n");
245         printf(" [Initial Percentage of Active Dumbbells]\n");
246         printf(" [Initial Percentage of Dangling Dumbbells]\n");
247         printf(" [A Coefficient]\n [B Coefficient]\n");
248         printf(" [GPU Device (0 or 1)]\n [Write Raw Data (Y or N)]\n");
249         printf(" [Output Filename]\n");
250         return EXIT_FAILURE;
251     } else if (argc ==1){
252

```

```

253     //Use default values
254     printf("Using default values.\n");
255
256     hostNumberOfParticles = 1048576;
257     hostStepSizeMicroFirst = 0.1;
258     hostStepSizeMicroSecon = 0.001;
259     hostTimeStepsMicro = 100;
260     hostTimeStepsMacro = 100;
261     hostMacroStepSizeSplitPt = 50;
262     hostFlowRate = 1.0;
263     hostMaxSpringLength = 5.0;
264     hostFreq = 1.0;
265     hostD_free = D_FREE;
266     hostZee = ZEE;
267     hostChi = CHI;
268     hostAlpha = ALPHA;
269     hostA_coeff = A_COEFF;
270     hostB_coeff = B_COEFF;
271     Init_Active_Ratio = 0.5;
272     Init_Dangle_Ratio = 0.5;
273
274     GPU_select = 0;
275
276     strcpy(RawData_select, "N");
277     strcpy(DataFileName, "DEFAULT");
278
279     return(0);
280 }
281

```

```

282
283     errno = 0;
284
285     //Num of dumbbells
286     hostNumberOfParticles = strtoul(argv[1], NULL, 10);
287     //micro step size stage 1
288     hostStepSizeMicroFirst = strtod(argv[2], NULL);
289     //micro step size stage 2
290     hostStepSizeMicroSecon = strtod(argv[3], NULL);
291     //number of micro time steps looped on GPU per single CPU macro step
292     hostTimeStepsMicro = strtoul(argv[4], NULL, 10);
293     //total number of macro time steps for the simulation
294     hostTimeStepsMacro = strtol(argv[5], NULL, 10);
295     //number of macro steps using micro steps of size stage 1
296     hostMacroStepSizeSplitPt = strtol(argv[6], NULL, 10);
297     hostFlowRate = strtod(argv[7], NULL);
298     hostMaxSpringLength = strtod(argv[8], NULL);
299     hostFreq = strtod(argv[9], NULL);
300
301     //additional command line arguments
302     hostD_free = strtod(argv[10], NULL);
303     hostZee = strtod(argv[11], NULL);
304     hostChi = strtod(argv[12], NULL);
305     hostAlpha = strtod(argv[13], NULL);
306     hostBeta = strtod(argv[14], NULL);
307     Init_Active_Ratio = strtod(argv[15], NULL);
308     Init_Dangle_Ratio = strtod(argv[16], NULL);
309     #ifdef NO_REPORT
310     hostA_coeff = strtoull(argv[17], NULL, 10);

```



```

311 #else
312     hostA_coeff = strtod(argv[17], NULL);
313     //New use: Number of macro steps to skip before recording data.
314     //(Speed sim runtime)
315 #endif
316     hostB_coeff = strtod(argv[18], NULL);
317
318     GPU_select = (int) strtol(argv[19], NULL,10);
319     strcpy(RawData_select, argv[20]);
320     strcpy(DataFileName, argv[21]);
321
322
323     if (hostNumberOfParticles==0){
324         printf("Unable to convert %s to positive integer\n", argv[1]);
325         return EXIT_FAILURE;
326     }
327
328     if (hostStepSizeMicroFirst==0){
329         printf("Unable to convert %s to double\n", argv[2]);
330         return EXIT_FAILURE;
331     }
332
333     if (hostStepSizeMicroSecon==0){
334         printf("Unable to convert %s to double\n", argv[3]);
335         return EXIT_FAILURE;
336     }
337
338     if (hostTimeStepsMicro==0){
339         printf("Unable to convert %s to positive integer\n", argv[4]);

```

```

340         return EXIT_FAILURE;
341     }
342
343     if (hostTimeStepsMacro==0){
344         printf("Unable to convert %s to positive integer\n", argv[5]);
345         return EXIT_FAILURE;
346     }
347
348     if (hostMacroStepSizeSplitPt==0){
349         printf("Unable to convert %s to positive integer\n", argv[6]);
350         return EXIT_FAILURE;
351     }
352
353     if (hostMaxSpringLength == 0){
354         printf("Unable to convert %s to positive double\n", argv[8]);
355         return EXIT_FAILURE;
356     }
357
358     if (hostFreq == 0){
359         printf("Unable to convert %s to positive double\n", argv[9]);
360         return EXIT_FAILURE;
361     }
362
363     //__ additional command line arguments __
364     if (hostD_free == 0){
365         printf("Unable to convert %s to positive double\n", argv[10]);
366         return EXIT_FAILURE;
367     }
368     if (hostZee == 0){

```

```

369         printf("Unable to convert %s to positive double\n", argv[11]);
370         return EXIT_FAILURE;
371     }
372
373     if (hostA_coeff == 0){
374         printf("hostA_coeff input error:"
375             " Unable to convert %s to positive double\n", argv[17]);
376         return EXIT_FAILURE;
377     }
378     if (hostB_coeff == 0){
379         printf("Unable to convert %s to positive double\n", argv[18]);
380         return EXIT_FAILURE;
381     }
382
383     switch(RawData_select[0]){
384         case 'N':
385         case 'n':
386             strcpy(RawData_select, "No");
387             break;
388         case 'Y':
389         case 'y':
390             strcpy(RawData_select, "Yes");
391             break;
392         default:
393             printf("The only valid choices to write raw data file are:"
394                 " Y,y,N,n\n");
395             return EXIT_FAILURE;
396     }
397

```

```

398     if ((RawData_select[0]!='Y')&&(RawData_select[0]!='N')
399         &&(RawData_select[0]!='y')&&(RawData_select[0]!='n'))
400     {
401         printf("The only valid choices to write raw data file are: Y,y,N,n\n");
402         return EXIT_FAILURE;
403     }
404     //////////////////////////////////////////////////
405
406     //Check to see if same filename for output exists.
407     // If the file exists, exit the program.
408     // This was done to fix the restarting issue
409
410     char CheckFilename[264];
411
412     sprintf(CheckFilename, "%s.csv", DataFileName);
413
414     if ( access ( CheckFilename, F_OK) != - 1 ){
415
416         printf("File: %s exists, exiting program.\n", CheckFilename);
417         return EXIT_FAILURE;
418     }
419
420     else {
421         //create empty file to hold the sapce.
422
423         FILE *OutputFile = NULL;
424         OutputFile = fopen(CheckFilename, "w");
425
426         if (OutputFile == NULL){

```

```

427         fprintf(stderr, "Couldn't open output file: %s!\n", CheckFilename);
428         exit(1);
429     }
430
431     fclose(OutputFile);
432 }
433
434 //Also check for bin file
435 sprintf(CheckFilename, "%s.bin", DataFileName);
436
437 if ( access ( CheckFilename, F_OK) != - 1 ){
438
439     printf("File: %s exists, exiting program.\n", CheckFilename);
440     return EXIT_FAILURE;
441 }
442
443
444 if (errno == ERANGE){
445     printf("%s\n", strerror(errno));
446     return EXIT_FAILURE;
447 }
448
449
450 return 0;
451 }
452
453
454
455

```

```

456
457
458
459 //Function PrinSimInfo
460 //Prints to terminal information about the current simulation
461 void PrintSimInfo(){
462
463     // ____ Calculate and output program parameters ____
464     printf("_____ Running Simulation _____ \n");
465     #ifdef SIMPLE_SHEAR
466         printf("|| Simple Shear Flow \n");
467     #else
468         printf("|| Small Oscillatory Shear Flow\n");
469     #endif
470     #ifdef LOOPED_DUMBBELLS
471         printf("|| Dumbbell Types: Active, Dangling and Looped\n");
472     #else
473         printf("|| Dumbbell Types: Active, and Dangling\n");
474     #endif
475
476
477
478     printf("|| Total Time: %g \n",
479         (hostStepSizeMicroFirst * hostMacroStepSizeSplitPt
480         + hostStepSizeMicroSecon
481         * (hostTimeStepsMacro - hostMacroStepSizeSplitPt))
482         * hostTimeStepsMicro );
483     printf("|| ----- Time Step Parameters ----- \n" );
484     printf("|| Total Number of Macro Steps: %u\n", hostTimeStepsMacro);

```

```

485     printf("|| Micro Steps Per Macro Iteration: %u\n", hostTimeStepsMicro);
486     printf("|| Macro Step Size Split Point: %u\n", hostMacroStepSizeSplitPt);
487     printf("||\n");
488     printf("|| ---- Stage One ---- \n");
489     printf("|| Micro Step Size: %1.12g\n", hostStepSizeMicroFirst);
490     printf("|| Macro Step Size: %1.12g\n", hostStepSizeMicroFirst
491             * hostTimeStepsMicro);
492     printf("|| Number of Macro Steps: %u\n", hostMacroStepSizeSplitPt);
493     printf("|| Stage One Total Time: %1.12g\n", hostStepSizeMicroFirst
494             * hostTimeStepsMicro * hostMacroStepSizeSplitPt);
495     printf("|| Flow Rate: 0 \n");
496     printf("||\n");
497     printf("|| ---- Stage Two ---- \n");
498     printf("|| Micro Step Size: %1.12g\n", hostStepSizeMicroSecon);
499     printf("|| Macro Step Size: %1.12g\n", hostStepSizeMicroSecon
500             * hostTimeStepsMicro);
501     printf("|| Number of Macro Steps: %u\n", hostTimeStepsMacro
502             - hostMacroStepSizeSplitPt);
503     printf("|| Stage Two Total Time: %1.12g\n", hostStepSizeMicroSecon
504             * hostTimeStepsMicro * (hostTimeStepsMacro - hostMacroStepSizeSplitPt));
505     printf("|| Flow Rate: %g \n", hostFlowRate);
506     printf("||\n");
507     printf("|| ----- Simulation Parameters ----- \n");
508     printf("|| Number of Particles: %u\n", hostNumberOfParticles);
509     printf("|| Maximum Spring Length: %g\n", hostMaxSpringLength );
510     printf("|| SAOS Frequency: %g\n", hostFreq );
511     printf("|| d: %g\n", hostD_free );
512     printf("|| Z: %g\n", hostZee );
513     printf("|| Chi: %g\n", hostChi);

```

```

514     printf("|| Alpha: %g\n", hostAlpha);
515     printf("|| Beta: %g\n", hostBeta);
516     printf("|| Initial Active Ratio: %g\n", Init_Active_Ratio);
517     printf("|| Initial Dangling Ratio: %g\n", Init_Dangle_Ratio);
518     printf("|| Initial Looped Ratio: %g\n",
519           1-Init_Dangle_Ratio-Init_Active_Ratio);
520 #ifdef NO_REPORT
521     printf("|| Macro Step Jump: %llu\n", hostA_coeff);
522 #else
523     printf("|| A Coefficient: %g\n", hostA_coeff);
524 #endif
525     printf("|| B Coefficient: %g\n", hostB_coeff);
526     printf("||\n");
527     printf("|| ----- Program Options ----- \n");
528     printf("|| Running on GPU device: %d\n", GPU_select);
529     printf("|| Write Raw Data: %s\n", RawData_select);
530     printf("|| Output Filename: %s\n", DataFileName);
531     printf(" - - - - - \n");
532
533     //*****
534 }
535
536 //Function OutputToFile
537 //Writes header containing information about the simulation
538 //and contents of three vectors to file
539
540 /*
541  * Write data to a .csv file
542  *

```



```

543 * Writes detailed parameter information and meta data to a csv
544 * whose file name is specified by OUTPUT_FILENAME
545 *
546 *
547 */
548 #ifndef SPEC_CHNG
549
550 void OutputToFile ( double XX[], double XY[], double YY[],
551                   double TimeTrack[], double time_spent, int count,
552                   char ProgName[],
553                   double ActiveRatio[], double DangleRatio[],
554                   double LoopedRatio[],
555                   SpeciesValue AvgLen[], SpeciesValue Variance[],
556                   int NumOfBins, SpeciesCount **Hist,
557                   Stress Time_k_Stress[], Stress Active_Stress[],
558                   Stress Dangle_Stress[],
559                   double AvgSpringLife[],
560                   unsigned int Dng2Act[], unsigned int Dng2Lpd[],
561                   unsigned int Act2Dng[], unsigned int Lpd2Dng[],
562                   char OutputFileName[]){
563
564 #else
565
566     // Function Description: output results to .CSV file
567 void OutputToFile ( double XX[], double XY[], double YY[],
568                   double TimeTrack[], double time_spent, int count,
569                   char ProgName[],
570                   double ActiveRatio[], double DangleRatio[],
571                   double LoopedRatio[],

```

```

572         SpeciesValue AvgLen[], SpeciesValue Variance[],
573         int NumOfBins, SpeciesCount **Hist,
574         Stress Time_k_Stress[], Stress Active_Stress[],
575         Stress Dangle_Stress[],
576         double AvgSpringLife[],
577         char OutputFileName[]){
578
579 #endif
580
581
582     FILE *OutputFile = NULL;
583
584     sprintf(OutputFileName, "%s.csv", OutputFileName); //<--- Filename
585
586     OutputFile = fopen(OutputFileName, "w+"); //w+ to overwrite file
587
588     if (OutputFile == NULL){
589         fprintf(stderr, "Couldn't open output file: %s!\n", OutputFileName);
590         exit(1);
591     }
592
593     // _____ Header for textfile _____
594     //Description
595
596     fprintf(OutputFile,
597     "*****",
598     "*****\n");
599     fprintf(OutputFile, "* %60s *\n", ProgName);
600     fprintf(OutputFile, "* Header - 8 lines, 1 thru 8,",

```

```

601             "Parameters+2 – 25 lines, 9 thru 33 *\n");
602     fprintf(OutputFile, "* Data header – 3 lines, 34 thru 36,",
603             " Stress Data – lines, 37+ *\n");
604
605     /*
606     * List preprocessor options so that it is clear in output.
607     */
608
609     fprintf(OutputFile, " Preprocessor Options: ");
610     #ifdef SIMPLE_SHEAR
611     fprintf(OutputFile, "SIMPLE_SHEAR, ");
612     #else
613     fprintf(OutputFile, "OSCILLATORY_SHEAR, ");
614     #endif
615
616     #ifdef LOOPED_DUMBBELLS
617     fprintf(OutputFile, "LOOPED_DUMBBELLS, ");
618     #else
619     fprintf(OutputFile, "ACTIVE_AND_DANGLING_ONLY, ");
620     #endif
621
622     #ifdef NEW_TAU
623     fprintf(OutputFile, "NEW_TAU, ");
624     #endif
625
626     #ifdef RAW_OUT
627     fprintf(OutputFile, "RAW_OUT, ");
628     #endif
629

```

```

630 #ifdef DEBUG
631     fprintf(OutputFile, "DEBUG, ");
632 #endif
633
634 #ifdef SPEC_CHNG
635     fprintf(OutputFile, "SPEC_CHNG, ");
636 #endif
637
638 #ifdef SINGLE_MICRO
639     fprintf(OutputFile, "SINGLE_MICRO: ID(unit):%d Type(int):%lu",
640             " Length(double):%lu ",
641             SINGLE_MICRO, sizeof(int), sizeof(double));
642 #endif
643 #ifdef MICRO_RAW
644     fprintf(OutputFile, "MICRO_RAW: ID(unit):%lu Type(int):%lu",
645             " Length(double):%lu ",
646             sizeof(unsigned int), sizeof(int), sizeof(double));
647 #endif
648
649
650 #ifdef FIXED_SEED
651     fprintf(OutputFile, "FIXED_SEED, ");
652 #endif
653
654 #ifdef SINGLE_MICRO
655     fprintf(OutputFile, "SINGLE_MICRO, ");
656 #endif
657
658 #ifdef MICRO_RAW

```

```
659     fprintf(OutputFile, "MICRO_RAW, ");
660 #endif
661
662 #ifdef COND_PROB_METHOD
663     fprintf(OutputFile, "COND_PROB_METHOD, ");
664 #endif
665
666 #ifdef CHK_DNG
667     fprintf(OutputFile, "CHK_DNG, ");
668 #endif
669
670 #ifdef LEN_CHG
671     fprintf(OutputFile, "LEN_CHG, ");
672 #endif
673
674 #ifdef PROB_TEST
675     fprintf(OutputFile, "PROB_TEST, ");
676 #endif
677
678 #ifdef SINGLE_TRACK
679     fprintf(OutputFile, "SINGLE_TRACK, ");
680 #endif
681
682 #ifdef LOOP_PROB_TWO
683     fprintf(OutputFile, "LOOP_PROB_TWO, ");
684 #endif
685
686 #ifdef LOOP_PROB_THREE
687     fprintf(OutputFile, "LOOP_PROB_THREE, ");
```

```
688 #endif
689
690 #ifdef LOOP_PROB_FOUR
691     fprintf(OutputFile, "LOOP_PROB_FOUR, ");
692 #endif
693
694 #ifdef NO_REPORT
695     fprintf(OutputFile, "NO_REPORT: %llu,", hostA_coeff);
696 #endif
697
698 #ifdef SKEW_START
699     fprintf(OutputFile, "SKEW_START, ");
700 #endif
701
702 #ifdef LEN_CHN_NORM
703     fprintf(OutputFile, "LEN_CHN_NORM, ");
704 #endif
705
706 #ifdef LOOP_FREEZE
707     fprintf(OutputFile, "LOOP_FREEZE, ");
708 #endif
709
710 #ifdef FULL_DATA
711     fprintf(OutputFile, "FULL_DATA");
712 #endif
713
714     fprintf(OutputFile, "\n");
715
716
```

```

717 #ifdef SIMPLE_SHEAR
718     fprintf(OutputFile,"* Simple Shear Flow ",
719             " *\n");
720 #else
721     fprintf(OutputFile,"* Small Oscillatory Shear Flow ",
722             " *\n");
723 #endif
724 #ifdef LOOPED_DUMBBELLS
725     fprintf(OutputFile,"* Dumbbell Types: Active, Dangling and Looped ",
726             " *\n");
727 #else
728     fprintf(OutputFile,"* Dumbbell Types: Active, and Dangling ",
729             " *\n");
730 #endif
731
732 #ifdef RAW_OUT
733     fprintf(OutputFile,"***** Has Raw Output Bin File",
734             " *****\n");
735 #else
736     fprintf(OutputFile,"*****",
737             "*****\n");
738 #endif
739
740
741 #ifdef NO_REPORT
742     fprintf(OutputFile,"Total_Time: %g \n",
743             hostStepSizeMicroFirst * (hostMacroStepSizeSplitPt - 1) *
744             hostTimeStepsMicro + //Stage 1
745             hostStepSizeMicroSecon * hostA_coeff + //Macro Jump

```

```

746     hostStepSizeMicroSecon *
747     (hostTimeStepsMacro – hostMacroStepSizeSplitPt )
748     * hostTimeStepsMicro ); //Stage 2
749 #else
750     fprintf(OutputFile,"Total_Time: %g \n", (hostStepSizeMicroFirst *
751     hostMacroStepSizeSplitPt + hostStepSizeMicroSecon *
752     (hostTimeStepsMacro – hostMacroStepSizeSplitPt)) *
753     hostTimeStepsMicro );
754 #endif
755     fprintf(OutputFile,"Total_Number_of_Macro_Steps: %u\n",
756     hostTimeStepsMacro);
757     fprintf(OutputFile,"Micro_Steps_Per_Macro_Iteration: %u\n",
758     hostTimeStepsMicro);
759     fprintf(OutputFile,"Macro_Step_Size_Split_Point: %u\n",
760     hostMacroStepSizeSplitPt);
761     fprintf(OutputFile,"Micro_Step_Size_One: %1.12g\n",
762     hostStepSizeMicroFirst);
763     fprintf(OutputFile,"Macro_Step_Size_One: %1.12g\n",
764     hostStepSizeMicroFirst * hostTimeStepsMicro);
765     fprintf(OutputFile,"Number_of_Macro_Steps_Stage_One: %u\n",
766     hostMacroStepSizeSplitPt);
767     fprintf(OutputFile,"Stage_One_Total_Time: %1.12g\n",
768     hostStepSizeMicroFirst * hostTimeStepsMicro *
769     hostMacroStepSizeSplitPt);
770     fprintf(OutputFile,"Micro_Step_Size_Two: %1.12g\n",
771     hostStepSizeMicroSecon);
772     fprintf(OutputFile,"Macro_Step_Size_Two: %1.12g\n",
773     hostStepSizeMicroSecon * hostTimeStepsMicro);
774     fprintf(OutputFile,"Number_of_Macro_Steps_Stage_Two: %u\n",

```



```

775         hostTimeStepsMacro – hostMacroStepSizeSplitPt);
776     fprintf(OutputFile,"Stage_Two_Total_Time: %1.12g\n",
777         hostStepSizeMicroSecon * hostTimeStepsMicro *
778         (hostTimeStepsMacro – hostMacroStepSizeSplitPt));
779     fprintf(OutputFile,"Number_of_Particles: %u\n", hostNumberOfParticles);
780     fprintf(OutputFile,"Flow_Rate: %g \n", hostFlowRate);
781     fprintf(OutputFile,"Maximum_Spring_Length: %g\n", hostMaxSpringLength );
782     fprintf(OutputFile,"SAOS_Frequency: %g\n", hostFreq );
783     fprintf(OutputFile,"d: %g\n", hostD_free );
784     fprintf(OutputFile,"Z: %g\n", hostZee );
785     fprintf(OutputFile,"Chi: %g\n", hostChi);
786     fprintf(OutputFile,"Alpha: %g\n", hostAlpha);
787     fprintf(OutputFile,"Beta: %g\n", hostBeta);
788     fprintf(OutputFile,"Initial_Active_Ratio: %g\n", Init_Active_Ratio);
789     fprintf(OutputFile,"Initial_Dangling_Ratio: %g\n", Init_Dangle_Ratio);
790     fprintf(OutputFile,"Initial_Looped_Ratio: %g\n",
791         1–Init_Dangle_Ratio–Init_Active_Ratio);
792     #ifdef NO_REPORT
793         fprintf(OutputFile,"Macro_Step_Jump: %llu\n", hostA_coeff);
794     #else
795         fprintf(OutputFile,"A_Coefficient: %g\n", hostA_coeff);
796     #endif
797     fprintf(OutputFile,"B_Coefficient: %g\n", hostB_coeff);
798     fprintf(OutputFile,"Runtime: %g\n", time_spent);
799
800
801     //.....
802
803

```

```

804  /*Nicer table output */
805
806      fprintf(OutputFile," %20s," , "Time");
807      fprintf(OutputFile," %20s," , "StressXX");
808      fprintf(OutputFile," %20s," , "StressXY");
809      fprintf(OutputFile," %20s," , "StressYY");
810      fprintf(OutputFile," %20s," , "Active_Stress_XX");
811      fprintf(OutputFile," %20s," , "Active_Stress_XY");
812      fprintf(OutputFile," %20s," , "Active_Stress_YY");
813      fprintf(OutputFile," %20s," , "Dangle_Stress_XX");
814      fprintf(OutputFile," %20s," , "Dangle_Stress_XY");
815      fprintf(OutputFile," %20s," , "Dangle_Stress_YY");
816      fprintf(OutputFile," %20s," , "ActiveRatio");
817      fprintf(OutputFile," %20s," , "DangleRatio");
818      fprintf(OutputFile," %20s," , "LoopedRatio");
819      fprintf(OutputFile," %20s," , "AvgLen.ActiveLen");
820      fprintf(OutputFile," %20s," , "AvgLen.ActiveAng");
821      fprintf(OutputFile," %20s," , "AvgLen.ActiveX");
822      fprintf(OutputFile," %20s," , "AvgLen.ActiveY");
823      fprintf(OutputFile," %20s," , "AvgLen.DangleLen");
824      fprintf(OutputFile," %20s," , "AvgLen.DangleAng");
825      fprintf(OutputFile," %20s," , "AvgLen.DangleX");
826      fprintf(OutputFile," %20s," , "AvgLen.DangleY");
827      fprintf(OutputFile," %20s," , "AvgLen.LoopedLen");
828      fprintf(OutputFile," %20s," , "AvgLen.LoopedAng");
829      fprintf(OutputFile," %20s," , "AvgLen.LoopedX");
830      fprintf(OutputFile," %20s," , "AvgLen.LoopedY");
831      fprintf(OutputFile," %20s," , "Variance.ActiveLen");
832      fprintf(OutputFile," %20s," , "Variance.ActiveAng");

```

```

833     fprintf(OutputFile," %20s," , "Variance.ActiveX");
834     fprintf(OutputFile," %20s," , "Variance.ActiveY");
835     fprintf(OutputFile," %20s," , "Variance.DangleLen");
836     fprintf(OutputFile," %20s," , "Variance.DangleAng");
837     fprintf(OutputFile," %20s," , "Variance.DangleX");
838     fprintf(OutputFile," %20s," , "Variance.DangleY");
839     fprintf(OutputFile," %20s," , "Variance.LoopedLen");
840     fprintf(OutputFile," %20s," , "Variance.LoopedAng");
841     fprintf(OutputFile," %20s," , "Variance.LoopedX");
842     fprintf(OutputFile," %20s," , "Variance.LoopedY");
843     fprintf(OutputFile," %20s," , "AvgSpringLife");
844
845     #ifdef SPEC_CHNG
846         fprintf(OutputFile," %20s," , "Dng2Act");
847         fprintf(OutputFile," %20s," , "Dng2Lpd");
848         fprintf(OutputFile," %20s," , "Act2Dng");
849         fprintf(OutputFile," %20s," , "Lpd2Dng");
850     #endif
851
852     fprintf(OutputFile," %50s" , "Histogram Bins: Active, Dangle, Looped – ");
853     fprintf(OutputFile,"%d each\n", NumOfBins);
854
855
856
857
858     /* write data to file */
859
860     unsigned int k;
861     for (k=0; k<count; k++){

```

```

862     fprintf(OutputFile," % 20.6f," , TimeTrack[k]);
863     fprintf(OutputFile," % 20.10f," , XX[k]);
864     fprintf(OutputFile," % 20.10f," , XY[k]);
865     fprintf(OutputFile," % 20.10f," , YY[k]);
866     fprintf(OutputFile," % 20.10f," , Active_Stress[k].XX);
867     fprintf(OutputFile," % 20.10f," , Active_Stress[k].XY);
868     fprintf(OutputFile," % 20.10f," , Active_Stress[k].YY);
869     fprintf(OutputFile," % 20.10f," , Dangle_Stress[k].XX);
870     fprintf(OutputFile," % 20.10f," , Dangle_Stress[k].XY);
871     fprintf(OutputFile," % 20.10f," , Dangle_Stress[k].YY);
872     fprintf(OutputFile," % 20.6f," , ActiveRatio[k]);
873     fprintf(OutputFile," % 20.6f," , DangleRatio[k]);
874     fprintf(OutputFile," % 20.6f," , LoopedRatio[k]);
875     fprintf(OutputFile," % 20.6f," , AvgLen[k].ActiveLen);
876     fprintf(OutputFile," % 20.6f," , AvgLen[k].ActiveAng);
877     fprintf(OutputFile," % 20.6f," , AvgLen[k].ActiveX);
878     fprintf(OutputFile," % 20.6f," , AvgLen[k].ActiveY);
879     fprintf(OutputFile," % 20.6f," , AvgLen[k].DangleLen);
880     fprintf(OutputFile," % 20.6f," , AvgLen[k].DangleAng);
881     fprintf(OutputFile," % 20.6f," , AvgLen[k].DangleX);
882     fprintf(OutputFile," % 20.6f," , AvgLen[k].DangleY);
883     fprintf(OutputFile," % 20.6f," , AvgLen[k].LoopedLen);
884     fprintf(OutputFile," % 20.6f," , AvgLen[k].LoopedAng);
885     fprintf(OutputFile," % 20.6f," , AvgLen[k].LoopedX);
886     fprintf(OutputFile," % 20.6f," , AvgLen[k].LoopedY);
887     fprintf(OutputFile," % 20.6f," , Variance[k].ActiveLen);
888     fprintf(OutputFile," % 20.6f," , Variance[k].ActiveAng);
889     fprintf(OutputFile," % 20.6f," , Variance[k].ActiveX);
890     fprintf(OutputFile," % 20.6f," , Variance[k].ActiveY);

```

```

891         fprintf(OutputFile," % 20.6f," , Variance[k].DangleLen);
892         fprintf(OutputFile," % 20.6f," , Variance[k].DangleAng);
893         fprintf(OutputFile," % 20.6f," , Variance[k].DangleX);
894         fprintf(OutputFile," % 20.6f," , Variance[k].DangleY);
895         fprintf(OutputFile," % 20.6f," , Variance[k].LoopedLen);
896         fprintf(OutputFile," % 20.6f," , Variance[k].LoopedAng);
897         fprintf(OutputFile," % 20.6f," , Variance[k].LoopedX);
898         fprintf(OutputFile," % 20.6f," , Variance[k].LoopedY);
899     fprintf(OutputFile," % 20.6f," , AvgSpringLife[k]);
900
901     #ifdef SPEC_CHNG
902         fprintf(OutputFile," %20u," , Dng2Act[k]);
903         fprintf(OutputFile," %20u," , Dng2Lpd[k]);
904         fprintf(OutputFile," %20u," , Act2Dng[k]);
905         fprintf(OutputFile," %20u," , Lpd2Dng[k]);
906     #endif
907
908
909     for(unsigned int n=0; n<NumOfBins; n++){
910         fprintf(OutputFile," % 12d," , Hist[n][k].Active);
911     }
912     for(unsigned int n=0; n<NumOfBins; n++){
913         fprintf(OutputFile," % 12d," , Hist[n][k].Dangle);
914     }
915     for(unsigned int n=0; n<NumOfBins-1; n++){
916         fprintf(OutputFile," % 12d," , Hist[n][k].Looped);
917     }
918
919     fprintf(OutputFile, " % 12d\n" , Hist[NumOfBins-1][k].Looped);

```

```

920
921
922     }
923     //.....
924
925     fclose(OutputFile);
926
927 }
928
929 /*
930  * No longer being used
931  * CPU Function: Raw Data
932  *
933  * Output all x, y and species data for each dumbbell and write it to
934  * a second raw data csv file.
935  *
936  *
937  */
938
939 void WriteRawDataFile(double TimeTrack[], Dumbbell *RawDBellData[])
940 {
941     FILE *RawOutput = NULL;
942     char RawDataFilename[] = RAWDATA_FILENAME;
943
944
945     RawOutput = fopen(RawDataFilename, "w");
946
947     if (RawOutput == NULL)
948     {

```

```

949     fprintf(stderr, "Could not open output file: %s!\n", RawDataFilename);
950     exit(1);
951 }
952
953 for(unsigned int k=0; k<hostTimeStepsMacro+1; k++)
954 {
955     fprintf(RawOutput, "%9.6f, ", TimeTrack[k]);
956     for(unsigned int j=0; j<hostNumberOfParticles; j++)
957         fprintf(RawOutput, "% .2d, % 20.14f, % 20.14f, ",
958                 RawDBellData[k][j].type,
959                 RawDBellData[k][j].x,
960                 RawDBellData[k][j].y);
961     fprintf(RawOutput, "\n");
962 }
963
964
965
966     fclose(RawOutput);
967 }
968
969
970
971
972 //Function:
973 //GPU Function
974 //Caclulates the change of state probability of an active dumbbell
975 //given the spring length
976 //Tao must be commputed each time: See paper, use equations 10 AND 11.
977 device double ActiveToDanglingProb (double SpringLen, double MicroStepSize){

```

```

978
979
980  /*
981   * These probabilities are based on the reasoning in notebook:
982   * Transition Probability Physical Argugments
983   *
984   */
985 #ifndef PROB_TEST
986   //transition probabilities held constant
987   return devBeta;
988
989 #else
990   //Normal transition probabilities
991
992
993   double F_fene = SpringLen /
994     ( 1 - SpringLen * SpringLen / devMaxSpringLength / devMaxSpringLength );
995
996
997   return 1 - exp( - devBeta * exp( 0.0325 * abs( F_fene )) * MicroStepSize);
998
999 #endif
1000 }
1001
1002 //Function:
1003 //GPU Function
1004 //Cacluates the change of state probability for a dangling dumbbell.
1005 __device__ double DanglingToActiveProb (double SpringLen, double MicroStepSize){
1006

```



```

1007
1008 #ifndef PROB_TEST
1009     //transition probabilities held constant
1010     return devAlpha;
1011
1012 #else
1013     //Normal transition probabilities
1014
1015     double F_fene = SpringLen /
1016     ( 1 - SpringLen * SpringLen / devMaxSpringLength / devMaxSpringLength );
1017
1018     return 1.0 - exp( - devAlpha * SpringLen * F_fene * MicroStepSize );
1019 #endif
1020 }
1021
1022 //Function:
1023 //GPU Function
1024 //Calculates the probability of an chain going active becoming
1025 // a loop instead of a bridge
1026 __device__ double DanglingToLoopedProb (double SpringLen,
1027                                         double MicroStepSize){
1028
1029 #ifndef LOOP_PROB_TWO
1030     double F_fene_two = SpringLen /
1031     ( 1 - (devMaxSpringLength - SpringLen) *
1032     (devMaxSpringLength - SpringLen) /
1033     devMaxSpringLength / devMaxSpringLength );
1034
1035     return 1 - exp( - devChi * (devMaxSpringLength - SpringLen)*

```

```

1036     (devMaxSpringLength – SpringLen) / F_fene_two * MicroStepSize );
1037 #else
1038 #ifdef LOOP_PROB_THREE
1039     double F_fene_two = 1 / ( 1 – (devMaxSpringLength – SpringLen) *
1040     (devMaxSpringLength – SpringLen) /
1041     devMaxSpringLength / devMaxSpringLength );
1042
1043     return 1 – exp( – devChi * (devMaxSpringLength – SpringLen) *
1044     (devMaxSpringLength – SpringLen) * F_fene_two * MicroStepSize );
1045 #else
1046 #ifdef LOOP_PROB_FOUR
1047     double F_fene_two = 1 / ( 1 – (devMaxSpringLength – SpringLen) *
1048     (devMaxSpringLength – SpringLen) /
1049     devMaxSpringLength / devMaxSpringLength );
1050
1051     return 1 – exp( – devChi * SpringLen *
1052     (devMaxSpringLength – SpringLen) *
1053     (devMaxSpringLength – SpringLen) * F_fene_two * MicroStepSize );
1054 #else
1055     return exp( – SpringLen * SpringLen / devChi * MicroStepSize );
1056 #endif
1057 #endif
1058 #endif
1059
1060
1061
1062 }
1063
1064 //Function:

```

```

1065 //GPU Function
1066 //Calculates the probability looped chain becoming a dangling chain
1067 __device__ double LoopedToDanglingProb (double SpringLen,
1068                                         double MicroStepSize){
1069
1070     /*
1071      * These probabilities are based on the reasoning in notebook:
1072      * Proposed Transition Probabilities One
1073      *
1074      * This probability doesn't depend on the length of the dumbbell
1075      * because the behavior of looped dumbbells are not modeled
1076      * [Although there are still some numbers in the simulation].
1077      *
1078      */
1079
1080     return 1.0 - exp( - devBeta * MicroStepSize );
1081 }
1082
1083 //Function:
1084 //GPU Function
1085 //Calculate the conditional probability of becoming a loop given
1086 //that a dangling dumbbell does not become active.
1087 __device__ double DangleNotActToLoop (double SpringLen,
1088                                       double MicroStepSize, int dbell, double time){
1089
1090     double F_fene = SpringLen / ( 1 - SpringLen * SpringLen /
1091                                   devMaxSpringLength / devMaxSpringLength );
1092
1093

```

```

1094     double cond_prob = exp( - SpringLen * SpringLen *
1095         ( 1 / devChi - devAlpha / F_fene ) * MicroStepSize );
1096
1097
1098     if (cond_prob <= 1.0){
1099         return cond_prob;
1100     } else {
1101         return 1.0;
1102     }
1103
1104
1105 }
1106
1107
1108 __device__ double DanglingToAttachProb(double SpringLen, double MicroStepSize){
1109
1110     double AttachProb;
1111     AttachProb = DanglingToActiveProb(SpringLen, MicroStepSize) +
1112         DanglingToLoopedProb(SpringLen, MicroStepSize);
1113
1114     if (AttachProb > 1.0) {
1115         return 1.0;
1116     } else {
1117         return AttachProb;
1118     }
1119
1120 }
1121
1122

```

```

1123
1124 //Function: AttachedLoop
1125 ___device___ double AttachedToLoopedProb(double SpringLen, double MicroStepSize){
1126
1127     return DanglingToLoopedProb( SpringLen, MicroStepSize) /
1128         ( DanglingToLoopedProb( SpringLen, MicroStepSize) +
1129           DanglingToActiveProb( SpringLen, MicroStepSize) );
1130
1131 }
1132
1133
1134 //Function: AttachedLoop
1135 ___device___ double AttachedToActiveProb(double SpringLen,
1136                                           double MicroStepSize){
1137
1138     return DanglingToActiveProb( SpringLen, MicroStepSize) /
1139         ( DanglingToLoopedProb( SpringLen, MicroStepSize) +
1140           DanglingToActiveProb( SpringLen, MicroStepSize) );
1141
1142 }
1143
1144
1145 //Function: Evolve
1146 //GPU Function
1147 // Describes how length evolves over the specified time step size
1148 ___device___ void Evolve(double *SpringLenX, double *SpringLenY, double randx,
1149                          double randy, double drag_coeff, double *SimTime,
1150                          double MicroStepSize, double FlowRate){
1151

```

```

1152     double SpringLenXStep, SpringLenYStep;
1153
1154     //__ Intermediate step variables
1155     double SpringLenXOne, SpringLenYOne;
1156     double ItermValueOne, ItermValueTwo;
1157     double LengthLimitingFactor;
1158     //"....."
1159
1160
1161     //_____ Non-Dim Evolution Equations for dangling FENE dumbbells _____
1162
1163
1164
1165     #ifndef SIMPLE_SHEAR //Uses a compiler flag to switch to simple_shear
1166
1167     /* Simple Shear with Variable Flow Rate */
1168
1169         SpringLenXOne = *SpringLenX
1170         + (U11 * *SpringLenX + U21 * *SpringLenY) * FlowRate * MicroStepSize
1171         + sqrt( drag_coeff * MicroStepSize) * randx;
1172     #else
1173
1174     /* Small Amplitude Oscillatory Shear Flow
1175     * with Variable Flow Rate (Allows for equilibrium period)
1176     */
1177
1178         SpringLenXOne = *SpringLenX
1179         + (U11 * *SpringLenX + U21 * devFreq * cos(devFreq * *SimTime) *
1180         *SpringLenY) * FlowRate * MicroStepSize

```

```

1181         + sqrt( drag_coeff * MicroStepSize) * randx;
1182
1183 #endif
1184
1185     /* note: flow in the y-direction is unaffected */
1186
1187     SpringLenYOne = *SpringLenY
1188         + (U12 * *SpringLenX + U22 * *SpringLenY)
1189         * FlowRate * MicroStepSize
1190         + sqrt( drag_coeff * MicroStepSize) * randy;
1191
1192
1193     LengthLimitingFactor = ( SpringLenXOne * SpringLenXOne +
1194                             SpringLenYOne * SpringLenYOne )
1195                             / devMaxSpringLength / devMaxSpringLength;
1196
1197     ItermValueOne = 1.0 + 2.0 * drag_coeff * MicroStepSize +
1198         LengthLimitingFactor;
1199
1200     ItermValueTwo = 2 / ( ItermValueOne +
1201 sqrt( ItermValueOne * ItermValueOne - 4 * LengthLimitingFactor) );
1202
1203     SpringLenXStep = sqrt ( ItermValueTwo ) * SpringLenXOne;
1204
1205     SpringLenYStep = sqrt ( ItermValueTwo ) * SpringLenYOne;
1206
1207     //.....
1208
1209

```

```

1210     *SpringLenX = SpringLenXStep;
1211     *SpringLenY = SpringLenYStep;
1212
1213 }
1214
1215 //Function: Micro_Steps
1216 //Loops through the Micro loop of the SDE
1217 #ifndef SPEC_CHNG
1218
1219 __global__ void Micro_Steps( double *SpringLenX, double *SpringLenY,
1220     int *SpeciesType,
1221     curandState *states, curandState *ProbStates,
1222     double AvgSpringLifes, double *SimTime, double MicroStepSize,
1223     unsigned int TimeStepsMicro,
1224     double DangleAvgLen, double FlowRate,
1225     unsigned int *Dng2Act, unsigned int *Dng2Lpd,
1226     unsigned int *Act2Dng, unsigned int *Lpd2Dng){
1227
1228 #else
1229 #ifndef MICRO_RAW
1230
1231 __global__ void Micro_Steps( double *SpringLenX, double *SpringLenY,
1232     int *SpeciesType,
1233     curandState *states, curandState *ProbStates,
1234     double AvgSpringLifes, double *SimTime, double MicroStepSize,
1235     unsigned int TimeStepsMicro,
1236     double DangleAvgLen, double FlowRate,
1237     DBSpecChng *SCArr, unsigned int NumberOfParticles){
1238 #else

```



```

1239 #ifdef NO_REPORT
1240 __global__ void Micro_Steps( double *SpringLenX, double *SpringLenY,
1241     int *SpeciesType,
1242     curandState *states, curandState *ProbStates,
1243     double AvgSpringLifes, double *SimTime, double MicroStepSize,
1244     unsigned long long TimeStepsMicro,
1245     double DangleAvgLen, double FlowRate){
1246
1247 #else
1248 #ifdef SINGLE_MICRO
1249
1250 __global__ void Micro_Steps( double *SpringLenX, double *SpringLenY,
1251     int *SpeciesType,
1252     curandState *states, curandState *ProbStates,
1253     double AvgSpringLifes, double *SimTime, double MicroStepSize,
1254     unsigned int TimeStepsMicro,
1255     double DangleAvgLen, double FlowRate,
1256     DBSpecChng *SCArr, unsigned int NumberOfParticles){
1257 #else
1258 __global__ void Micro_Steps( double *SpringLenX, double *SpringLenY,
1259     int *SpeciesType,
1260     curandState *states, curandState *ProbStates,
1261     double AvgSpringLifes, double *SimTime, double MicroStepSize,
1262     unsigned int TimeStepsMicro,
1263     double DangleAvgLen, double FlowRate){
1264 #endif //SINGLE_MICRO
1265 #endif //NO_REPORT
1266 #endif //MICRO_RAW
1267 #endif //SPEC_CHNG

```

```

1268
1269
1270
1271
1272
1273
1274     int i = threadIdx.x + blockIdx.x * blockDim.x;
1275
1276
1277     //___Device API for Random Number Generation___
1278     //copy state to local state for efficiency
1279     curandState localState = states[i];
1280     curandState localProbState = ProbStates[i];
1281
1282
1283     //___ Calculation values and constants
1284
1285
1286
1287     #ifdef SPEC_CHNG
1288         // set counters to 0
1289         Dng2Act[i]=0;
1290         Dng2Lpd[i]=0;
1291         Act2Dng[i]=0;
1292         Lpd2Dng[i]=0;
1293     #endif
1294
1295
1296     #ifdef MICRO_RAW

```

```

1297     /* printf("Thread:%d Precur:%d Time:%f Length:%f \n", i, */
1298     /* SCArr[i*TimeStepsMicro].type, */
1299     /* SCArr[i*TimeStepsMicro].time, */
1300     /* SCArr[i*TimeStepsMicro].length); */
1301 #endif
1302
1303     //____ Node drag value calculations ____
1304
1305     double D_node = 0.5 * devZee * 6.0 * devD_free;
1306     //Equation (25) – non-dimensional
1307
1308     double drag_coeff_active = devD_free / (2 * D_node);
1309     //Nondimensionalized
1310
1311     double drag_coeff_dangle = (D_node + devD_free) / 4.0 / D_node;
1312
1313
1314     //*****
1315
1316
1317
1318     //*****
1319
1320
1321     double2 RandNorm;
1322     double RandUniform;
1323
1324 #ifdef LOOPED_DUMBBELLS
1325

```

```

1326         double RandUniform2;
1327
1328
1329 #endif
1330
1331 #ifdef DEBUG
1332     //printf("TimeStepsMicro = %d\n", TimeStepsMicro);
1333 #endif
1334
1335         double SpringLen;
1336         for(unsigned long long j=0; j < TimeStepsMicro; j++){
1337             //changed to unsigned long long for large loop cnts
1338
1339
1340
1341
1342
1343 #ifdef SINGLE_TRACK
1344     if (i==0){
1345         printf("SingleTrack:%f,%d:%f:%f\n",SimTime[i],SpeciesType[i],
1346             SpringLenX[i],SpringLenY[i]);
1347     }
1348 #endif
1349
1350
1351
1352         //generate new random number each time
1353         RandNorm = curand_normal2_double(&localState);
1354         RandUniform = curand_uniform_double(&localProbState);

```

```

1355
1356 #ifndef LOOPED_DUMBBELLS
1357     RandUniform2 = curand_uniform_double(&localProbState);
1358
1359
1360 #endif
1361
1362 #ifdef LEN_CHG
1363     /*
1364     * Added to check if looped re-entry is responsible for phenomena
1365     * Reinserts loops as randomly angled short dumbbells.
1366     */
1367     double RandUniform3;
1368     double RandUniform4;
1369
1370     RandUniform3 = curand_uniform_double(&localProbState);
1371     RandUniform4 = curand_uniform_double(&localProbState);
1372 #endif
1373
1374
1375 #ifdef LEN_CHN_NORM
1376     /*
1377     * Reinserts loops with length and orientation from a Gaussian dist.
1378     * Careful using this a short maximum dumbbell length.
1379     */
1380     double2 RandNorm2;
1381     RandNorm2 = curand_normal2_double(&localState);
1382 #endif
1383

```

```

1384
1385
1386
1387         //Calculate Spring Length
1388         SpringLen = sqrt(SpringLenX[i] * SpringLenX[i] +
1389             SpringLenY[i] * SpringLenY[i]);
1390
1391 #ifndef SINGLE_MICRO
1392     //record type, time, and length of each step
1393     if (i==SINGLE_MICRO){
1394         SCArr[j].type = SpeciesType[i];
1395         SCArr[j].time = SimTime[i];
1396         SCArr[j].x = SpringLenX[i];
1397         SCArr[j].y = SpringLenY[i];
1398     }
1399 #endif
1400
1401 #ifndef MICRO_RAW
1402     //record type, time, and length of each step
1403     SCArr[i*TimeStepsMicro+j].type = SpeciesType[i];
1404     SCArr[i*TimeStepsMicro+j].length = SpringLen;
1405 #endif
1406
1407
1408
1409 #ifndef LOOPED_DUMBBELLS
1410     switch(SpeciesType[i]) {
1411
1412         case 0: //Active Type

```

```

1413             Evolve(&SpringLenX[i], &SpringLenY[i],
1414             RandNorm.x, RandNorm.y,
1415             drag_coeff_active, &SimTime[i],
1416             MicroStepSize, FlowRate);
1417
1418             if (ActiveToDanglingProb(SpringLen, MicroStepSize) >
1419             RandUniform){
1420             // if threshold prob is higher than uniform rand number then..
1421             SpeciesType[i] = 1; //Change dumbbell to Dangling species
1422 #ifndef SPEC_CHNG
1423             Act2Dng[i]++;
1424 #endif
1425             }
1426
1427             break;
1428
1429             case 1: //Dangling Type
1430
1431             Evolve(&SpringLenX[i], &SpringLenY[i],
1432             RandNorm.x, RandNorm.y,
1433             drag_coeff_dangle, &SimTime[i],
1434             MicroStepSize, FlowRate);
1435
1436
1437 #ifndef COND_PROB_METHOD
1438
1439
1440             if (DanglingToAttachProb(SpringLen, MicroStepSize) >
1441             RandUniform){

```

```

1442         //Dumbbell will become active or looped
1443         if (AttachedToActiveProb(SpringLen, MicroStepSize) >
1444             RandUniform2){
1445             SpeciesType[i] = 0; //Change to Active Dumbbell
1446         } else {
1447             SpeciesType[i] = 2; //Change to Looped Dumbbell
1448         }
1449     }
1450
1451
1452     #else
1453         if ((DanglingToLoopedProb(SpringLen, MicroStepSize) >
1454             RandUniform)
1455             && (DanglingToActiveProb(SpringLen, MicroStepSize) <
1456             RandUniform2)){
1457
1458             SpeciesType[i] = 2; //Change to looped type
1459
1460         } else if ((DanglingToLoopedProb(SpringLen, MicroStepSize) <
1461             RandUniform) && (DanglingToActiveProb(SpringLen, MicroStepSize)
1462             > RandUniform2)){
1463
1464             SpeciesType[i] = 0; //Change to Active species
1465
1466         } //In all other cases dumbbells remain dangling
1467     #endif
1468
1469
1470

```



```

1471         break;
1472
1473 #ifdef LOOP_FREEZE
1474 #else //LOOP_FREEZE
1475         case 2: //Loooped Type
1476
1477         if ( LoopedToDanglingProb(SpringLen, MicroStepSize) >
1478             RandUniform){
1479
1480
1481
1482
1483
1484 #ifdef LEN_CHG
1485         SpringLenX[i] = (RandUniform3 - 0.5) * 2;
1486         SpringLenY[i] = (RandUniform4 - 0.5) * 2;
1487 #endif //LEN_CHG
1488
1489 #ifdef LEN_CHN_NORM
1490
1491     /*
1492     * Note: There is no failsafe for this loop and it could continue infinitely.
1493     */
1494
1495     do {
1496         SpringLenX[i] = RandNorm2.x;
1497         SpringLenY[i] = RandNorm2.y;
1498     } while ( SpringLenX[i] * SpringLenX[i] +
1499             SpringLenY[i] * SpringLenY[i] >=

```

```

1500             devMaxSpringLength * devMaxSpringLength );
1501
1502 #endif //LEN_CHN_NORM
1503
1504 #ifdef CHK_DNG
1505             printf("New DangleDumbbell[%d] X-len: %f",
1506                 " Y-Len: %f Time: %f\n", i, SpringLenX[i], SpringLenY[i],
1507                 SimTime[i]);
1508 #endif //CHK_DNG
1509             SpeciesType[i] = 1; //Change to dangling type
1510 #ifdef SPEC_CHNG
1511             Lpd2Dng[i]++;
1512 #endif //SPEC_CHNG
1513         }
1514         break;
1515 #endif //LOOP_FREEZE
1516     }
1517 #else
1518
1519     //Default to two dumbbell types
1520
1521     switch(SpeciesType[i]) {
1522
1523     case 0: //Active Type
1524         Evolve(&SpringLenX[i], &SpringLenY[i], RandNorm.x, RandNorm.y,
1525             drag_coeff_active, &SimTime[i], MicroStepSize, FlowRate);
1526
1527         if (ActiveToDanglingProb(SpringLen, MicroStepSize)
1528             > RandUniform){

```

```

1529         // if threshold prob is higher than uniform rand number then
1530         SpeciesType[i] = 1; //Change dumbbell to Dangling species
1531 #ifdef SPEC_CHNG
1532         Act2Dng[i]++;
1533 #endif
1534     }
1535
1536     break;
1537
1538     case 1: //Dangling Type
1539         Evolve(&SpringLenX[i], &SpringLenY[i],
1540             RandNorm.x, RandNorm.y,
1541             drag_coeff_dangle, &SimTime[i],
1542             MicroStepSize, FlowRate);
1543
1544     if (DanglingToActiveProb(SpringLen, MicroStepSize) > RandUniform){
1545         // if dangling prob is higher than uniform rand number then
1546         SpeciesType[i] = 0; //Change dumbbell to Active species
1547 #ifdef SPEC_CHNG
1548         Dng2Act[i]++;
1549 #endif
1550     }
1551
1552     break;
1553 }
1554
1555 #endif
1556
1557 //.....

```

```

1558
1559         SimTime[i] += MicroStepSize;
1560
1561
1562
1563         //.....
1564
1565
1566     }
1567
1568     //copy random number generator state back
1569     states[i] = localState;
1570     ProbStates[i] = localProbState;
1571 }
1572
1573 //Function: RandomGenInit
1574 //Initialize the random number generator on each of the threads
1575 //Gives each thread a different seed form *SeedList vector
1576 __global__ void RandomGenInit(unsigned long long *SeedList,
1577                               curandState *states){
1578
1579     int tid = blockIdx.x * blockDim.x + threadIdx.x;
1580
1581     //curand_init(SeedList[tid], tid, 0, &states[tid]);
1582     //previous method seems to be quite slow.
1583
1584     curand_init((unsigned long long)SeedList[tid], 0, 0, &states[tid]);
1585
1586 }

```

```

1587
1588
1589 //Function: RndNorm
1590 //CPU Function to transform uniform random variable [0,1] to normal random
1591 //variable with meand 0 and Variance defined in the function
1592 double RndNorm (void){
1593     double Variance = 1;
1594
1595     static int HasSpareRandomNum = 0;
1596     static double SpareRandomNum;
1597
1598     if(HasSpareRandomNum == 1){
1599         HasSpareRandomNum = 0;
1600         return Variance * SpareRandomNum;
1601     }
1602
1603     HasSpareRandomNum = 1;
1604
1605     static double u,v,s;
1606
1607     do{
1608         u = ( rand() / ((double) RAND_MAX)) * 2 - 1;
1609         v = ( rand() / ((double) RAND_MAX)) * 2 - 1;
1610         s = u * u + v * v;
1611     } while (s >= 1 || s == 0);
1612
1613     s = sqrt (-2.0 * log(s) / s);
1614
1615     SpareRandomNum = v * s; //Save spare random number for next function call

```

```

1616
1617     return Variance * u * s;
1618 }
1619
1620
1621
1622 double AvgSpringLife ( double *SpringLenX, double *SpringLenY,
1623                       int *SpeciesType){
1624
1625     //TODO: decide on method and clean up debug output
1626     #ifndef NEW_TAU
1627         return 6.0;
1628     #else
1629
1630     #ifdef DEBUG
1631         double Total1 = 0.0;
1632     #endif
1633     double Total2 = 0.0;
1634
1635     double SpringLen;
1636     int ActiveCount = 0;
1637
1638     for (unsigned int j=0; j<hostNumberOfParticles; j++){
1639
1640         if (SpeciesType[j] == 0){ //If active type
1641
1642             ActiveCount++;
1643             SpringLen = sqrt( SpringLenX[j] * SpringLenX[j] +
1644                             SpringLenY[j] * SpringLenY[j]);

```

```

1645
1646         //__Hookean Springs__
1647         //Total += Tao_zero * exp ( - LITTLE_D * LITTLE_D *
1648         // SpringLen * SpringLen / U_ZERO );
1649         //*****
1650
1651         //__FENE Springs__
1652
1653
1654 #ifdef DEBUG
1655
1656         /*
1657         * If in debug mode, compute both and compare.
1658         */
1659
1660         Total1 += 2 / hostBeta * exp ( - 0.0325 * abs( SpringLen /
1661         ( 1 - SpringLen * SpringLen /
1662         hostMaxSpringLength / hostMaxSpringLength ) ));
1663
1664         Total2 += TAO_FUND * hostA_coeff *
1665         exp ( - ( hostB_coeff * SpringLen * SpringLen ) /
1666         (( 1 - ( SpringLen / hostMaxSpringLength ) *
1667         ( SpringLen / hostMaxSpringLength ) ) *
1668         ( 1 - ( SpringLen / hostMaxSpringLength ) *
1669         ( SpringLen / hostMaxSpringLength ) ) )
1670         ); //Eqn (12)
1671 #else
1672
1673         //Hernandez-Cifre Tau Calculation

```

```

1674         Total2 += TAO_FUND * hostA_coeff *
1675             exp ( - ( hostB_coeff * SpringLen * SpringLen ) /
1676                 (( 1 - ( SpringLen / hostMaxSpringLength) *
1677                 ( SpringLen / hostMaxSpringLength) ) *
1678                 ( 1 - ( SpringLen / hostMaxSpringLength) *
1679                 ( SpringLen / hostMaxSpringLength) ) )
1680             ); //Eqn (12)
1681
1682
1683 #endif //DEBUG
1684
1685
1686     }
1687
1688 }
1689
1690 /* Fixed bug were -nan values returned */
1691 /*
1692  * A second possible solution would be to return
1693  * a value in [5.999 - 6.012] range. As this parameter
1694  * does not seem to vary much. In fact, for speed it
1695  * could be beneficial to simply set this parameter.
1696  *
1697  */
1698
1699 if (ActiveCount == 0)
1700 {
1701     /*
1702     * Instead of exiting out here, return 0 value.

```



```

1703     * Then use zero value to exit main loop.
1704     *
1705     * This will hopefully preserve the data up
1706     * until the 0 value is reached.
1707     */
1708
1709     return 0;
1710 }
1711
1712 #ifdef DEBUG
1713     printf("AvgSpringLife...Hernandez-Cife: %f Sing-McKinley: %f \n",
1714           Total2/ActiveCount, Total1/ActiveCount);
1715 #endif //DEBUG
1716
1717
1718
1719     return Total2 / (double) ActiveCount;
1720
1721 #endif //NEW_TAU
1722
1723 }
1724
1725
1726 void SpeciesRatioCount( int SpeciesType[], double *ActiveRatio,
1727                        double *DangleRatio, double *LoopedRatio){
1728     unsigned int j;
1729     int NumOfActive=0;
1730     int NumOfDangling=0;
1731     int NumOfLooped=0;

```

```

1732
1733     for (j=0; j<hostNumberOfParticles; j++){
1734
1735         switch (SpeciesType[j]){
1736             case 0:
1737                 NumOfActive++;
1738             break;
1739
1740             case 1:
1741                 NumOfDangling++;
1742             break;
1743
1744             case 2:
1745                 NumOfLooped++;
1746             break;
1747
1748             default:
1749                 printf("Error: Undetermined Species Type!\n");
1750             break;
1751
1752         }
1753     }
1754
1755     *ActiveRatio = (double)NumOfActive / hostNumberOfParticles;
1756     *DangleRatio = (double)NumOfDangling / hostNumberOfParticles;
1757     *LoopedRatio = (double)NumOfLooped / hostNumberOfParticles;
1758
1759 }
1760

```

```

1761
1762 //Function
1763 //CPU
1764 //Calculate Ratios, Return Average Lengths and Variation, Histogram per type.
1765 void Detailed_Info (int SpeciesType[], double SpringLenX[], double SpringLenY[],
1766                   SpeciesValue *AvgLen, SpeciesValue *Variance,
1767 #ifdef NEW_DNG_LN
1768                   TwoDimSpring *AvgDng,
1769 #endif
1770                   int NumOfBins, SpeciesCount **Hist, int t_step){
1771
1772 //NOTES: *AvgLen.Active = AvgLen->Active
1773
1774 //histogram
1775 int BinNumber = 0;
1776
1777 //Initialize Bins to 0
1778 for(unsigned int i=0; i<NumOfBins; i++){
1779     Hist[i][t_step].Active = 0;
1780     Hist[i][t_step].Dangle = 0;
1781     Hist[i][t_step].Looped = 0;
1782 }
1783
1784
1785
1786 double max = sqrt( 2 * hostMaxSpringLength * hostMaxSpringLength );
1787 double min = 0;
1788
1789

```

```

1790
1791     double SpringLen = 0.0;
1792     double SpringAng = 0.0;
1793
1794
1795
1796     SpeciesCount NumOf = {0};
1797
1798     /*
1799     * Need to initialize average lengths to 0.
1800     */
1801     AvgLen->ActiveLen = 0;
1802     AvgLen->DangleLen = 0;
1803     AvgLen->LoopedLen = 0;
1804
1805     AvgLen->ActiveAng = 0;
1806     AvgLen->DangleAng = 0;
1807     AvgLen->LoopedAng = 0;
1808
1809     AvgLen->ActiveX = 0;
1810     AvgLen->DangleX = 0;
1811     AvgLen->LoopedX = 0;
1812     AvgLen->ActiveY = 0;
1813     AvgLen->DangleY = 0;
1814     AvgLen->LoopedY = 0;
1815
1816     Variance->ActiveLen = 0;
1817     Variance->DangleLen = 0;
1818     Variance->LoopedLen = 0;

```

```

1819
1820     Variance->ActiveAng = 0;
1821     Variance->DangleAng = 0;
1822     Variance->LoopedAng = 0;
1823
1824     Variance->ActiveX = 0;
1825     Variance->DangleX = 0;
1826     Variance->LoopedX = 0;
1827     Variance->ActiveY = 0;
1828     Variance->DangleY = 0;
1829     Variance->LoopedY = 0;
1830
1831     NumOf.Active = 0;
1832     NumOf.Dangle = 0;
1833     NumOf.Looped = 0;
1834
1835
1836     #ifdef NEW_DNG_LN
1837         AvgDng->x = 0;
1838         AvgDng->y = 0
1839     #endif
1840
1841
1842     for (unsigned int j=0; j<hostNumberOfParticles; j++){
1843
1844         SpringLen = sqrt( SpringLenX[j] * SpringLenX[j] +
1845                         SpringLenY[j] * SpringLenY[j] );
1846
1847

```

```

1848     BinNumber = (int)(( SpringLen - min) / ((max-min)/ NumOfBins));
1849
1850
1851     switch (SpeciesType[j]){
1852         case 0:
1853             //Average Length
1854             NumOf.Active++;
1855             AvgLen->ActiveLen += SpringLen;
1856             AvgLen->ActiveAng += atan(SpringLenY[j] / SpringLenX[j]);
1857             AvgLen->ActiveX += SpringLenX[j];
1858             AvgLen->ActiveY += SpringLenY[j];
1859             Hist[BinNumber][t_step].Active++;
1860
1861         break;
1862
1863         case 1:
1864             //Average Length
1865             NumOf.Dangle++;
1866             AvgLen->DangleLen += SpringLen;
1867             AvgLen->DangleAng += atan(SpringLenY[j] / SpringLenX[j]);
1868             AvgLen->DangleX += SpringLenX[j];
1869             AvgLen->DangleY += SpringLenY[j];
1870             Hist[BinNumber][t_step].Dangle++;
1871     #ifdef NEW_DNG_LN
1872             AvgDng->x += SpringLenX[j];
1873             AvgDng->y += SpringLenY[j];
1874     #endif
1875         break;
1876

```

```

1877         case 2:
1878             //Average Length
1879             NumOf.Looped++;
1880             AvgLen->LoopedLen += SpringLen;
1881             AvgLen->LoopedAng += atan(SpringLenY[j] / SpringLenX[j]);
1882             AvgLen->LoopedX += SpringLenX[j];
1883             AvgLen->LoopedY += SpringLenY[j];
1884             Hist[BinNumber][t_step].Looped++;
1885
1886         break;
1887
1888         default:
1889             printf("Error: Undetermined Species Type!\n");
1890         break;
1891
1892     }
1893 }
1894
1895
1896 #ifdef NEW_DNG_LN
1897     AvgDng->x = AvgDng->x / NumOf.Dangle;
1898     AvgDng->y = AvgDng->y / NumOf.Dangle;
1899 #endif
1900
1901
1902     if ((AvgLen->ActiveLen/NumOf.Active > hostMaxSpringLength) ||
1903         (AvgLen->DangleLen/NumOf.Dangle > hostMaxSpringLength) ||
1904         (AvgLen->LoopedLen/NumOf.Looped > hostMaxSpringLength)){
1905         printf("Average Length – Active[%f] Dangling[%f] Looped[%f]\n",

```

```

1906         AvgLen->ActiveLen, AvgLen->DangleLen, AvgLen->LoopedLen);
1907     printf("NumofActive: %d NumofDangle: %d NumofLooped: %d \n",
1908           NumOf.Active, NumOf.Dangle, NumOf.Looped);
1909 }
1910
1911
1912
1913 if (NumOf.Active == 0){
1914     AvgLen->ActiveLen = 0;
1915     AvgLen->ActiveAng = 0;
1916     AvgLen->ActiveX = 0;
1917     AvgLen->ActiveY = 0;
1918 } else {
1919     AvgLen->ActiveLen = (double) AvgLen->ActiveLen / NumOf.Active;
1920     AvgLen->ActiveAng = (double) AvgLen->ActiveAng / NumOf.Active;
1921     AvgLen->ActiveX = (double) AvgLen->ActiveX / NumOf.Active;
1922     AvgLen->ActiveY = (double) AvgLen->ActiveY / NumOf.Active;
1923 }
1924
1925 if (NumOf.Dangle == 0){
1926     AvgLen->DangleLen = 0;
1927     AvgLen->DangleAng = 0;
1928     AvgLen->DangleX = 0;
1929     AvgLen->DangleY = 0;
1930 } else {
1931     AvgLen->DangleLen = (double) AvgLen->DangleLen / NumOf.Dangle;
1932     AvgLen->DangleAng = (double) AvgLen->DangleAng / NumOf.Dangle;
1933     AvgLen->DangleX = (double) AvgLen->DangleX / NumOf.Dangle;
1934     AvgLen->DangleY = (double) AvgLen->DangleY / NumOf.Dangle;

```



```

1935     }
1936
1937     if (NumOf.Looped == 0){
1938         AvgLen->LoopedLen = 0;
1939         AvgLen->LoopedAng = 0;
1940         AvgLen->LoopedX = 0;
1941         AvgLen->LoopedY = 0;
1942     } else {
1943         AvgLen->LoopedLen = (double) AvgLen->LoopedLen / NumOf.Looped;
1944         AvgLen->LoopedAng = (double) AvgLen->LoopedAng / NumOf.Looped;
1945         AvgLen->LoopedX = (double) AvgLen->LoopedX / NumOf.Looped;
1946         AvgLen->LoopedY = (double) AvgLen->LoopedY / NumOf.Looped;
1947     }
1948
1949
1950     /*
1951     * Calculate Variance
1952     *
1953     */
1954
1955     for (unsigned int j=0; j<hostNumberOfParticles; j++){
1956
1957         SpringLen = sqrt( SpringLenX[j] * SpringLenX[j] +
1958                         SpringLenY[j] * SpringLenY[j] );
1959         SpringAng = atan( SpringLenY[j] / SpringLenX[j]);
1960
1961         switch (SpeciesType[j]){
1962             case 0:
1963                 Variance->ActiveLen += (SpringLen - AvgLen->ActiveLen) *

```

```

1964             (SpringLen - AvgLen->ActiveLen);
1965     Variance->ActiveAng += (SpringAng - AvgLen->ActiveAng) *
1966             (SpringAng - AvgLen->ActiveAng);
1967     Variance->ActiveX += (SpringLenX[j] - AvgLen->ActiveX) *
1968             (SpringLenX[j] - AvgLen->ActiveX);
1969     Variance->ActiveY += (SpringLenY[j] - AvgLen->ActiveY) *
1970             (SpringLenY[j] - AvgLen->ActiveY);
1971     break;
1972
1973     case 1:
1974         Variance->DangleLen += (SpringLen - AvgLen->DangleLen) *
1975             (SpringLen - AvgLen->DangleLen);
1976         Variance->DangleAng += (SpringAng - AvgLen->DangleAng) *
1977             (SpringAng - AvgLen->DangleAng);
1978         Variance->DangleX += (SpringLenX[j] - AvgLen->DangleX) *
1979             (SpringLenX[j] - AvgLen->DangleX);
1980         Variance->DangleY += (SpringLenY[j] - AvgLen->DangleY) *
1981             (SpringLenY[j] - AvgLen->DangleY);
1982     break;
1983
1984     case 2:
1985         Variance->LoopedLen += (SpringLen - AvgLen->LoopedLen) *
1986             (SpringLen - AvgLen->LoopedLen);
1987         Variance->LoopedAng += (SpringAng - AvgLen->LoopedAng) *
1988             (SpringAng - AvgLen->LoopedAng);
1989         Variance->LoopedX += (SpringLenX[j] - AvgLen->LoopedX) *
1990             (SpringLenX[j] - AvgLen->LoopedX);
1991         Variance->LoopedY += (SpringLenY[j] - AvgLen->LoopedY) *
1992             (SpringLenY[j] - AvgLen->LoopedY);

```

```

1993         break;
1994
1995         default:
1996             printf("Error: Undetermined Species Type!\n");
1997         break;
1998
1999     }
2000 }
2001
2002
2003 if (NumOf.Active == 0){
2004     Variance->ActiveLen = 0.0;
2005     Variance->ActiveAng = 0.0;
2006     Variance->ActiveX = 0.0;
2007     Variance->ActiveY = 0.0;
2008 } else {
2009     Variance->ActiveLen = (double) Variance->ActiveLen / NumOf.Active;
2010     Variance->ActiveAng = (double) Variance->ActiveAng / NumOf.Active;
2011     Variance->ActiveX = (double) Variance->ActiveX / NumOf.Active;
2012     Variance->ActiveY = (double) Variance->ActiveY / NumOf.Active;
2013 }
2014
2015 if (NumOf.Dangle == 0){
2016     Variance->DangleLen = 0.0;
2017     Variance->DangleAng = 0.0;
2018     Variance->DangleX = 0.0;
2019     Variance->DangleY = 0.0;
2020 } else {
2021     Variance->DangleLen = (double) Variance->DangleLen / NumOf.Dangle;

```

```

2022     Variance->DangleAng = (double) Variance->DangleAng / NumOf.Dangle;
2023     Variance->DangleX = (double) Variance->DangleX / NumOf.Dangle;
2024     Variance->DangleY = (double) Variance->DangleY / NumOf.Dangle;
2025 }
2026
2027 if (NumOf.Looped == 0){
2028     Variance->LoopedLen = 0.0;
2029     Variance->LoopedAng = 0.0;
2030     Variance->LoopedX = 0.0;
2031     Variance->LoopedY = 0.0;
2032 } else {
2033     Variance->LoopedLen = (double) Variance->LoopedLen / NumOf.Looped;
2034     Variance->LoopedAng = (double) Variance->LoopedAng / NumOf.Looped;
2035     Variance->LoopedX = (double) Variance->LoopedX / NumOf.Looped;
2036     Variance->LoopedY = (double) Variance->LoopedY / NumOf.Looped;
2037 }
2038
2039
2040
2041 }
2042
2043
2044
2045
2046
2047
2048 // Function:
2049 // CPU Function
2050 // Given Types, X and Y lengths, calculate ensemble

```

```

2051 // average stress XX, XY, and YY.
2052 void EnsembleAverage (int SpeciesType[], double SpringLenX[],
2053                       double SpringLenY[],
2054                       struct Stress *TotalStress, struct Stress *Active,
2055                       struct Stress *Dangling, int k){
2056
2057     /*
2058     * Notes on Stress Calculation
2059     *
2060     * Weighted average calculated based on real-time numbers of active and
2061     * dangling dumbbells. Simplification causes division in the mean
2062     * calculation by the number of each type to cancel with the weighting
2063     * average factor. Leaving only division by the total number
2064     * of dumbbells.
2065     *
2066     * see the calculations in StressCalculation.pdf
2067     *
2068     */
2069
2070     Active[k].XX = 0;
2071     Active[k].XY = 0;
2072     Active[k].YY = 0;
2073
2074     Dangling[k].XX = 0;
2075     Dangling[k].XY = 0;
2076     Dangling[k].YY = 0;
2077
2078
2079     TotalStress[k].XX = 0;

```

```

2080     TotalStress[k].XY = 0;
2081     TotalStress[k].YY = 0;
2082
2083     double LengthLimiter = 1.0;
2084     int NumberOfActive = 0;
2085     int NumberOfDangle = 0;
2086
2087     /* DEBUG */
2088     /*****/
2089     int ErrorFlag_ZeroSpringLength = 0;
2090     int ZeroSpringCount = 0;
2091     /*****/
2092
2093     /*
2094     * DETAILED METHOD
2095     *
2096     * It is also possible to simplify this calculation further if necessary.
2097     * However, this method is tested and provides additional information
2098     * To be exact, this methods shows stress contribution from each type
2099     * of dumbbell, and the total stress.
2100     */
2101
2102
2103     for (unsigned int j=0; j<hostNumberOfParticles; j++){
2104
2105         /* DEBUG */
2106         /*****/
2107         ZeroSpringCount = 0;
2108         /*****/

```

```

2109
2110
2111     switch (SpeciesType[j]){
2112
2113     case 0:
2114         NumberOfActive++;
2115
2116         //__FENE Springs_____
2117
2118         LengthLimiter =
2119             (1.0 - (SpringLenX[j] * SpringLenX[j]
2120                 + SpringLenY[j] * SpringLenY[j])
2121              / (hostMaxSpringLength*hostMaxSpringLength));
2122
2123         Active[k].XX += SpringLenX[j] * SpringLenX[j] / LengthLimiter;
2124         Active[k].XY += SpringLenX[j] * SpringLenY[j] / LengthLimiter;
2125         Active[k].YY += SpringLenY[j] * SpringLenY[j] / LengthLimiter;
2126
2127         //*****
2128         /* DEBUG */
2129         /******
2130         if ((SpringLenX[j] == 0 ) && (SpringLenY[j] == 0))
2131         {
2132             ErrorFlag_ZeroSpringLength = 1;
2133             ZeroSpringCount++;
2134         }
2135         /******
2136         break;
2137

```

```

2138     case 1:
2139         NumberOfDangle++;
2140
2141         //__FENE Springs_____
2142
2143         LengthLimiter =
2144             (1.0 - (SpringLenX[j] * SpringLenX[j]
2145                 + SpringLenY[j] * SpringLenY[j])
2146              / (hostMaxSpringLength*hostMaxSpringLength));
2147
2148         Dangling[k].XX += SpringLenX[j] * SpringLenX[j] / LengthLimiter;
2149         Dangling[k].XY += SpringLenX[j] * SpringLenY[j] / LengthLimiter;
2150         Dangling[k].YY += SpringLenY[j] * SpringLenY[j] / LengthLimiter;
2151
2152         //*****
2153         /* DEBUG */
2154         /******
2155         if ((SpringLenX[j] == 0 ) && (SpringLenY[j] == 0))
2156         {
2157             ErrorFlag_ZeroSpringLength = 1;
2158             ZeroSpringCount++;
2159         }
2160         /******
2161
2162         break;
2163
2164     case 2:
2165         break;
2166

```



```

2167     default:
2168         printf("Error: Unable to Classify Species Type[%d] Of Dumbbell[%d]\n",
2169             SpeciesType[j], j);
2170         exit(4);
2171     }
2172 }
2173
2174
2175 if (NumberOfActive == 0){
2176     TotalStress[k].XX = - 2.0 / (double) hostNumberOfParticles *
2177         Dangling[k].XX;
2178     TotalStress[k].XY = - 2.0 / (double) hostNumberOfParticles *
2179         Dangling[k].XY;
2180     TotalStress[k].YY = - 2.0 / (double) hostNumberOfParticles *
2181         Dangling[k].YY;
2182
2183     Active[k].XX = 0;
2184     Active[k].XY = 0;
2185     Active[k].YY = 0;
2186
2187     Dangling[k].XX = - 2.0 / (double) hostNumberOfParticles *
2188         Dangling[k].XX;
2189     Dangling[k].XY = - 2.0 / (double) hostNumberOfParticles *
2190         Dangling[k].XY;
2191     Dangling[k].YY = - 2.0 / (double) hostNumberOfParticles *
2192         Dangling[k].YY;
2193
2194
2195 } else {

```

```

2196     if (NumberOfDangle == 0){
2197         TotalStress[k].XX = - 2.0 / (double) hostNumberOfParticles *
2198             ( Active[k].XX );
2199         TotalStress[k].XY = - 2.0 / (double) hostNumberOfParticles *
2200             ( Active[k].XY );
2201         TotalStress[k].YY = - 2.0 / (double) hostNumberOfParticles *
2202             ( Active[k].YY );
2203
2204         Active[k].XX = - 2.0 / (double) hostNumberOfParticles *
2205             Active[k].XX;
2206         Active[k].XY = - 2.0 / (double) hostNumberOfParticles *
2207             Active[k].XY;
2208         Active[k].YY = - 2.0 / (double) hostNumberOfParticles *
2209             Active[k].YY;
2210
2211         Dangling[k].XX = 0;
2212         Dangling[k].XY = 0;
2213         Dangling[k].YY = 0;
2214
2215
2216     } else {
2217         TotalStress[k].XX = - 2.0 / (double) hostNumberOfParticles *
2218             ( Active[k].XX + Dangling[k].XX );
2219         TotalStress[k].XY = - 2.0 / (double) hostNumberOfParticles *
2220             ( Active[k].XY + Dangling[k].XY );
2221         TotalStress[k].YY = - 2.0 / (double) hostNumberOfParticles *
2222             ( Active[k].YY + Dangling[k].YY );
2223
2224         Active[k].XX = - 2.0 / (double) hostNumberOfParticles *

```

```

2225         Active[k].XX;
2226     Active[k].XY = - 2.0 / (double) hostNumberOfParticles *
2227         Active[k].XY;
2228     Active[k].YY = - 2.0 / (double) hostNumberOfParticles *
2229         Active[k].YY;
2230
2231     Dangling[k].XX = - 2.0 / (double) hostNumberOfParticles *
2232         Dangling[k].XX;
2233     Dangling[k].XY = - 2.0 / (double) hostNumberOfParticles *
2234         Dangling[k].XY;
2235     Dangling[k].YY = - 2.0 / (double) hostNumberOfParticles *
2236         Dangling[k].YY;
2237
2238     }
2239 }
2240
2241
2242 /*
2243  * END DETAILED METHOD
2244 */
2245
2246
2247 /* DEBUG */
2248 /*****/
2249 if (ErrorFlag_ZeroSpringLength)
2250     printf("%d Active or Dangling springs had zero length at",
2251           " time step %d\n", ZeroSpringCount, k);
2252 /*****/
2253

```

```

2254
2255 }
2256
2257
2258 int RawOut_OSFlow(int loop_step){
2259
2260     /*
2261     * For Oscillatory Shear Flow
2262     * Sample the last <Cycle_Num> cycles of the simutlation.
2263     * Records dumbbell positions and types for 100 snap shots during simulation.
2264     *
2265     */
2266
2267
2268     int Cycle_Num = 2; //take snap shots over final two cycles
2269
2270     double Time = Cycle_Num * 2 * M_PI / hostFreq; //second for Cycle_Num cycles
2271
2272     double MacroSizeStg2 = hostStepSizeMicroSecon * hostTimeStepsMicro;
2273     //seconds per Macro step in stage 2
2274
2275     int MacroStepsXCycle = (int) floor(Time / MacroSizeStg2) + 1;
2276
2277     int StartPt = 0; // = hostTimeStepsMacro – MacroStepsXCycle;
2278
2279     int SampRate = 0;  //(int) floor(MacroStepsXCycle / 100);
2280
2281     int NumOfSamples = 200; //desired number of sample snapshots to take.
2282

```

```

2283     int Remdr = 0;
2284
2285
2286     if ((NumOfSamples > MacroStepsXCycle) ||
2287         (NumOfSamples > hostTimeStepsMacro)){
2288         //then sample last NumOfSamples macro steps
2289         StartPt = hostTimeStepsMacro - NumOfSamples;
2290
2291
2292         if (loop_step > StartPt){
2293             return 1; //take raw data snap shot
2294         } else {
2295             return 0;
2296         }
2297
2298     } else {
2299         //evenly space NumOfSamples among the final macro steps.
2300         SampRate = (int) floor(MacroStepsXCycle / 200);
2301
2302         StartPt = hostTimeStepsMacro - MacroStepsXCycle;
2303
2304         Remdr = (loop_step - StartPt) % SampRate;
2305
2306
2307         if ((loop_step > StartPt) && (Remdr == 0)){
2308             //printf("[%d]: Take Snapshot!\n",loop_step);
2309             return 1;
2310         } else {
2311             return 0;

```

```

2312     }
2313
2314 }
2315 }
2316
2317
2318 /*
2319  * For Steady Shear Flow
2320  * Records 100 snapshots of dumbbell positions and types
2321  * at even spaced intervals.
2322  *
2323  */
2324
2325 int RawOut_SSFlow(int loop_step){
2326
2327     //For splitting up only the second stage
2328
2329
2330 #ifdef FULL_DATA
2331     int SampleNum = (int) hostTimeStepsMacro / 800;
2332 #else
2333     int SampleNum = (int) hostTimeStepsMacro / 100;
2334 #endif
2335
2336     if (loop_step % SampleNum == 0){
2337         return 1;
2338     } else {
2339         return 0;
2340     }

```

```

2341
2342 }
2343
2344
2345 #ifndef SPEC_CHNG
2346 //sums the entries of a vector
2347 unsigned int VectorSum( unsigned int *Vector, unsigned int length){
2348
2349     unsigned int sum = 0;
2350
2351     for(unsigned int n=0; n<length; n++){
2352         sum += Vector[n];
2353     }
2354
2355     return sum;
2356 }
2357 #endif
2358
2359
2360 int main(int argc, char *argv[]){
2361
2362 #ifndef DEBUG
2363     printf("START DEBUG MODE\n");
2364     printf("DEBUG: Start Sim\n");
2365 #endif
2366
2367     //_____Record Program Run Time
2368     clock_t begin, end, end2;
2369     begin = clock();

```

```

2370     double time_spent, time_spent2;
2371     //*****
2372
2373
2374     // _____ Read Command Line Arguments _____
2375
2376     if (ParseInput(argc, argv)==EXIT_FAILURE){
2377         //return EXIT_FAILURE;
2378         exit(2);
2379     }
2380     //*****
2381
2382     /*
2383     * Select GPU Device
2384     */
2385     cudaSetDevice(GPU_select);
2386
2387     PrintSimInfo(); //Output Simulation Variables to Terminal
2388
2389     //---- Set Global Variable Values -----
2390     cudaMemcpyToSymbol(devFlowRate, &hostFlowRate, sizeof(double));
2391     cudaMemcpyToSymbol(devMaxSpringLength, &hostMaxSpringLength,
2392         sizeof(double));
2393     cudaMemcpyToSymbol(devFreq, &hostFreq, sizeof(double));
2394
2395     // additional command line arguments
2396     cudaMemcpyToSymbol(devD_free, &hostD_free, sizeof(double));
2397     cudaMemcpyToSymbol(devZee, &hostZee, sizeof(double));
2398     cudaMemcpyToSymbol(devChi, &hostChi, sizeof(double));

```



```

2399     cudaMemcpyToSymbol(devAlpha, &hostAlpha, sizeof(double));
2400     cudaMemcpyToSymbol(devBeta, &hostBeta, sizeof(double));
2401
2402     //*****
2403
2404
2405     //----define block and thread structure ----
2406     dim3 block;
2407
2408     if (hostNumberOfParticles < 512){
2409         block.x = hostNumberOfParticles;
2410         block.y = 1;
2411     }
2412     else {
2413         block.x=512;
2414         block.y=1;
2415     }
2416
2417     dim3 grid ((hostNumberOfParticles + block.x -1) / block.x,1);
2418     //*****
2419
2420
2421     //__Variables for random number generation on GPU kernels
2422     curandState *states = NULL;
2423     curandState *ProbStates = NULL;
2424     //*****
2425
2426     //____allocate memory on GPU for random number generator states____
2427     CUDA_CALL(cudaMalloc((void **)&states, sizeof(curandState) *

```

```

2428             hostNumberOfParticles ));
2429     CUDA_CALL(cudaMalloc((void **)&ProbStates, sizeof(curandState) *
2430             hostNumberOfParticles ));
2431     //.....
2432
2433     //__create vectors of seeds____
2434     unsigned long long *hostSeeds = NULL;
2435     unsigned long long *devSeeds = NULL;
2436
2437     unsigned long long *hostProbSeeds = NULL;
2438     unsigned long long *devProbSeeds = NULL;
2439
2440
2441     hostSeeds = (unsigned long long *)malloc(hostNumberOfParticles *
2442             sizeof(unsigned long long));
2443     hostProbSeeds = (unsigned long long *)malloc(hostNumberOfParticles *
2444             sizeof(unsigned long long));
2445
2446     /*
2447     * Verify memory allocated successfully.
2448     */
2449     if (hostSeeds == NULL)
2450         printf("hostSeeds memory error.\n");
2451     if (hostProbSeeds == NULL)
2452         printf("hostProbSeeds memory error.\n");
2453
2454
2455     CUDA_CALL(cudaMalloc((void **)&devSeeds, sizeof(unsigned long long) *
2456             hostNumberOfParticles));

```

```

2457     CUDA_CALL(cudaMalloc((void **)&devProbSeeds,
2458                          sizeof(unsigned long long) *
2459                          hostNumberOfParticles));
2460
2461     #ifndef FIXED_SEED
2462         srand(1);
2463     #else
2464         srand(time(NULL));
2465     #endif
2466     //Start from one random number and count from there.
2467
2468     hostSeeds[0] = abs(rand());
2469     hostProbSeeds[0] = abs(rand());
2470
2471     for (unsigned int i=1; i<hostNumberOfParticles; i++){
2472         hostSeeds[i] = hostSeeds[i-1] + 1;
2473         hostProbSeeds[i] = hostProbSeeds[i-1] + 1;
2474
2475     }
2476     //.....
2477
2478
2479     CUDA_CALL(cudaMemcpy(devSeeds, hostSeeds, sizeof(unsigned long long) *
2480                          hostNumberOfParticles, cudaMemcpyHostToDevice));
2481     CUDA_CALL(cudaMemcpy(devProbSeeds, hostProbSeeds,
2482                          sizeof(unsigned long long) *
2483                          hostNumberOfParticles, cudaMemcpyHostToDevice));
2484
2485

```

```

2486 //____initialize kernel random number generator on GPU threads____
2487 RandomGenInit<<< grid, block >>>(devSeeds, states);
2488 gpuErrchk( cudaPeekAtLastError() ); //Error catching
2489 gpuErrchk( cudaDeviceSynchronize() );
2490 //for catching errors. If removed, may give errors from other places
2491 RandomGenInit<<< grid, block >>>(devProbSeeds, ProbStates);
2492 gpuErrchk( cudaPeekAtLastError() );
2493 gpuErrchk( cudaDeviceSynchronize() );
2494 //*****
2495
2496 //____Spring Length variables____
2497 double *devSpringLenX = NULL;
2498 double *devSpringLenY = NULL;
2499 double *hostSpringLenX = NULL;
2500 double *hostSpringLenY = NULL;
2501 //*****
2502
2503 //____Dumbbell Species Type Variable____
2504 int *devSpeciesType = NULL;
2505 int *hostSpeciesType = NULL;
2506 //*****
2507
2508 //____alloc memory on CPU
2509 hostSpringLenX = (double*)malloc(hostNumberOfParticles*sizeof(double));
2510 hostSpringLenY = (double*)malloc(hostNumberOfParticles*sizeof(double));
2511 hostSpeciesType = (int*)malloc(hostNumberOfParticles*sizeof(int));
2512
2513 if (hostSpringLenX == NULL)
2514     printf("hostSpringLenX memory error.\n");

```

```

2515     if (hostSpringLenY == NULL)
2516         printf("hostSpringLenY memory error.\n");
2517     if (hostSpeciesType == NULL)
2518         printf("hostSpeciesType memory error.\n");
2519         //*****
2520
2521         //_____ allocate memory on GPU for spring length
2522         CUDA_CALL(cudaMalloc((double**)&devSpringLenX,
2523                               hostNumberOfParticles*sizeof(double)));
2524         CUDA_CALL(cudaMalloc((double**)&devSpringLenY ,
2525                               hostNumberOfParticles*sizeof(double)));
2526         CUDA_CALL(cudaMalloc((int**)&devSpeciesType,
2527                               hostNumberOfParticles*sizeof(int)));
2528         //*****
2529
2530
2531         //_____ initialize memory _____
2532         for(unsigned int n=0; n < hostNumberOfParticles; n++)
2533         {
2534             hostSpringLenX[n] = 0.0;
2535             hostSpringLenY[n] = 0.0;
2536             hostSpeciesType[n] = 0;
2537         }
2538
2539
2540
2541     #ifdef SPEC_CHNG
2542
2543         // Count species changes per macro time step

```

```

2544
2545   unsigned int *hostDng2Act = NULL;
2546   unsigned int *hostDng2Lpd = NULL;
2547   unsigned int *hostAct2Dng = NULL;
2548   unsigned int *hostLpd2Dng = NULL;
2549
2550   unsigned int *devDng2Act = NULL;
2551   unsigned int *devDng2Lpd = NULL;
2552   unsigned int *devAct2Dng = NULL;
2553   unsigned int *devLpd2Dng = NULL;
2554
2555   hostDng2Act = (unsigned int*)malloc(hostNumberOfParticles *
2556                                   sizeof(unsigned int));
2557   hostDng2Lpd = (unsigned int*)malloc(hostNumberOfParticles *
2558                                   sizeof(unsigned int));
2559   hostAct2Dng = (unsigned int*)malloc(hostNumberOfParticles *
2560                                   sizeof(unsigned int));
2561   hostLpd2Dng = (unsigned int*)malloc(hostNumberOfParticles *
2562                                   sizeof(unsigned int));
2563
2564   if (hostDng2Act == NULL) printf("hostDng2Act memory error.\n");
2565   if (hostDng2Lpd == NULL) printf("hostDng2Lpd memory error.\n");
2566   if (hostAct2Dng == NULL) printf("hostAct2Dng memory error.\n");
2567   if (hostLpd2Dng == NULL) printf("hostLpd2Dng memory error.\n");
2568
2569   CUDA_CALL(cudaMalloc((unsigned int**)&devDng2Act, hostNumberOfParticles *
2570                       sizeof(unsigned int)));
2571   CUDA_CALL(cudaMalloc((unsigned int**)&devDng2Lpd, hostNumberOfParticles *
2572                       sizeof(unsigned int)));

```

```

2573   CUDA_CALL(cudaMalloc((unsigned int**)&devAct2Dng, hostNumberOfParticles *
2574                       sizeof(unsigned int)));
2575   CUDA_CALL(cudaMalloc((unsigned int**)&devLpd2Dng, hostNumberOfParticles *
2576                       sizeof(unsigned int)));
2577
2578   for(unsigned int n=0; n < hostNumberOfParticles; n++)
2579   {
2580       hostDng2Act[n] = 0;
2581       hostDng2Lpd[n] = 0;
2582       hostAct2Dng[n] = 0;
2583       hostLpd2Dng[n] = 0;
2584   }
2585
2586   // Save count for each loop
2587   unsigned int *Dng2ActSum = NULL;
2588   unsigned int *Dng2LpdSum = NULL;
2589   unsigned int *Act2DngSum = NULL;
2590   unsigned int *Lpd2DngSum = NULL;
2591
2592
2593   Dng2ActSum = (unsigned int*)malloc((hostTimeStepsMacro+1) *
2594                                     sizeof(unsigned int));
2595   Dng2LpdSum = (unsigned int*)malloc((hostTimeStepsMacro+1) *
2596                                     sizeof(unsigned int));
2597   Act2DngSum = (unsigned int*)malloc((hostTimeStepsMacro+1) *
2598                                     sizeof(unsigned int));
2599   Lpd2DngSum = (unsigned int*)malloc((hostTimeStepsMacro+1) *
2600                                     sizeof(unsigned int));
2601

```

```

2602     if (Dng2ActSum == NULL) printf("Dng2ActSum memory error.\n");
2603     if (Dng2LpdSum == NULL) printf("Dng2LpdSum memory error.\n");
2604     if (Act2DngSum == NULL) printf("Act2DngSum memory error.\n");
2605     if (Lpd2DngSum == NULL) printf("Lpd2DngSum memory error.\n");
2606
2607     #endif
2608
2609     #ifndef SINGLE_MICRO
2610         // Tracks every species transition of every time step (micro)
2611
2612         DBSpecChng *hostSCArr = NULL;
2613
2614         DBSpecChng *devSCArr = NULL;
2615
2616         hostSCArr = (DBSpecChng *) malloc ( hostTimeStepsMicro *
2617             sizeof (DBSpecChng));
2618         CUDA_CALL(cudaMalloc((DBSpecChng **)&devSCArr, hostTimeStepsMicro *
2619             sizeof(DBSpecChng)));
2620
2621
2622
2623         // intialize array values to 0
2624
2625         for(unsigned int m=0; m < hostTimeStepsMicro; m++){
2626             hostSCArr[m].type = 0;
2627             hostSCArr[m].time = 0.0;
2628             hostSCArr[m].x = 0.0;
2629             hostSCArr[m].y = 0.0;
2630         }

```



```

2631
2632
2633     CUDA_CALL(cudaMemcpy(devSCArr, hostSCArr,
2634                         hostTimeStepsMicro * sizeof(DBSpecChng),
2635                         cudaMemcpyHostToDevice));
2636
2637
2638     //file to write data to.
2639
2640     char MicroDataFilename[256];
2641
2642     sprintf(MicroDataFilename, "%s_single_micro.bin", DataFileName);
2643
2644     FILE *MicroDataFilePtr = NULL;
2645
2646     MicroDataFilePtr = fopen(MicroDataFilename, "wb");
2647     if (!MicroDataFilePtr) printf("Unable to open micro data file!\n");
2648
2649     size_t MicroData_FileSize; //For checking file size.
2650
2651
2652     #endif
2653
2654     #ifdef MICRO_RAW
2655         // Tracks every species transition of every time step (micro)
2656
2657         DBSpecChng *hostSCArr = NULL;
2658
2659         DBSpecChng *devSCArr = NULL;

```

```

2660
2661 hostSCArr = (DBSpecChng *) malloc ( hostNumberOfParticles *
2662         hostTimeStepsMicro * sizeof (DBSpecChng));
2663 CUDA_CALL(cudaMalloc((DBSpecChng **)&devSCArr, hostNumberOfParticles *
2664         hostTimeStepsMicro * sizeof(DBSpecChng)));
2665
2666
2667
2668 // intialize array values to 0
2669
2670 for(unsigned int n=0; n < hostNumberOfParticles; n++){
2671     for(unsigned int m=0; m < hostTimeStepsMicro; m++){
2672         hostSCArr[n*hostTimeStepsMicro+m].type = 0;
2673         hostSCArr[n*hostTimeStepsMicro+m].length = 0.0;
2674     }
2675 }
2676
2677
2678 CUDA_CALL(cudaMemcpy(devSCArr, hostSCArr,
2679         hostNumberOfParticles * hostTimeStepsMicro * sizeof(DBSpecChng),
2680         cudaMemcpyHostToDevice));
2681
2682
2683 //file to write data to.
2684
2685 char MicroDataFilename[256];
2686
2687 sprintf(MicroDataFilename, "%s_micro.bin", DataFileName);
2688

```

```

2689 FILE *MicroDataFilePtr = NULL;
2690
2691 MicroDataFilePtr = fopen(MicroDataFilename, "wb");
2692 if (!MicroDataFilePtr) printf("Unable to open micro data file!\n");
2693
2694 size_t MicroData_FileSize; //For checking file size.
2695
2696
2697 #endif
2698
2699
2700 //____Simulation Time____
2701 //Variables for tracking time t throughout simulation
2702 //Highest memory cost solution I can think of. There is probably a better way.
2703
2704 /*
2705 *
2706 * First:
2707 * Create dynamically allocated array to store micro time step sizes.
2708 *
2709 * Second:
2710 * Transfer only the starting value to the GPU.
2711 * Return only the final value from the GPU.
2712 *
2713 *
2714 */
2715
2716 double *devSimTime = NULL;
2717 double *hostSimTime = NULL;

```

```

2718
2719     hostSimTime = (double *)malloc(hostNumberOfParticles*sizeof(double));
2720
2721     if (hostSimTime == NULL)
2722         printf("hostSimTime memory error.\n");
2723
2724     CUDA_CALL(cudaMalloc((double**)&devSimTime,
2725         hostNumberOfParticles*sizeof(double)));
2726
2727     //___ initialize memory ___
2728     for(unsigned int n=0; n < hostNumberOfParticles; n++)
2729         hostSimTime[n] = 0.0;
2730
2731     CUDA_CALL(cudaMemcpy(devSimTime, hostSimTime,
2732         hostNumberOfParticles*sizeof(double), cudaMemcpyHostToDevice));
2733     //"....."
2734
2735
2736
2737     //___ Set initial Spring Lengths to Normal Distribuion
2738     // "initially... equilibrium Gaussian distribution"
2739
2740
2741     double failsafe = 0.0;
2742
2743     for (unsigned int i=0; i < hostNumberOfParticles; i++){
2744
2745
2746

```



```

2776 // initial condition.
2777
2778 /*
2779  * This code inside the if can cause a sig fault if the first dumbbell
2780  * doesn't meet the condition.
2781  */
2782
2783
2784         if ( hostSpringLenX[i] * hostSpringLenX[i] +
2785             hostSpringLenY[i] * hostSpringLenY[i] >
2786             hostMaxSpringLength * hostMaxSpringLength){
2787     if ( i == 0 ) {
2788         printf("First dumbbell did not initialize under maximum length.\n");
2789         printf("Check parameters! Exiting to prevent seg fault.\n");
2790         exit(3);
2791     }
2792
2793         i--;
2794         failsafe++;
2795     }
2796     if ( failsafe > 4 * hostNumberOfParticles ) {
2797         printf("failed to initialize dumbbells\n");
2798         exit(3);
2799     }
2800     //.....
2801
2802
2803     //____set initial species type____
2804

```

```

2805
2806     /*
2807     * Initial Species Assignment
2808     *
2809     * Active = 0
2810     * Dangling = 1
2811     * Looped = 2
2812     *
2813     */
2814
2815     if ( i < hostNumberOfParticles * Init_Active_Ratio ){
2816         hostSpeciesType[i]=0;
2817
2818     } else {
2819
2820         if ( i < hostNumberOfParticles *
2821             ( Init_Active_Ratio + Init_Dangle_Ratio ))
2822         {
2823             hostSpeciesType[i]=1;
2824         } else {
2825             hostSpeciesType[i]=2;
2826         }
2827     }
2828
2829
2830     //.....
2831
2832
2833     //.....

```

```

2834
2835     }
2836
2837     printf("Dumbbells Successfully Initialized.\n");
2838
2839     //*****
2840
2841     //____ Copy to Gpu device
2842     CUDA_CALL(cudaMemcpy(devSpringLenX, hostSpringLenX,
2843                          hostNumberOfParticles*sizeof(double),
2844                          cudaMemcpyHostToDevice));
2845     CUDA_CALL(cudaMemcpy(devSpringLenY, hostSpringLenY,
2846                          hostNumberOfParticles*sizeof(double),
2847                          cudaMemcpyHostToDevice));
2848     CUDA_CALL(cudaMemcpy(devSpeciesType, hostSpeciesType,
2849                          hostNumberOfParticles*sizeof(int),
2850                          cudaMemcpyHostToDevice));
2851     //*****
2852
2853
2854
2855
2856     //____ initialize variables to calculate and store ensemble average
2857     double *Spring_AvgLen_XX = NULL;
2858     double *Spring_AvgLen_XY = NULL;
2859     double *Spring_AvgLen_YY = NULL;
2860
2861     Spring_AvgLen_XX = (double*)malloc((hostTimeStepsMacro+1)
2862                                         * sizeof(double));

```



```

2863     Spring_AvgLen_XY = (double*)malloc((hostTimeStepsMacro+1)
2864         * sizeof(double));
2865     Spring_AvgLen_YY = (double*)malloc((hostTimeStepsMacro+1)
2866         * sizeof(double));
2867
2868
2869     if (Spring_AvgLen_XX == NULL)
2870         printf("Spring_AvgLen_XX memory error.\n");
2871     if (Spring_AvgLen_XY == NULL)
2872         printf("Spring_AvgLen_XY memory error.\n");
2873     if (Spring_AvgLen_YY == NULL)
2874         printf("Spring_AvgLen_YY memory error.\n");
2875
2876
2877     //___ initialize memory ___
2878     for(unsigned int n=0; n < hostTimeStepsMacro+1; n++)
2879     {
2880         Spring_AvgLen_XX[n] = 0.0;
2881         Spring_AvgLen_XY[n] = 0.0;
2882         Spring_AvgLen_YY[n] = 0.0;
2883     }
2884
2885
2886     unsigned int k; //iterating variable used for main loop //Why here?
2887
2888     //"....."
2889
2890     //___ Track Species Ratios ___
2891     double *ActiveRatio = NULL;

```

```

2892     double *DangleRatio = NULL;
2893     double *LoopedRatio = NULL;
2894
2895     ActiveRatio = (double*)malloc((hostTimeStepsMacro+1)*sizeof(double));
2896     DangleRatio = (double*)malloc((hostTimeStepsMacro+1)*sizeof(double));
2897     LoopedRatio = (double*)malloc((hostTimeStepsMacro+1)*sizeof(double));
2898
2899     if (ActiveRatio == NULL)
2900         printf("ActiveRatio memory error.\n");
2901     if (DangleRatio == NULL)
2902         printf("DangleRatio memory error.\n");
2903     if (LoopedRatio == NULL)
2904         printf("LoopedRatio memory error.\n");
2905
2906     //.....
2907
2908
2909     //int NumberOfActive = 0;
2910     //int NumberOfDangling = 0;
2911
2912
2913     //__ Calculate Ensemble Average at time = 0__
2914     struct Stress *Time_k_Stress = NULL;
2915     struct Stress *Active_Stress = NULL;
2916     struct Stress *Dangle_Stress = NULL;
2917
2918     Time_k_Stress = (Stress*)malloc((hostTimeStepsMacro+1)*sizeof(Stress));
2919     Active_Stress = (Stress*)malloc((hostTimeStepsMacro+1)*sizeof(Stress));
2920     Dangle_Stress = (Stress*)malloc((hostTimeStepsMacro+1)*sizeof(Stress));

```

```

2921
2922     if (Time_k_Stress == NULL)
2923         printf("Time_k_Stress memory error.\n");
2924     if (Active_Stress == NULL)
2925         printf("Active_Stress memory error.\n");
2926     if (Dangle_Stress == NULL)
2927         printf("Dangle_Stress memory error.\n");
2928
2929
2930     //___ initialize memory ___
2931     for(unsigned int n=0; n < hostTimeStepsMacro+1; n++)
2932     {
2933         Time_k_Stress[n].XX = 0.0;
2934         Time_k_Stress[n].XY = 0.0;
2935         Time_k_Stress[n].YY = 0.0;
2936         Active_Stress[n].XX = 0.0;
2937         Active_Stress[n].XY = 0.0;
2938         Active_Stress[n].YY = 0.0;
2939         Dangle_Stress[n].XX = 0.0;
2940         Dangle_Stress[n].XY = 0.0;
2941         Dangle_Stress[n].YY = 0.0;
2942     }
2943
2944     //*****
2945
2946
2947     //__ Initial Species Count __
2948     SpeciesRatioCount(hostSpeciesType, &ActiveRatio[0], &DangleRatio[0],
2949                       &LoopedRatio[0]);

```

```

2950
2951 //___ NEW CODE ___
2952 SpeciesValue *AvgLen;
2953 AvgLen = (SpeciesValue*)malloc((hostTimeStepsMacro+1)*sizeof(SpeciesValue));
2954
2955 SpeciesValue *Variance;
2956 Variance = (SpeciesValue*)malloc((hostTimeStepsMacro+1) *
2957     sizeof(SpeciesValue));
2958
2959
2960 if (AvgLen == NULL)
2961     printf("AvgSpringLife_data memory error.\n");
2962 if (Variance == NULL)
2963     printf("AvgSpringLife_data memory error.\n");
2964
2965 //___ initialize memory ___
2966 for(unsigned int n=0; n < hostTimeStepsMacro+1; n++)
2967 {
2968     AvgLen[n].ActiveLen = 0.0;
2969     AvgLen[n].ActiveX = 0.0;
2970     AvgLen[n].ActiveY = 0.0;
2971     AvgLen[n].DangleLen = 0.0;
2972     AvgLen[n].DangleX = 0.0;
2973     AvgLen[n].DangleY = 0.0;
2974     AvgLen[n].LoopedLen = 0.0;
2975     AvgLen[n].LoopedX = 0.0;
2976     AvgLen[n].LoopedY = 0.0;
2977     Variance[n].ActiveLen = 0.0;
2978     Variance[n].ActiveX = 0.0;

```

```

2979     Variance[n].ActiveY = 0.0;
2980     Variance[n].DangleLen = 0.0;
2981     Variance[n].DangleX = 0.0;
2982     Variance[n].DangleY = 0.0;
2983     Variance[n].LoopedLen = 0.0;
2984     Variance[n].LoopedX = 0.0;
2985     Variance[n].LoopedY = 0.0;
2986 }
2987
2988 /*
2989  * Store Average Spring Life at each time step
2990  */
2991 double *AvgSpringLife_data = NULL;
2992
2993     AvgSpringLife_data = (double*)malloc((hostTimeStepsMacro+1)
2994         * sizeof(double));
2995
2996 if (AvgSpringLife_data == NULL)
2997     printf("AvgSpringLife_data memory error.\n");
2998
2999 //____ initialize memory ____
3000 for(unsigned int n=0; n < hostTimeStepsMacro+1; n++)
3001     AvgSpringLife_data[n] = 0.0;
3002
3003 /*
3004  * Histogram tracking:
3005  *
3006  * Dynamically allocate 2d struct array as points to pointers
3007  *

```

```

3008     * Notes: x-axis = bin number
3009     * y-axis = time
3010     *
3011     * Example Active bin2 and time step3: Hist[2][3].Active
3012     *
3013     */
3014
3015     int NumOfBins = 100;
3016
3017     SpeciesCount *Hist[100] = {NULL}; //Size should correspond to NumOfBins
3018
3019     for(int i=0; i < NumOfBins; i++){
3020         Hist[i]=(SpeciesCount *)malloc(sizeof(SpeciesCount) *
3021                                     (hostTimeStepsMacro+1));
3022
3023         if (Hist[i] == NULL)
3024             printf("Hist[%d] memory error.\n",i);
3025
3026         //___ initialize memory ___
3027         for(unsigned int n=0; n < hostTimeStepsMacro+1; n++)
3028             {
3029                 Hist[i][n].Active = 0.0;
3030                 Hist[i][n].Dangle = 0.0;
3031                 Hist[i][n].Looped = 0.0;
3032             }
3033     }
3034
3035
3036     //////////////////////////////////////////////////

```

```

3037
3038
3039 #ifdef RAW_OUT
3040
3041     /* Write Dumbbell Raw Data
3042     *
3043     * Enables the option to write dumbbell positions to
3044     * a binary file at a set interval.
3045     * Filename is the same as the csv file except *bin
3046     * appended.
3047     *
3048     * Notes: Writes 4+8+8 = 20 bytes for each dumbbell.
3049     * Therefore can quickly result in large files.
3050     *
3051     */
3052
3053     char RawDataFilename[256];
3054
3055     sprintf(RawDataFilename, "%s.bin", DataFileName);
3056
3057     FILE *RawDataFilePtr = NULL;
3058
3059
3060
3061
3062
3063     long int RawData_FileSize; //for checking file size
3064
3065     if (strcmp(RawData_select,"Yes")==0){

```

```

3066
3067     RawDataFilePtr = fopen(RawDataFilename, "wb");
3068     if (!RawDataFilePtr){
3069         printf("Unable to open raw data file!\n");
3070     }
3071 }
3072
3073 #ifdef DEBUG
3074     printf("DEBUG: RawData Filename = %s\n", RawDataFilename);
3075     printf("DEBUG: int = %zu double = %zu \n", sizeof(int), sizeof(double));
3076     printf("DEBUG: hostNumberOfParticles= %zu\n", hostNumberOfParticles);
3077 #endif
3078 #endif
3079
3080
3081     //_____ To Caclulate Average Length of all Active Dumbbells_____
3082
3083     double *hostAverageSpringLife = NULL;
3084     double *devAverageSpringLife = NULL;
3085
3086     hostAverageSpringLife = (double *)malloc(sizeof(double));
3087     CUDA_CALL(cudaMalloc((double**)&devAverageSpringLife,sizeof(double)));
3088
3089     if (hostAverageSpringLife == NULL)
3090         printf("hostAverageSpringLife memory error.\n");
3091
3092     //___ initialize memory ___
3093     *hostAverageSpringLife = 0.0;
3094     //"....."

```



```

3095
3096
3097
3098     //___ Array to record time steps ___
3099     double *TimeTrack = NULL;
3100
3101     TimeTrack = (double*)malloc((hostTimeStepsMacro+1)*sizeof(double));
3102
3103     if (TimeTrack == NULL)
3104         printf("TimeTrack memory error.\n");
3105
3106     //_____ Macro Time step Loop _____
3107     // Main simulation loop
3108
3109     double FlowRate = 0; /* FlowRate for each stage of simulation */
3110     double MicroStepSize = 0; /* Allocs two time step sizes */
3111
3112
3113     /*
3114     * Time step zero initializations
3115     */
3116     EnsembleAverage(hostSpeciesType, hostSpringLenX, hostSpringLenY,
3117                     Time_k_Stress, Active_Stress, Dangle_Stress, 0);
3118
3119
3120
3121     #ifdef NEW_DNG_LN
3122         TwoDimSpring *AvgDng;
3123     #endif

```

```

3124
3125
3126     Spring_AvgLen_XX[0] = Time_k_Stress[0].XX;
3127     Spring_AvgLen_XY[0] = Time_k_Stress[0].XY;
3128     Spring_AvgLen_YY[0] = Time_k_Stress[0].YY;
3129
3130
3131     Detailed_Info(hostSpeciesType, hostSpringLenX, hostSpringLenY,
3132                 AvgLen, Variance,
3133     #ifdef NEW_DNG_LN
3134                 AvgDng,
3135     #endif
3136                 NumOfBins, Hist, 0);
3137
3138     #ifdef NEW_DNG_LN
3139     printf("The average dangling length is x: %f y: %f \n",
3140           AvgDng->x, AvgDng->y);
3141     #endif
3142
3143
3144
3145
3146     TimeTrack[0]=0.0;
3147
3148     AvgSpringLife_data[0]=AvgSpringLife(hostSpringLenX, hostSpringLenY,
3149                                         hostSpeciesType);
3150
3151
3152

```

```

3153
3154 #ifndef SPEC_CHNG
3155     // At time step 0 there are no changes
3156     Dng2ActSum[0] = 0;
3157     Dng2LpdSum[0] = 0;
3158     Act2DngSum[0] = 0;
3159     Lpd2DngSum[0] = 0;
3160 #endif
3161
3162
3163     /*
3164     * Begin main simulation loop
3165     */
3166
3167     for (k=1; k<=hostTimeStepsMacro; k++){
3168
3169     #ifdef DEBUG
3170         printf("DEBUG: Main Loop [%u] ", k);
3171     #endif
3172         //Calculate Average Length of all Active dumbbells
3173         AvgSpringLife_data[k] = AvgSpringLife(hostSpringLenX,
3174                                             hostSpringLenY,
3175                                             hostSpeciesType);
3176
3177
3178         if (AvgSpringLife_data[k]==0){
3179             *hostAverageSpringLife = AvgSpringLife_data[0];
3180             AvgSpringLife_data[k] = AvgSpringLife_data[0];
3181         } else {

```

```

3182             *hostAverageSpringLife = AvgSpringLife_data[k];
3183     }
3184
3185
3186
3187     CUDA_CALL(cudaMemcpy(devAverageSpringLife,
3188             hostAverageSpringLife,
3189             sizeof(double),
3190             cudaMemcpyHostToDevice));
3191
3192     // set micro time step size based on whether the loop is in stage 1 or
3193     // stage 2 of the simulation
3194     /*
3195     * First stage is designed as zero flow rate. Second stage
3196     * is the inputed flow rate.
3197     * Notes: This is a quick fix for implementing the zero flow rate
3198     * equalizing phase into the simulations.
3199     *
3200     */
3201     if ( k < hostMacroStepSizeSplitPt){
3202         MicroStepSize = hostStepSizeMicroFirst;
3203         FlowRate = 0;
3204     #ifdef DEBUG
3205         printf("Stage 1\n");
3206     #endif
3207     } else {
3208         MicroStepSize = hostStepSizeMicroSecon;
3209         FlowRate = hostFlowRate;
3210     #ifdef DEBUG

```

```

3211         printf("Stage 2\n");
3212     #endif
3213         }
3214
3215
3216
3217     #ifdef NO_REPORT
3218         //Time is recorded in the next section when this option is selected
3219     #else
3220         //record time
3221         TimeTrack[k] = TimeTrack[k-1] + MicroStepSize
3222             * hostTimeStepsMicro;
3223     #endif
3224
3225     #ifdef SPEC_CHNG
3226         //Call function to perform computations on GPU
3227         Micro_Steps<<<grid,block>>>(devSpringLenX, devSpringLenY,
3228             devSpeciesType,
3229             states, ProbStates,
3230             AvgSpringLife_data[k],
3231             devSimTime, MicroStepSize,
3232             hostTimeStepsMicro,
3233             AvgLen[k-1].DangleLen, FlowRate,
3234             devDng2Act, devDng2Lpd,
3235             devAct2Dng, devLpd2Dng);
3236     #else
3237     #ifdef MICRO_RAW
3238         //Call function to perform computations on GPU
3239         Micro_Steps<<<grid,block>>>(devSpringLenX, devSpringLenY,

```

```

3240         devSpeciesType,
3241         states, ProbStates,
3242         AvgSpringLife_data[k],
3243         devSimTime, MicroStepSize,
3244         hostTimeStepsMicro,
3245         AvgLen[k-1].DangleLen, FlowRate,
3246         devSCArr, hostNumberOfParticles);
3247     //width in bytes -> hostTimeStepsMicro * sizeof(DBSpecChng)
3248     //height is hostNumberOfParticles
3249
3250     #else
3251     #ifdef NO_REPORT
3252     /*
3253     * This option ups the number of Microsteps during a single macro loop.
3254     * This has the effect of reducing the amount of CPU-GPU communication
3255     * for the part of the simulation that is not usually used.
3256     */
3257     if (k == hostMacroStepSizeSplitPt){
3258         //record time
3259         TimeTrack[k] = TimeTrack[k-1] + MicroStepSize * hostA_coeff;
3260         //Call function to perform computations on GPU
3261         Micro_Steps<<<grid,block>>>(devSpringLenX, devSpringLenY,
3262         devSpeciesType,
3263         states, ProbStates,
3264         AvgSpringLife_data[k],
3265         devSimTime, MicroStepSize,
3266         hostA_coeff,
3267         AvgLen[k-1].DangleLen, FlowRate);
3268     } else {

```

```

3269         //record time
3270         TimeTrack[k] = TimeTrack[k-1] + MicroStepSize
3271             * hostTimeStepsMicro;
3272         //Call function to perform computations on GPU
3273         Micro_Steps<<<grid,block>>>(devSpringLenX, devSpringLenY,
3274             devSpeciesType,
3275             states, ProbStates,
3276             AvgSpringLife_data[k],
3277             devSimTime, MicroStepSize,
3278             hostTimeStepsMicro,
3279             AvgLen[k-1].DangleLen, FlowRate);
3280     }
3281     #else
3282     #ifdef SINGLE_MICRO
3283         //Call function to perform computations on GPU
3284         Micro_Steps<<<grid,block>>>(devSpringLenX, devSpringLenY,
3285             devSpeciesType,
3286             states, ProbStates,
3287             AvgSpringLife_data[k],
3288             devSimTime, MicroStepSize,
3289             hostTimeStepsMicro,
3290             AvgLen[k-1].DangleLen, FlowRate,
3291             devSCArr, hostNumberOfParticles);
3292         //width in bytes -> hostTimeStepsMicro * sizeof(DBSpecChng)
3293         //height is hostNumberOfParticles
3294     #else
3295         //Call function to perform computations on GPU
3296         Micro_Steps<<<grid,block>>>(devSpringLenX, devSpringLenY,
3297             devSpeciesType,

```

```

3298         states, ProbStates,
3299         AvgSpringLife_data[k],
3300         devSimTime, MicroStepSize,
3301         hostTimeStepsMicro,
3302         AvgLen[k-1].DangleLen, FlowRate);
3303 #endif //SINGLE_MICRO
3304 #endif //NO_REPORT
3305 #endif //MICRO_RAW
3306 #endif //SPEC_CHNG
3307
3308
3309
3310
3311         //read result from gpu(device) back to cpu(host)
3312         CUDA_CALL(cudaMemcpy(hostSpringLenX, devSpringLenX,
3313             hostNumberOfParticles*sizeof(double),
3314             cudaMemcpyDeviceToHost));
3315         CUDA_CALL(cudaMemcpy(hostSpringLenY, devSpringLenY,
3316             hostNumberOfParticles*sizeof(double),
3317             cudaMemcpyDeviceToHost));
3318         CUDA_CALL(cudaMemcpy(hostSpeciesType, devSpeciesType,
3319             hostNumberOfParticles*sizeof(int),
3320             cudaMemcpyDeviceToHost));
3321
3322         //read sim time back from gpu(device) back to cpu(host)
3323         CUDA_CALL(cudaMemcpy(hostSimTime, devSimTime,
3324             hostNumberOfParticles*sizeof(double),
3325             cudaMemcpyDeviceToHost));
3326

```



```

3327 #ifdef SPEC_CHNG
3328     //read species transitions back from gpu
3329         CUDA_CALL(cudaMemcpy(hostDng2Act, devDng2Act,
3330             hostNumberOfParticles*sizeof(unsigned int),
3331             cudaMemcpyDeviceToHost));
3332         CUDA_CALL(cudaMemcpy(hostDng2Lpd, devDng2Lpd,
3333             hostNumberOfParticles*sizeof(unsigned int),
3334             cudaMemcpyDeviceToHost));
3335         CUDA_CALL(cudaMemcpy(hostAct2Dng, devAct2Dng,
3336             hostNumberOfParticles*sizeof(unsigned int),
3337             cudaMemcpyDeviceToHost));
3338         CUDA_CALL(cudaMemcpy(hostLpd2Dng, devLpd2Dng,
3339             hostNumberOfParticles*sizeof(unsigned int),
3340             cudaMemcpyDeviceToHost));
3341
3342     //call function that sums the values
3343     Dng2ActSum[k] = VectorSum(hostDng2Act,hostNumberOfParticles);
3344     Dng2LpdSum[k] = VectorSum(hostDng2Lpd,hostNumberOfParticles);
3345     Act2DngSum[k] = VectorSum(hostAct2Dng,hostNumberOfParticles);
3346     Lpd2DngSum[k] = VectorSum(hostLpd2Dng,hostNumberOfParticles);
3347
3348 #endif
3349
3350 #ifdef SINGLE_MICRO
3351
3352     //transfer data back from GPU
3353     CUDA_CALL(cudaMemcpy(hostSCArr, devSCArr,
3354         hostTimeStepsMicro * sizeof(DBSpecChng),
3355         cudaMemcpyDeviceToHost));

```

```

3356
3357 //check file size, error if too big
3358 MicroData_FileSize = ftell(MicroDataFilePtr);
3359
3360
3361 for(unsigned int m=0; m < hostTimeStepsMicro; m++){
3362
3363     if (MicroData_FileSize < MICRODATA_MAX_FILESIZE){
3364         fwrite( &(hostSCArr[m].type),sizeof(int), 1, MicroDataFilePtr);
3365         fwrite( &(hostSCArr[m].time),sizeof(double),1, MicroDataFilePtr);
3366         fwrite( &(hostSCArr[m].x), sizeof(double),1, MicroDataFilePtr);
3367         fwrite( &(hostSCArr[m].y), sizeof(double),1, MicroDataFilePtr);
3368     } else {
3369         printf("WARNING: Micro data file size exceeded maximum. No longer ",
3370             "writing to file. \n");
3371     }
3372 }
3373
3374
3375 #endif
3376
3377 #ifdef MICRO_RAW
3378
3379 //transfer data back from GPU
3380 CUDA_CALL(cudaMemcpy(hostSCArr, devSCArr,
3381     hostNumberOfParticles * hostTimeStepsMicro * sizeof(DBSpecChng),
3382     cudaMemcpyDeviceToHost));
3383
3384 //check file size, error if too big

```

```

3385     MicroData_FileSize = ftell(MicroDataFilePtr);
3386
3387
3388     for(unsigned int n=0; n < hostNumberOfParticles; n++){
3389         for(unsigned int m=0; m < hostTimeStepsMicro; m++){
3390
3391             if (MicroData_FileSize < MICRODATA_MAX_FILESIZE){
3392                 fwrite( &(n),
3393                     sizeof(unsigned int), 1, MicroDataFilePtr);
3394                 fwrite( &(hostSCArr[n*hostTimeStepsMicro+m].type),
3395                     sizeof(int), 1, MicroDataFilePtr);
3396                 fwrite( &(hostSCArr[n*hostTimeStepsMicro+m].length),
3397                     sizeof(double), 1, MicroDataFilePtr);
3398             } else {
3399                 printf("WARNING: Micro data file size exceeded maximum. No longer ",
3400                     "writing to file. \n");
3401             }
3402         }
3403     }
3404
3405
3406 #endif
3407
3408
3409     EnsembleAverage(hostSpeciesType, hostSpringLenX, hostSpringLenY,
3410                     Time_k_Stress, Active_Stress, Dangle_Stress,k);
3411
3412     Spring_AvgLen_XX[k] = Time_k_Stress[k].XX;
3413     Spring_AvgLen_XY[k] = Time_k_Stress[k].XY;

```

```

3414         Spring_AvgLen_YY[k] = Time_k_Stress[k].YY;
3415         //*****
3416
3417
3418         SpeciesRatioCount(hostSpeciesType, &ActiveRatio[k], &DangleRatio[k],
3419                             &LoopedRatio[k]);
3420
3421         //___ NEW CODE ___
3422         Detailed_Info (hostSpeciesType, hostSpringLenX, hostSpringLenY,
3423                         &AvgLen[k], &Variance[k],
3424                         NumOfBins, Hist, k);
3425
3426
3427 #ifdef RAW_OUT
3428
3429         /* Write file output directly to file */
3430
3431         #ifdef SIMPLE_SHEAR
3432         if ((strcmp(RawData_select,"Yes")==0) && RawOut_SSFlow(k))
3433         #else
3434
3435         /*
3436         * FULL_DATA option to allow for 800 steps over entire
3437         * Oscillatory shear simulation
3438         */
3439
3440         #ifdef FULL_DATA
3441         if ((strcmp(RawData_select,"Yes")==0) && RawOut_SSFlow(k))
3442         #else

```

```

3443     //default is oscillatory shear
3444     if ((strcmp(RawData_select,"Yes")==0) && RawOut_OSFlow(k))
3445     #endif
3446     #endif
3447     {
3448
3449     //check file size, error if too big
3450     RawData_FileSize = ftell(RawDataFilePtr);
3451
3452
3453
3454     #ifdef DEBUG
3455         printf("DEBUG: Current file size: %ld\n", RawData_FileSize);
3456         printf("DEBUG: Writing to file: %s on step: %d at time: %f\n",
3457             RawDataFilename, k, TimeTrack[k]);
3458
3459     #endif
3460     if (RawData_FileSize < RAWDATA_MAX_FILESIZE){
3461
3462
3463         fwrite(&(TimeTrack[k]),sizeof(double), 1,
3464             RawDataFilePtr);
3465         fwrite(hostSpeciesType,sizeof(int) ,hostNumberOfParticles,
3466             RawDataFilePtr);
3467         fwrite(hostSpringLenX ,sizeof(double),hostNumberOfParticles,
3468             RawDataFilePtr);
3469         fwrite(hostSpringLenY ,sizeof(double),hostNumberOfParticles,
3470             RawDataFilePtr);
3471     } else {

```

```

3472         printf("WARNING: Raw data file size exceeded %f bytes. No longer ",
3473                "writing to file.\n", RAWDATA_MAX_FILESIZE);
3474     }
3475 }
3476
3477 #endif
3478 }
3479 // "End Macro loop"
3480
3481 #ifdef RAW_OUT
3482
3483     if (strcmp(RawData_select,"Yes")==0){
3484         fclose(RawDataFilePtr);
3485     }
3486
3487 #endif
3488
3489
3490 #ifdef MICRO_RAW
3491     fclose(MicroDataFilePtr);
3492 #endif
3493
3494 #ifdef SINGLE_MICRO
3495     fclose(MicroDataFilePtr);
3496 #endif
3497
3498     // __ stop computational clock __
3499     end = clock();
3500     time_spent = double(end-begin)/ CLOCKS_PER_SEC;

```

```

3501 //*****
3502
3503
3504 #ifdef SPEC_CHNG
3505     OutputToFile( Spring_AvgLen_XX, Spring_AvgLen_XY, Spring_AvgLen_YY,
3506                 TimeTrack, time_spent, k, argv[0],
3507                 ActiveRatio, DangleRatio, LoopedRatio,
3508                 AvgLen, Variance,
3509                 NumOfBins, Hist,
3510                 Time_k_Stress, Active_Stress, Dangle_Stress,
3511                 AvgSpringLife_data,
3512                 Dng2ActSum, Dng2LpdSum, Act2DngSum,
3513                 Lpd2DngSum,
3514                 DataFileName);
3515
3516 #else
3517
3518     OutputToFile( Spring_AvgLen_XX, Spring_AvgLen_XY, Spring_AvgLen_YY,
3519                 TimeTrack, time_spent, k, argv[0],
3520                 ActiveRatio, DangleRatio, LoopedRatio,
3521                 AvgLen, Variance,
3522                 NumOfBins, Hist,
3523                 Time_k_Stress, Active_Stress, Dangle_Stress,
3524                 AvgSpringLife_data,
3525                 DataFileName);
3526 //*****
3527 #endif
3528
3529

```

```
3530  /*
3531  * Memory freed in the order it was initialized.
3532  *
3533  */
3534
3535
3536  CUDA_CALL(cudaFree(states));
3537  CUDA_CALL(cudaFree(ProbStates));
3538
3539
3540  free(hostSeeds);
3541  free(hostProbSeeds);
3542
3543
3544  CUDA_CALL(cudaFree(devSeeds));
3545  CUDA_CALL(cudaFree(devProbSeeds));
3546
3547  free(hostSpringLenX);
3548  free(hostSpringLenY);
3549  free(hostSpeciesType);
3550
3551  CUDA_CALL(cudaFree(devSpringLenX));
3552  CUDA_CALL(cudaFree(devSpringLenY));
3553  CUDA_CALL(cudaFree(devSpeciesType));
3554
3555
3556  free(hostSimTime);
3557  CUDA_CALL(cudaFree(devSimTime));
3558
```



```

3559     free(Spring_AvgLen_XX);
3560     free(Spring_AvgLen_XY);
3561     free(Spring_AvgLen_YY);
3562
3563     free(ActiveRatio);
3564     free(DangleRatio);
3565     free(LoopedRatio);
3566
3567     free(Time_k_Stress);
3568     free(Active_Stress);
3569     free(Dangle_Stress);
3570
3571     free(AvgLen);
3572
3573     free(Variance);
3574
3575     free(AvgSpringLife_data);
3576
3577     for(int i=0; i<NumOfBins; i++)
3578         free(Hist[i]);
3579
3580     #ifdef SPEC_CHNG
3581
3582     free(hostDng2Act);
3583     free(hostDng2Lpd);
3584     free(hostAct2Dng);
3585     free(hostLpd2Dng);
3586
3587     CUDA_CALL(cudaFree(devDng2Act));

```

```
3588     CUDA_CALL(cudaFree(devDng2Lpd));
3589     CUDA_CALL(cudaFree(devAct2Dng));
3590     CUDA_CALL(cudaFree(devLpd2Dng));
3591
3592     free(Dng2ActSum);
3593     free(Dng2LpdSum);
3594     free(Act2DngSum);
3595     free(Lpd2DngSum);
3596
3597 #endif
3598
3599 #ifdef SINGLE_MICRO
3600
3601     free(hostSCArr);
3602     CUDA_CALL(cudaFree(devSCArr));
3603
3604 #endif
3605 #ifdef MICRO_RAW
3606
3607     free(hostSCArr);
3608     CUDA_CALL(cudaFree(devSCArr));
3609
3610 #endif
3611
3612
3613
3614     free(hostAverageSpringLife);
3615     CUDA_CALL(cudaFree(devAverageSpringLife));
3616
```

```
3617     free(TimeTrack);
3618
3619     //*****
3620
3621
3622     cudaDeviceReset();
3623
3624
3625     // __ stop computational clock __
3626     end2 = clock();
3627     time_spent2 = double(end2-begin)/ CLOCKS_PER_SEC;
3628     printf("Runtime: %f\n\n", time_spent2);
3629     //*****
3630
3631
3632     return EXIT_SUCCESS;
3633
3634 }
```